BIULETYN
INSTYTUTU SPAWALNICTWA

CONTENTS

Summaries of the articles

J. Matusiak, J. Wyciślik, A. Pilarczyk – I-EcoWelding - Internet system of guidance supporting calculations of welding fumes emissions in welding and allied processes

The article presents a new tool for environmental analyses concerning pollutant emissions, i.e. the I-EcoWelding software programme. This Internet guidance system is an innovative tool supporting the decision-making related to health and safety in production processes and supporting calculations of pollutant emissions into work environment during welding and allied processes. The Internet guidance system helps determine emissions and compositions of welding fumes during fusion welding, resistance welding, vibration welding of thermoplastics, brazing as well as thermal gas and plasma cutting. In addition, the system enables calculating emissions in relation to the entire welding production of a given company, taking into consideration the duration of a technological process or the declared weight of filler metal used.

Z. Mikno, Sz. Kowieski, W. Zhang – Simulation and optimisation of resistance welding using the SORPAS® software programme

The implementation of new materials such as dual phase (DP) steels, TRIP steels (Transformation Induced Plasticity Steel) and aluminium alloys or joining more complex dissimilar materials (three sheets/plates) having various thicknesses and various chemical compositions pose serious challenges in terms of resistance welding technologies. The article presents the possibilities of the professional Sorpas® software programme used for simulating and optimising resistance welding processes. This software programme assesses the weldability of materials by simulating welding processes and forecasting the final result, including the size of the weld nugget. In addition, the software enables the optimisation of welding processes, the simulation of post-weld joint properties, the assessment of weld quality in terms of microstructural transformations, hardness distribution and strength in specific load conditions as well as makes it possible to determine the field of welding parameters. Available versions of the software are designated as 2D and 3D. The latter version enables the modelling of complex phenomena, e.g. shunting or multi-projection welding.

M. Restecka, R. Jachym – IT systems used for welding process simulations and simulators of thermal-strain cycles

The first part of the article presents an overview of software programmes assisting welding-related engineering works as well as discusses possibilities and advantages related to the use of such programmes. Software programmes available today enable, among other things, the monitoring of welding processes, calculations of temperature distribution, the determination of mechanical and plastic properties, simulations of distributions of residual stresses as well as simulations of transformations triggered by welding thermal cycles. The second part of the article is dedicated to simulators enabling physical simulations of welding processes as well as describes principles of simulations tests and presents advantages related to the use of this technique.

E. Turyk – Qualifying the technology of the aluminothermic welding of tramway rails on the basis of quality assurance system requirements in welding engineering

The article discusses the issue of demonstrating the correctness of a technology dedicated to the aluminothermic welding of tramway rails, recommends that the technology be qualified in accordance with standard PN-EN ISO 15613:2006 concerning the pre-production testing of technologies used when welding atypical joints, proposes the scope of qualification tests and presents test results concerning defective welded joints.

M. Różański, S. Stano, A. Grajcar – Laser welding and heat treatment of steel 0H15N7M2J

DOI: 10.17729/ebis.2016.4/5

The article presents the results of tests concerning the mechanical and structural properties of single-spot and twin-spot laser beam welded joints made of a steel strip, the chemical composition of which corresponds to that of steel 0H15N7M2J. In addition, the article presents the comparison concerning the geometry of joints made using the single and twin-spot laser beam. The test joints were subjected to heat treatment involving austenitisation, cold treatment and ageing. The study also involved the comparison of the mechanical and structural properties of the joints subjected and those not subjected to the above named heat treatment.

R. Kaczmarek, K. Kaczmarek, J. Słania, R. Krawczyk - Performing of ultrasonic inspection using TOFD technique in terms of the requirements of related standards

DOI: 10.17729/ebis.2016.4/6

The article concerns the time of flight diffraction testing technique (TOFD), which is, next to the simultaneous TOFD + Phased Array testing, one of the most effective methods of volumetric non-destructive tests. The article discusses the advantages of the TOFD technique as well as the basis of diffraction phenomenon and the formation of imaging signals. In addition, the article presents a TOFD image of a welded joint and describes its characteristic elements. Also, the article discusses the TOFD-related testing standards and analyses their requirements related to welded joints and their acceptance criterion, i.e. the quality level according to PN-EN ISO 5817. The target readers of the article include NDT personnel, inspectors, welding engineers and welding equipment manufacturers wishing to implement an effective tool enabling the detection of welding imperfections.

P. Irek, Ł. Rawicki, K. Kaczmarek – Dye penetrant testing of welded joints made of nickel and its alloys

DOI: 10.17729/ebis.2016.4/7

The article presents tests involving natural cracks, including measurements of the width of cracks and the profile of their surface roughness. The investigation also involved tests performed in order to observe how a given factor affects development times in penetrant tests as well as to determine what time of development is recommended for nickel and its alloys in order to detect unacceptable welding imperfections (cracks). The article also discusses the effect of penetration times on the duration of development times and sizes of indications in penetrant tests.

R. Krawczyk, J. Kozłowski – Analysing the effect of changes in overlay weld geometry on test SEP 1390

DOI: 10.17729/ebis.2016.4/8

The article presents issues related to the assessment of the weldability of thick-walled materials used when making welded steel structures. The article also discusses the analysis of test results based on the technological test concerning the weldability of thick-walled structural materials according to the guidelines of SEP 1390. The tests took into consideration the effect of the change in overlay weld geometry on the technological test, and, as a result, the final result of weldability assessment.

Investigations

J. Matusiak, J. Wyciślik, A. Pilarczyk

I-EcoWelding – Internet System of Guidance Supporting Calculations of Welding Fumes Emissions in Welding and Allied Processes

Abstract: The article presents a new tool for environmental analyses concerning pollutant emissions, i.e. the I-EcoWelding software programme. This Internet guidance system is an innovative tool supporting the decision-making related to health and safety in production processes and supporting calculations of pollutant emissions into work environment during welding and allied processes. The Internet guidance system helps determine emissions and compositions of welding fumes during fusion welding, resistance welding, vibration welding of thermoplastics, brazing as well as thermal gas and plasma cutting. In addition, the system enables calculating emissions in relation to the entire welding production of a given company, taking into consideration the duration of a technological process or the declared weight of filler metal used.

Keywords: I-EcoWelding, welding software, welding fumes, pollutant emissions

The welding sector in Poland provides employment for thousands of fusion welders, brazers, pressure welders, welding machine operators, specialists in production, control and monitoring in machine-building, ship-building, automotive and aviation industries as well as in electrical engineering and civil engineering. The use of welding processes requires maintaining special conditions of industrial health and safety. Welding processes entail numerous chemical and physical hazards. For this reason, there has been continuous demand for information, hints and recommendations concerning harmful pollutant emissions accompanying welding processes, the effect of these pollutants on worker health and the possible optimisation of technological processes in terms of pollutant emission reductions. Both welding coordination as well as industrial health and safety services have been emphasizing the importance of the necessity for solving problems involving the protection of worker health during welding processes.

For several years, within the confines of European projects, national projects and statutory works, Instytut Spawalnictwa has been involved

dr inż. Jolanta Matusiak (PhD (DSc) Eng.); mgr inż. Joanna Wyciślik (MSc Eng.) – Instytut Spawalnictwa, Department of Resistance and Friction Welding and Environmental Engineering;
mgr inż. Adam Pilarczyk (MSc Eng.) – Instytut Spawalnictwa, IT Department

Joining/ cutting

- gas-shielded metal arc welding
- manual metal arc welding
- gas-shielded tungsten electrode arc welding
- gas-shielded metal arc braze welding
- pressure welding
- thermal cutting
- brazing

Fusion welding/ braze welding/ pressure welding cutting method

- MMA
- MIG/MAG
- ColdArc,
- CMT
- AC MIG Pulse
- Pulse CP
- TIG
- resistance welding
- vibration welding
- gas cutting
- plasma cutting
- flame brazing

Base material

- structural unalloyed steels
- stainless steels
- aluminium alloys
- nickel
- coated steel plates/sheets
- thermoplastics

Filler metal

- covered electrodes
- solid wires, flux-cored wires
- wires for welding aluminium
- wires for welding coated plates/sheets
- wires for braze welding
- wires for welding stainless steels
- filler metals for braze welding

Shielding gas

- Ar
- CO_2
- $Ar+O_2$
- $Ar+CO_2$
- $Ar+H_2$
- Ar+He
- $Ar+CO_2+O_2$
- $Ar+CO_2+H_2$
- none

Process technological parameters

- Welding current
- Arc voltage
- Pressure force
- Vibration amplitude

Fig. 1. Scheme presenting the sequence of data search in the system

Fig. 2 panel — Selection of process and conditions:

- Welding process
- Method
- Base material
- Grade
- Thickness [mm]
- Filler metal
- **Grade**
- Diameter [mm]
- Shielding gas
- I [A]
- U [V]

Selected data:

DESIGN:
Gas-shielded metal arc welding
MAG (135)
Unalloyed and fine-grained steels
S235JR (St3S)
8.0.
Electrode wire
G3Si1 (SG2, SpG3S)
1.2
80% Ar = 20% CO_2
200
27

i-Eco Welding

27

| Weight of filler metal used [kg] | 15 |
| Process duration [h] | 0 |

🔍 **Show (pdf)**

Sidebar: i-Eco Welding · Database · Welding Engineer Web Portal · Research Institutions · Users

Fig. 2. Screen after entering input data

Time emission [mg/s]

fumes	NOx	CO
4.55	0.13	1.78

Computational model

time emission	Ec [mg/s]	process duration [h]	total emission [kg]
fumes	4.55	0	0
nitrogen oxides (NOx)	0.13	0	0
carbon oxide (CO)	1.78	0	0
weight emission	Ew [mg/kg of wire]	weight of filler metal used[kg]	total emission [kg]
fumes	7010.78	15	0.1051617
nitrogen oxides (NOx)	195.68	15	0.0029352
carbon oxide (CO)	4680.3	15	0.0702045

Weight emission [mg/kg of wire]

fumes	NOx	CO
7010.78	195.68	4680.3

Chemical composition of welding fumes [%]

Fe	Mn	Si	Cr	Ni
57.23	11.64	3.57	0.03	0.03

Fig. 3. Screen with results related to gas-shielded metal arc welding –MAG, filler metal wire grade G3Si1, shielding gas 80% Ar + 20% CO_2

in research dedicated to the influence of welding technological and material conditions of welding and allied processes on emissions of welding fumes into work environment. The research has involved tests concerning new joining methods as well as new base materials and filler metals. Results of research works, in the form of fumes emission factors, were disseminated via catalogues concerning characteristics of materials as regards pollutant emissions, single emission sheets related to individual joining procedures, publications in various magazines and, last but not least, in the form of a software programme named Еко-Spawanie (Eco-Welding). This software programme, developed in 2004, within the confines of Multi-Annual Programme (MAP) *Adaptation of work conditions in Poland to standards in the European Union* is dedicated to determining pollutant emissions accompanying MMA, MIG/MAG and TIG welding.

The development and improvement of welding methods as well as the growing awareness concerning hazards in the work environment of companies making welded structures and products have imposed the necessity of providing the welding engineering sector with a new tool for performing environmental analysis focused on pollutant emissions. This new tool is the Internet guidance system

i-EkoSpawanie (I-EcoWelding) based on databases containing emission factors. The system is an innovative tool supporting decision-making related to health and safety in production processes and supporting calculations of pollutant emissions into a work environment during welding and allied processes. The Internet guidance system helps determining emissions and compositions of welding fumes in traditional welding methods, i.e. MIG/MAG, TIG and MIG/MAG performed using pulsed arc and double pulse, MMAW and welding/braze welding using innovative low-energy arc methods such as CMT, ColdArc, STT, AC Pulse and ColdProcess. The system also includes databases of emission factors related to resistance welding, the vibration welding of plastics, brazing as well as thermal gas and plasma cutting processes. The system also enables calculating emissions in relation to the entire welding production of a given company, taking into consideration the duration of a technological process or the declared weight of filler metal used.

The target group of the guidance system includes companies using welding processes in their production, institutions calculating environmental fees in accordance with the Environmental Protection Law and labour inspections. In addition, the system can be used by designer bureaus or companies designing or providing ventilation systems for welding processes.
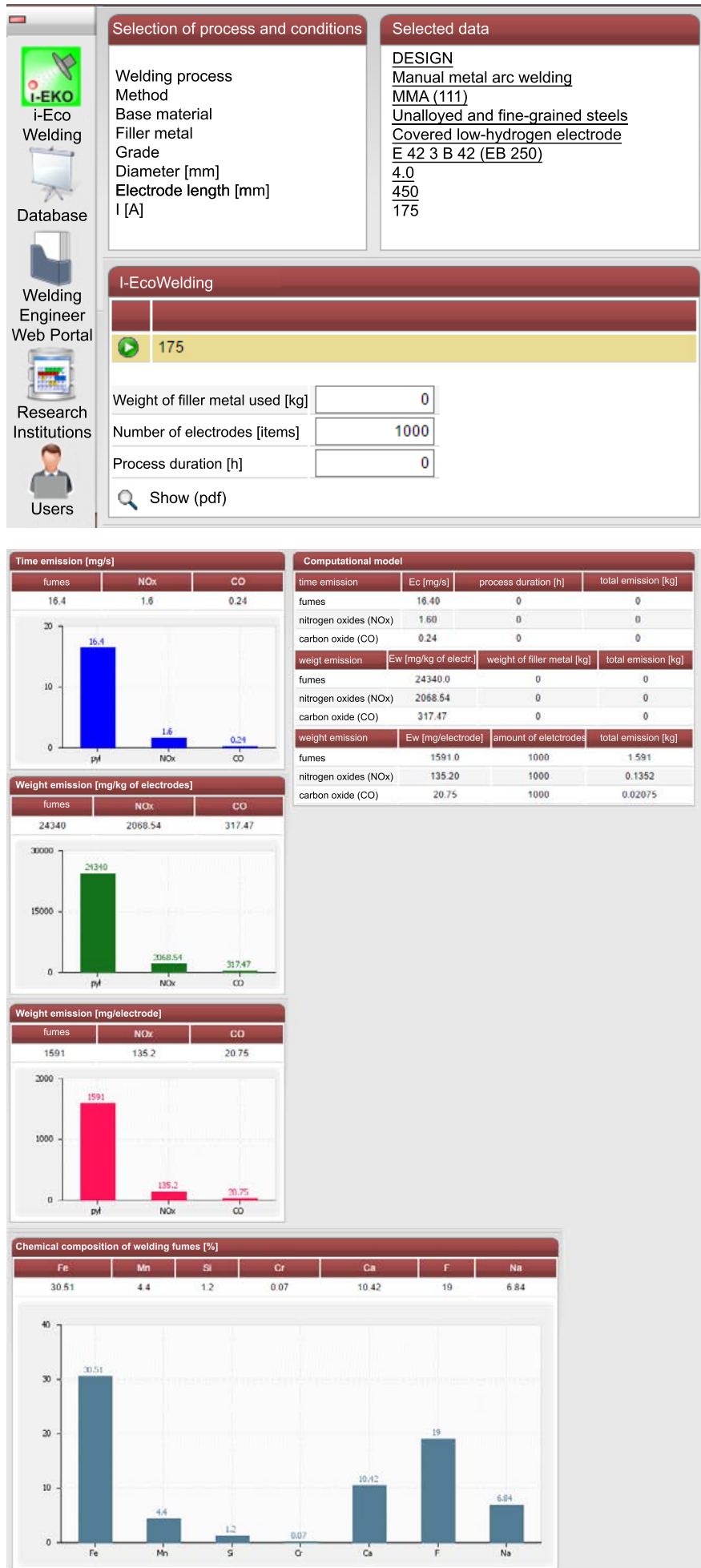
Fig. 4. Screen with results following the selection of MMA welding and covered electrode grade EB 250
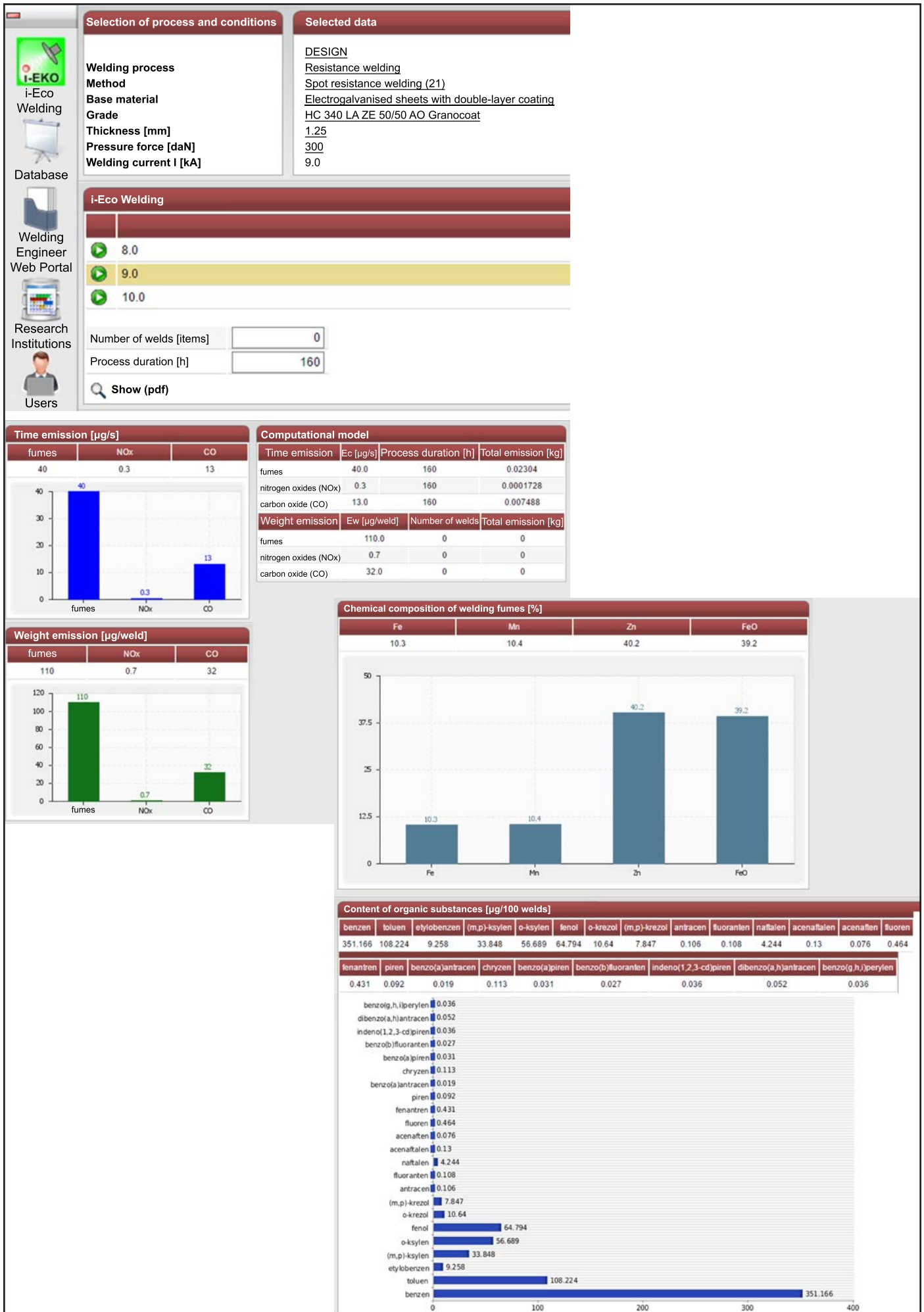
Fig. 5. Screen with results following the selection of resistance welding process

INSTYTUT SPAWALNICTWA
44-100 Gliwice, ul. Bł. Czesława 16-18
Department of Resistance and Friction Welding and Environmental Engineering

I-ECOWELDING PROGRAMME SOFTWARE

POLLUTANT EMISSION DATA SHEET

PROGRAMME USER DATA

Company name	Instytut Spawalnictwa
Address	ul. Bl. Czeslawa 16-18, 44-100 Gliwice
NIP (Taxpayer ID Number)	631-010-22-58
User name	Joanna Wycislik
Sheet generation date	2016-04-29

EMISSION OF WELDING FUMES AND GASES

Welding process	Flame brazing
Method/ name	Flame brazing (912)
Base material	High-alloy steels; copper and its alloys; nickel and its alloys
Filler metal	Flux-cored silver brazing metal
Grade	AG 203 (PR-LS 45)
Diameter	1,8
Rod length	450

DATA FOR TOTAL EMISSION CALCULATION

Process duration [h]	160
Weight of filler metal used [kg]	0
Number of rods	0

COMPUTATIONAL MODULE

Time emission	Ec [mg/s]	Process duration [h]	Total emission [kg]
welding fumes	10.52	160	6.05952
nitrogen oxides (NOx)	3.00	160	1.728
carbon oxide (CO)	0.44	160	0.25344

Weight emission	Ew [mg/kg of brazing metal]	Weight of filler metal used [kg]	Total emission [kg]
welding fumes	38563.70	0	0
nitrogen oxides (NOx)	10679.70	0	0
carbon oxide (CO)	1569.60	0	0

Weight emission	Ew [mg/rod of brazing metal]	Number of rods	Total emission [kg]
welding fumes	250.20	0	0
nitrogen oxides (NOx)	67.11	0	0
carbon oxide (CO)	9.87	0	0

EMISSION OF WELDING FUMES AND GASES

Time emission	Ec [mg/s]
welding fumes	10.52
nitrogen oxides (NOx)	3.00
carbon oxide (CO)	0.44

Weight emission	Ew [mg/kg of brazing metal]
welding fumes	38563.70
nitrogen oxides (NOx)	10679.70
carbon oxide (CO)	1569.60

Weight emission	Ew [mg/rod of brazing metal]
welding fumes	250.20
nitrogen oxides (NOx)	67.11
carbon oxide (CO)	9.87
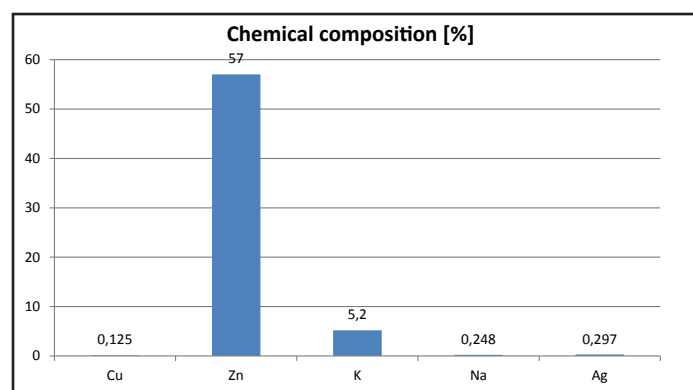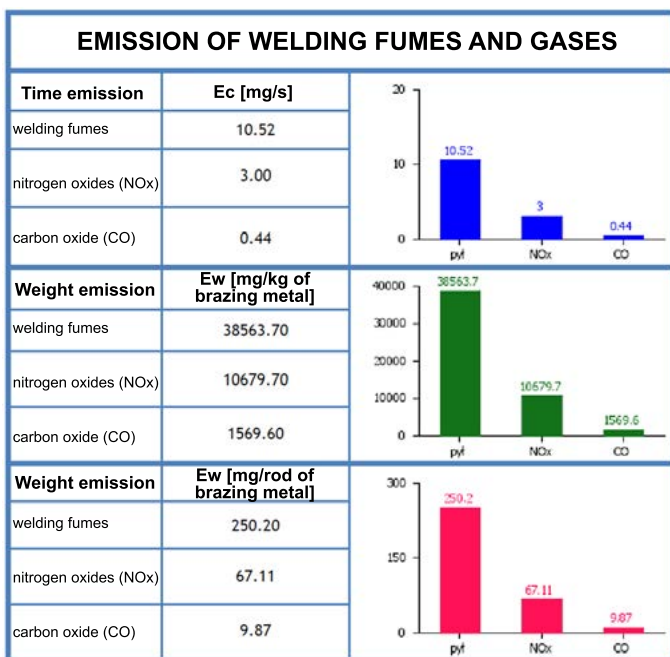
Fig. 6. Pollutant emission data sheet for the flame brazing using silver brazing metal AG 203

Description of I-EcoWelding

The guidance system i-EkoSpawanie (I-Eco-Welding) has been made available on the Internet Welding Platform and provides the possibility of the on-line use of knowledge and results of tests concerning pollutant emissions accompanying welding processes as well as makes it possible to determine emission factors of selected fusion welding, braze welding, pressure welding, brazing and cutting methods in relation to selected structural materials and filler metals. The start-up screen of the I-Eco-Welding system contains all welding and allied processes along with pollutant emission-related data. The user starts designing their calculations using the above named screen. The selection of a joining process option is automatically followed by moving on to the selection of

a joining method. Further steps are concerned with types, grades and thicknesses of base materials, and then, types and grades of filler metals and technological conditions appropriate for related joining or cutting processes. The scheme presenting the sequence of data search in the system is presented in Figure 1.

A selected joining process, method, and material-technological conditions are saved in the dedicated window *Selected data: design* (Fig. 2). The subsequent step involves the use of a computational model determining total emissions. The entering of data related to the duration of a process or the weight of filler metal used is followed by the display of a screen presenting all information related to pollutant emissions. Figure 3 presents the screen with results concerning the MAG welding of unalloyed steel sheets/plates using filler metal wire grade G3Si1 and the shielding gas mixture of 80% Ar + 20% CO_2. The screen presents values of time and weight emissions of welding fumes, nitrogen and carbon oxides as well as the chemical composition of welding fumes. The computational module table provides information concerning total emissions in relation to the declared weight of consumed electrode wire. Exemplary result-related screens of the I-EcoWelding system concerning the MMA welding and the resistance welding of sheets/plates with double protective coatings are presented in Figures 4-5.

For each calculation, the system enables the generation of a *Pollutant Emission Data Sheet*. The sheet is prepared in the PDF format and, as a result, can be saved on a disc and printed out.

An exemplary *Pollutant Emission Data Sheet* is presented in Figure 6.

Summary

The Internet guidance system I-EcoWelding is dedicated to determining emissions of fumes generated during welding and allied processes. In its databases, the system contains results of research performed at Instytut Spawalnictwa and concerning emissions and chemical compositions of pollutants emitted to a work environment during various joining and cutting processes. In comparison with the already existing Eco-Welding software programme, the I-EcoWelding system provides the possibility of updating data directly following the completion of successive research works. The system also features a computational module enabling the determination of the total emission of pollutants. The system structure allows its continuous development and the addition of new information using the administrator interface.

The I-EcoWelding system is available on the Internet Welding Platform and is addressed at a variety of companies using welding processes in production. Users can access the system on using their individual login and password.

References

[1] Matusiak J., Wyciślik J., Pilarczyk A.: *Opracowanie internetowego systemu doradczego wspomagającego określanie emisji zanieczyszczeń przy spawaniu i procesach pokrewnych*. Instytut Spawalnictwa Research Work no. Ma-40 (ST 342), Gliwice 2015

Zygmunt Mikno, Szymon Kowieski, Wengi Zhang

Simulation and Optimisation of Resistance Welding Using the SORPAS® Software Programme

Abstract: The implementation of new materials such as dual phase (DP) steels, TRIP steels (Transformation Induced Plasticity Steel) and aluminium alloys or joining more complex dissimilar materials (three sheets/plates) having various thicknesses and various chemical compositions pose serious challenges in terms of resistance welding technologies. The article presents the possibilities of the professional SORPAS® software programme used for simulating and optimising resistance welding processes. This software programme assesses the weldability of materials by simulating welding processes and forecasting the final result, including the size of the weld nugget. In addition, the software enables the optimisation of welding processes, the simulation of post-weld joint properties, the assessment of weld quality in terms of microstructural transformations, hardness distribution and strength in specific load conditions as well as makes it possible to determine the field of welding parameters. Available versions of the software are designated as 2D and 3D. The latter version enables the modelling of complex phenomena, e.g. shunting or multi-projection welding.

Keywords: resistance welding, FEM calculations, SORPAS software, 2D and 3D modelling

Introduction

For over 140 years, resistance welding has been used in the metal industry, particularly in the automotive industry and in the widely defined household appliances industry [1]. Although the technology has been known for many years, it continues to face new challenges, e.g. connected with new materials (advanced high strength steels {AHSS} and aluminium alloys), new solutions in terms of welding machine components (servomechanical actuators) or the (spot) welding of greater numbers of sheets (particularly complicated if sheets have different thicknesses and are made of various material grades, e.g. low-carbon steels, AHSS etc.).

The joining of thin-walled metal elements, commonly performed using resistance welding technologies, often faces problems connected with joint quality, process stability (e.g. liquid metal expulsion) or the longer life of electrodes. Simulations of welding processes offer not only the possibility of better understanding issues

dr inż. Zygmunt Mikno (PhD (DSc) Eng.), mgr inż. Szymon Kowieski (MSc Eng.)– Instytut Spawalnictwa, Department of Resistance and Friction Welding and Environmental Engineering;
Wengi Zhang (PhD (DSc) Eng.) – SWANTEC Software and Engineering ApS, Lyngby, Denmark.

concerning various materials and their weldability but also make it possible to optimise welding process parameters. In experimental conditions, obtaining such knowledge requires numerous welding and destructive tests, which are often time-consuming and expensive.

As regards welding processes, the advantages of numerical simulations (FEM calculations) include reduced costs and time of design, technological tests and process optimisation. In addition, FEM calculations make it possible to more adequately use optimisation procedures by determining the allowed field of technological parameters guaranteeing the obtainment of good quality joints.

Since the 1980s, FEM calculations have been used to model and forecast the results of welding processes in relation to specific materials and parameters [2-7]. The usability of FEM calculations has been positively verified by many theoretical and experimental tests. The positive results of the verification have resulted in the growing use of FEM calculations in practical applications, which, in turn, has entailed the growing demand for the optimisation of resistance welding processes in industry, in particular as regards the determination of the most favourable initial welding conditions.

The article presents the possibilities of performing calculations in various configurations of joints. The SWANTEC company, i.e. the developer of the SORPAS® software programme dedicated to resistance welding processes, also runs training courses concerning the operation of the programme. SORPAS® is continuously developed and improved by including new possibilities and options enabling 2D and 3D calculations [8-10]. Licensed users are provided with ready and proven computational models [10].

SORPAS® Software Programme

The Finite Element Method (FEM) in the SORPAS® software programme is used for building numerical models enabling simulations of, in particular, resistance welding processes. More than ten years of tests and industrial use as well as the continuous development of the software programme have resulted in the obtainment of the satisfactory accuracy and reliability of numerical models, data concerning materials as well as the interface and dynamics of welding equipment. The system has also been improved by activities aimed at the automation of preparatory procedures and faster simulation through a more comfortable user graphic interface and a display for the presentation of results. The coincidence of calculation results with those obtained in tests has also been confirmed in publications by welding specialists from Instytut Spawalnictwa [11-13]. The highly accurate representation of actual processes offered by SORPAS® is possible because of combined electric, thermal and mechanical calculations [10].

In the SORPAS® system, the Finite Element Method is used for creating numerical models enabling simulations of resistance welding processes. Simulations of welding processes are performed in order to determine (test) the weldability of new materials by predicting results arising from the use of specific base materials, electrode materials and welding process parameters. Simulations constitute the basis for more advanced tasks involving the optimisation and design of welding processes.

A user-friendly graphic interface presents automatic procedures making it possible to prepare input data, quicken the construction of a model, perform numerical calculations (simulations) as well as to present the results of welding processes. After performing a simulation, the software programme enables presenting the curves of dynamic process parameters in the function of time (e.g. waveforms of voltage, current, power and resistance, courses of electrode force and travel, increase in the weld nugget diameter etc.). During welding processes, the system enables the visualisation of temperature distribution, current, voltage, hardness as well as of strains and stresses in all materials (elements of a given model).

Four databases built in the SORPAS® software programme facilitate its use. The databases contain sets of information related to commonly used materials and their properties, new materials, data related to electrodes and their shapes normalised in the ISO system, data concerning workpieces (enabling preliminary design) as well as characteristics and properties of welding equipment.

Model 2D

Because of the arrangement (geometry) of two-sided spot welding, in most cases it is possible to perform simulations using the axisymmetric (2D) model. In comparison with the 3D model, the use of the simplified 2D model significantly reduces the time of calculations (calculations last on average 30 minutes instead of between ten and twenty hours) as well as significantly reduces memory-related demand for archived data.

Two-Sided Overlap Spot Welding of Two Sheets

Figure 1 presents the exemplary simulation of the two-sided overlap spot welding of two sheets. Part 1a of the figure presents the user graphic interface used for preparing input data, such as materials to be welded, electrodes and welding process parameters. Figure 1b presents a simulation report containing initial conditions and simulation results, including selected curves of process parameters and the final size of the weld nugget [10].

Two-Sided Overlap Spot Welding of Three Sheets

The SORPAS® system is used both by production companies and research centres for numerical calculations (simulations) of complex joints involving more materials than in cases of standard joints (two sheets). Figure 2 presents several examples of the welding of three sheets having various thicknesses and made of dissimilar materials in various combinations of joints and compares the results of simulation with the macrostructure of actual joints. The tests involved the use of four various steel sheets, i.e. DC06 (0.6 mm), HSLA340 (0.8 mm), DP600 (1.5 mm) and TRIP700 (1.2 mm). In all of the tests, the upper sheet was thin and made of low-carbon steel, whereas the other two sheets had various thicknesses and were made of various materials [14-15]. The FEM simulation performed using the SORPAS® software programme was used to determine the most favourable welding conditions before performing the principal technological welding tests. The actual welding conditions presented in Figure 2 (left) were compared with the results of simulation. The results of calculation (the right side of the photographs – Fig. 2) revealed
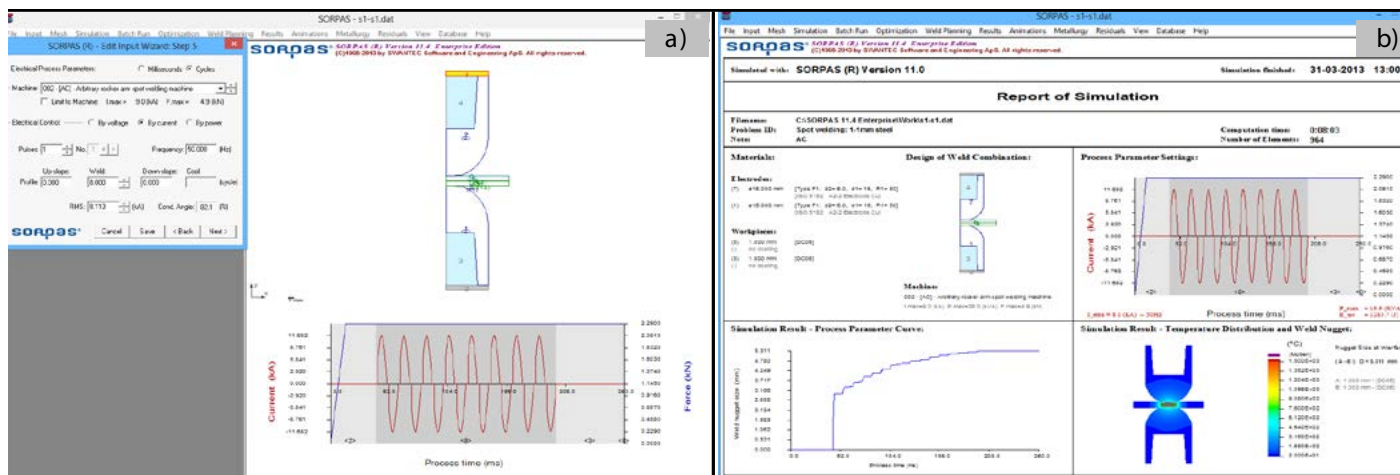

Fig. 1. Simulation of the two-sided overlap spot welding of two sheets, performed using the SORPAS® system: (a) graphic interface for preparing input data concerning materials to be welded, electrodes and welding process parameters; (b) simulation report containing pre-set (input) parameters and anticipated welding process results [10].

significant compatibility of the actual welding test results (the right side of the photographs – Fig. 2 – macrostructures).

Liquid Metal Expulsion

Expulsion during welding processes is simulated by forecasting the initial time of its occurrence and its intensity, i.e. low, medium and high. Figure 3a presents the curve of dynamic resistance with the initial time of expulsion occurrence and its intensity. Figure 3b presents the weld nugget and the area of expulsion occurrence (between the sheets).
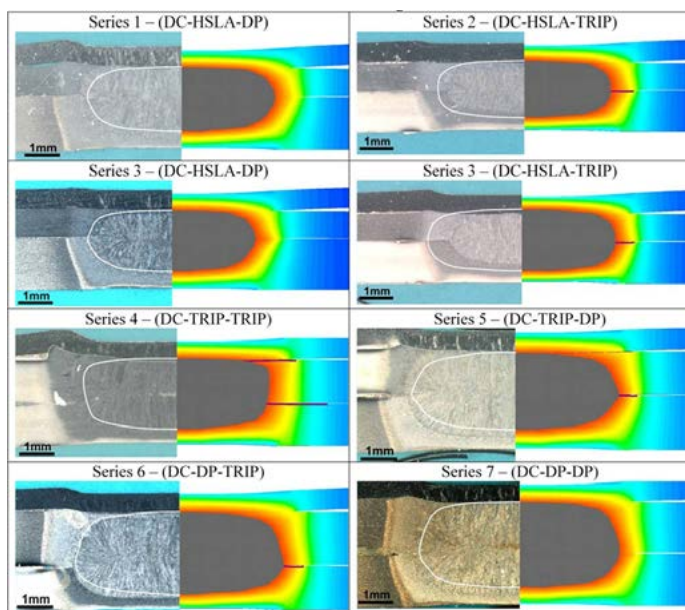
Fig. 2. Comparison of the microstructures obtained during experimental tests and in calculations (SORPAS®) related to the welding of three sheets in three combinations [14].

Examples of Resistance Welding Models

Resistance welding is performed in various configurations, e.g. as spot welding performed using electrodes having specific shapes, as projection welding, where the area of weld formation is determined by projections and as the short-circuit butt welding of rods or sections. Sorpas® enables creating models in relation to the above named methods (Fig. 4a-4c). Spot welding can be performed in the configuration of two-sided welding (Fig. 3b) or single-sided spot welding (Fig. 4a).

Process Optimisation

The results of process simulations were used to develop automated procedures enabling the optimisation of resistance welding process parameters. International standard En iso 14327 contains analyses of weldability and information concerning the optimisation of resistance welding along with two diagrams presenting
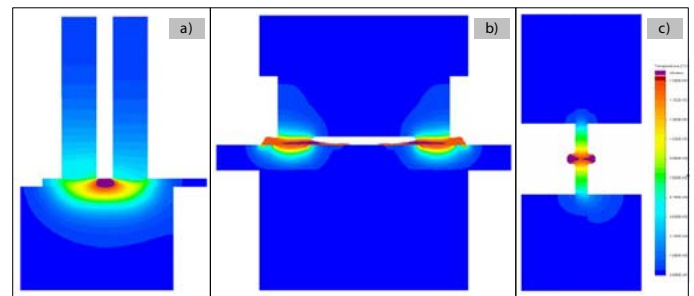
Fig. 4. Examples of resistance welding models: a) spot single-sided welding; b) projection welding of nuts; c) shirt-circuit butt welding of rods.
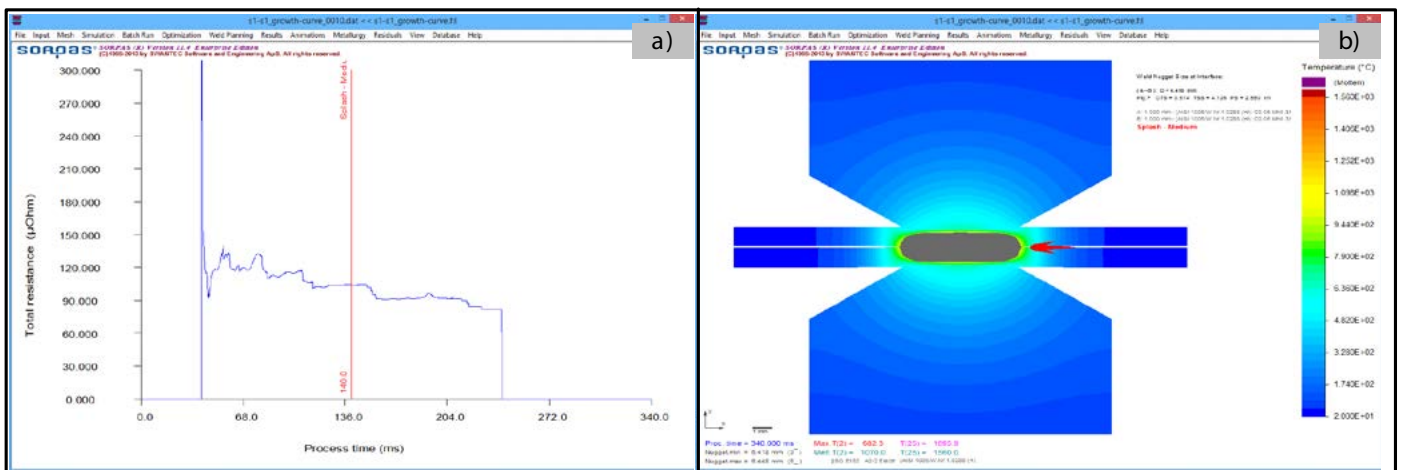
Fig. 3. Simulation of the expulsion of liquid metal from the weld nugget with the anticipated time of expulsion occurrence and intensity; (a) waveform of the selected parameter (static slope resistance) of the process with the time of expulsion initiation and formation intensity; (b) final weld nugget size with the area of expulsion formation.

the curve of weld nugget diameter increase and the determination of weldability (range of proper welding parameters). The Sorpas® system enabled the automatic determination of ranges including the limits of expected expulsion and the window of process parameters.

The curve of weld nugget diameter increase can be created by performing a series of welding tests and increasing welding current while doing so and by measuring the sizes of weld nuggets. In industrial practice, the above-presented tests are time-consuming and expensive. Because of automated procedures, Sorpas® makes it possible to perform simulations of all welds along the curve of weld formation and enables obtaining information about possible expulsion.

In a similar manner it is possible to simulate the range of parameters determining weldability, i.e. by simulating welds within the specific range of welding current and electrode force, making it possible to determine the window of welding process parameters. As regards the first range of parameter changes (window of parameters no. 1), current and welding time change, whereas electrode force stays the same. In the case of the second range of parameter changes (window of parameters no. 2), current and electrode force change, whereas welding time remains unchanged.

Figure 5 presents the optimisation of the spot welding of 1 mm thick sheets made of low-carbon steel. Figure 5a presents the simulated curve of the increase in the weld nugget diameter in the function of welding current. The weld nugget begins to form once a certain value of welding current has been exceeded and grows along increasing current. Black (square) points depict the lack of the weld or its insufficient size. Red (triangular) points represent expulsion. Green (round) points inside represent properly made welds and indicate the window of welding process parameters with the operating range of welding current. Figure 5b presents the range of weldability with current and electrode force as variable parameters and welding time as a constant parameter. Black (square) points represent the lack of the weld or its inadequate size. Red (triangular) points indicate expulsion. Green (round) points represent proper welds and, at the same time, indicate the window of proper welding parameters.

Model 3D

More complex phenomena, beyond the axisymmetric model (2D) such as the axial misalignment or the non-parallelism of electrodes, current shunting or multi-projection welding require the use of the three-dimensional (3D) model.
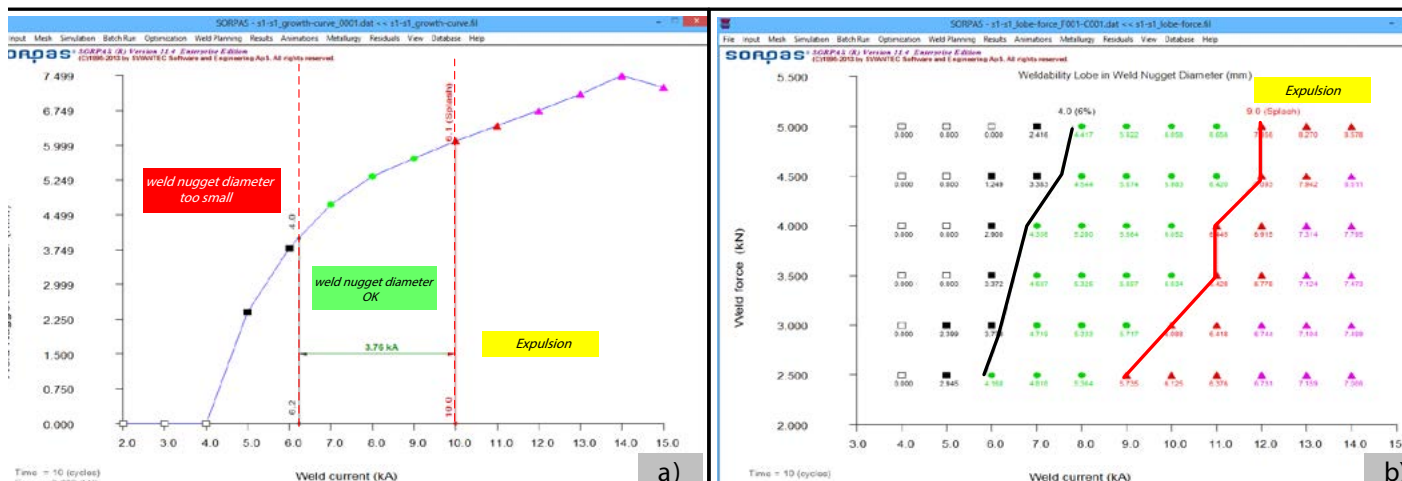

Fig. 5. Process optimisation involving the use of the SORPAS® software programme: (a) curve of the increase in the weld nugget diameter in relation to welding current; (b) range of (proper) weldability along with the window of welding process parameters.

Post-Weld Properties of Welds

The Sorpas® software programme makes it possible to calculate weld properties in relation to microstructural phase transformations or hardness distribution for typical grades of steel used, e.g. in the automotive industry. In addition, Sorpas® 3D enables simulating strength values on the basis of the weld nugget size and the anticipated hardness distribution, which in turn makes it possible to forecast the strength of welded joints (weld).

During heating, austenitisation-related calculations are based on temperature Ac1 and Ac3, regardless of the heating rate. It is assumed that entire austenitisation takes place when the maximum temperature of the process is higher than temperature Ac3. It turn it is assumed that austenitisation does not occur when the maximum temperature of the process is lower than temperature Ac1. The linear interpolation is used between temperatures Ac1 and Ac3. The austenitic transformation triggered by cooling following heating is based on critical cooling rates presented in CTT diagrams. In accordance with the formulas presented by R. Blondeau et al. [16], critical cooling rates leading to the formation of martensite, bainite and ferrite/pearlite are determined on the basis of the chemical composition. P. Maynier et al. [17] present formulas concerning the hardness of each phase in relation to the chemical composition. The value of total hardness is established on the basis of hardness values of individual phases, threated in such case as output hardness values.

Figure 6a presents the example of expected hardness distribution in the spot welded joint made of two sheets, each having a thickness of 1mm. The upper sheet was made of deep-drawing low-carbon steel DC06, whereas the lower sheet was made of dual-phase high strength steel DP600. The figure presents the

hardness of the base material around the weld nugget, the hardness following the process of austenitisation as well as the formation of subsequent phases in the weld nugget and in the heat affected zone (HAZ) during cooling. The HAZ revealed the difference between the sheets. Steel DP600 contained the significant amount of martensite, which resulted in increased hardness, whereas the HAZ of steel DC06 contained hardly any martensite, leaving the level of hardness unchanged. The weld nugget, containing phases of mixed chemical composition, contained a certain amount of martensite and was characterised by increased hardness in comparison with the hardness characterising both base materials [15].

Figure 6b presents the exemplary transverse tensile test [18]. The simulation presents the failure outside the weld nugget, which is consistent with observations during the experimental test resulting in a plug failure. Reference publications provide information concerning load curves, i.e. elongation related to tensile-shear strength tests, transverse tensile strength tests and peel strength tests. Further detailed information concerning changes in metallurgical nature as well as the forecasting of hardness and failures is presented in other publications [19].

Figure 7 presents other post-weld strength tests of joints possible to perform using the Sorpas® software programme, i.e. peeling test (Fig. 7B), static tensile strength test (Fig. 7A3) and the above named transverse tensile test
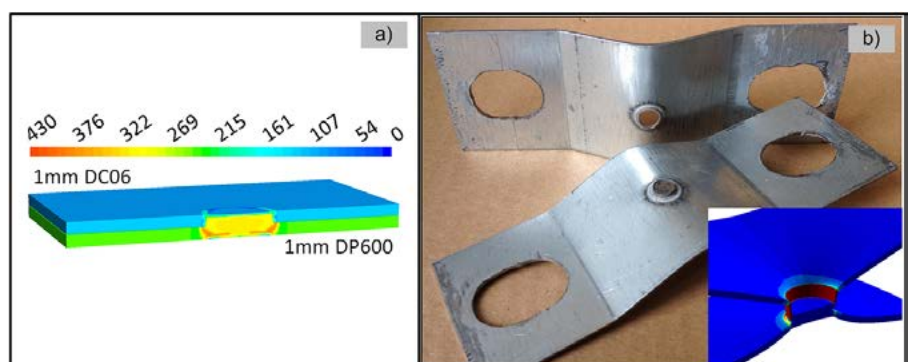

Fig. 6. Simulation (a) of hardness distribution according to the Vickers hardness test in the dissimilar spot welded joint DC06-DP600 and (b) transverse tensile strength tests of two sheets made of steel DP600 [14]. The simulation indicates the area of failure consistent with the experimentally observed plug failure [15].

leading to the plug failure of the joint (Fig. 7C1) and to the interface failure of the joint (Fig. 7C2.)

Shunting of Welding Current

The shunting of welding current is an undesired phenomenon during welding processes. The experimental tests enabled the determination of a distance between successive welds in order to minimise the undesired phenomenon [20-22]. However, the modelling and the analysis of the problem in the 3D model make it possible to deeply analyse the above-named phenomenon [23].

Figure 8 presents a welded joint containing three welds (Fig. 8A) made in the following sequence: weld no. 1 (Fig. 8B1), no. 2 (Fig. 8B3) and no. 3 (Fig. 8B2). The software programme enables calculating the principal welding current and shunting current flowing through previously made "points" (welds) as well as makes it possible to analyse the size of the weld nugget taking into account the shunting effect. This enables the adjustment of appropriately higher welding current for successively made welds in order to maintain the constant value of the weld nugget diameter.

Electrode Force

The software programme featured two built-in programme options enabling the selection of an electrode force system. Electrode force can be performed in two manners, i.e. using a standard, i.e. pneumatic or a servomechanical force system. The first manner, i.e. using pneumatic force, does not require extensive description; the setting of parameters is identical to that using a welding machine. It is necessary to take into consideration appropriate times of initial force, principal force and the separation of electrodes. The software programme automatically takes into consideration the time of delay resulting from the effect of the use of pneumatic
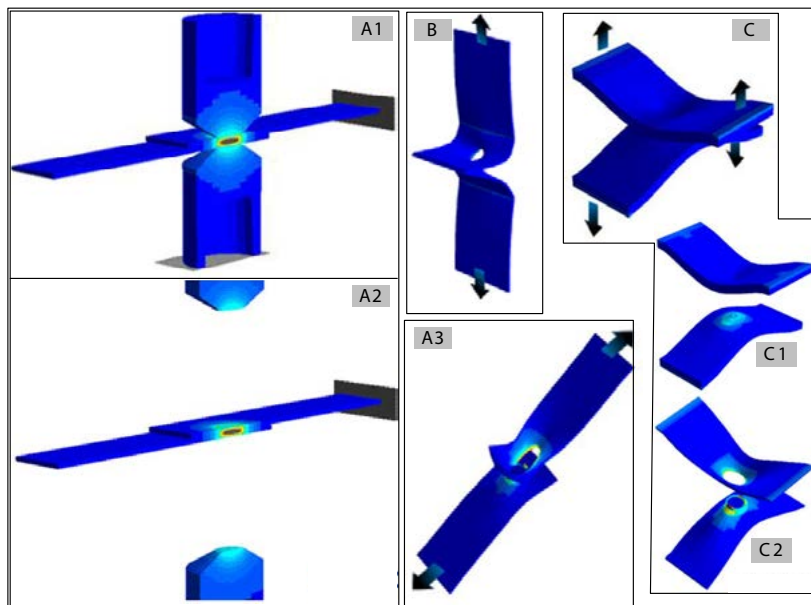

Fig. 7. Welding in the SORPAS® software programme (A1, A2). Computational strength test: A3) static tensile test, B) peeling test, C) transverse tensile test (C1 - plug failure, C2 – interface failure.
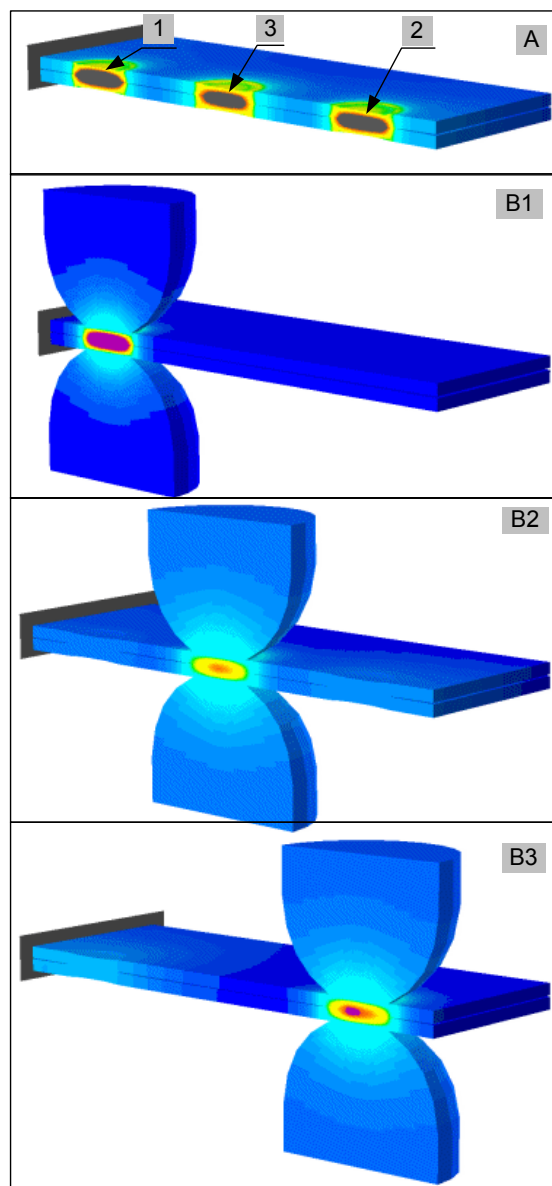

Fig. 8. Shunting of welding current for three welds (welding sequence B1, B3 and B2).

elements, i.e. primarily the size of cylinder, on the force of electrode.

The second manner involves the use of the servomechanical system of electrode force, consisting in setting the rate of electrode travel. Such a solution enables the controlled movement of electrodes. However, in such a case, the force of electrodes is the coincidence of the interaction of the electrode travel rate and the welding area heating rate resulting from the flow of current. The advantages of the system are particularly useful in projection welding, requiring the controlled movement of electrodes depending on the projection plasticisation rate. Pneumatic systems can also be used when projection welding, yet the window of parameters is very narrow if compared with that of servomechanical systems.

The exemplary course of the pre-set force in relation to the pneumatic system is presented in Figure 9a. Figure 9c presents the electrode travel rate (as regards the servomechanical system) varying depending on individual technologies. The use of force exerted by pneumatic systems

results in the, ultimately uncontrolled, movement of electrodes (Fig. 9b). In turn, the pre-set electrode travel rate enabling the controlled movement of electrodes (Fig. 9d) results in the force of electrodes (Fig. 9e).

Summary

Numerical calculations are very useful when assessing the weldability of new materials and optimising the parameters of welding processes. The Sorpas® software programme for the modelling of resistance welding processes enables performing various calculations, ranging from simple axisymmetric models (2D), e.g. spot overlap welding to advanced models, e.g. multi-projection welding or current shunting, requiring the use of the three-dimensional (3D) model.

Complex graphic options of the software programme enable the visualisation of data in the form of graphic presentations (courses/waveforms of related quantities during welding) and in the form of animated quantities subjected to analysis. The software programme
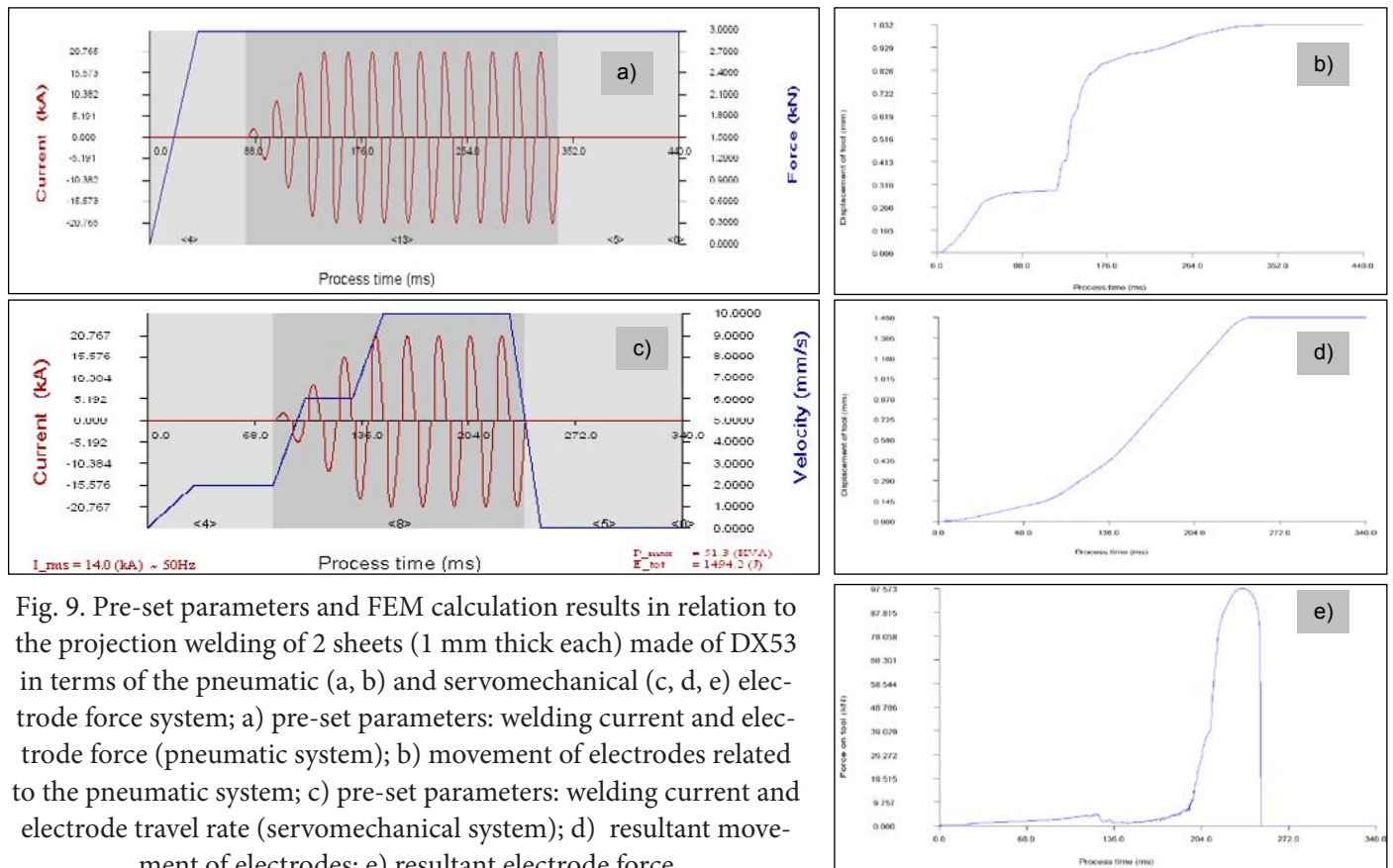
Fig. 9. Pre-set parameters and FEM calculation results in relation to the projection welding of 2 sheets (1 mm thick each) made of DX53 in terms of the pneumatic (a, b) and servomechanical (c, d, e) electrode force system; a) pre-set parameters: welding current and electrode force (pneumatic system); b) movement of electrodes related to the pneumatic system; c) pre-set parameters: welding current and electrode travel rate (servomechanical system); d) resultant movement of electrodes; e) resultant electrode force

makes an excellent tool for determining the initial welding parameters as well as enabling the in-depth analysis of phenomena taking place during resistance welding.

Workers of Instytut Spawalnictwa possess extensive experience in performing numerical calculations of welding processes using the Sorpas® software programme. Instytut collaborates with the Swantec company within the confines of joint national and international projects [24-27]. Instytut offers collaboration in the numerical modelling of resistance welding processes.

References

[1] Mikno Z., Papkala H., Piątek M.: *Zgrzewanie rezystancyjne – historia, teraźniejszość, przyszłość*. Seminar Proceedings. Paper title: *Kontrola i sterowanie w procesie zgrzewania rezystancyjnego. Jakość, rozwój, konkurencyjność i przyszłość*. March, 2004.

[2] Nied H.A.: *The Finite Element Modeling of the Resistance Spot Welding Process*. Welding Journal Research Supplement, 1984, no. 4, pp. 23-132.

[3] Cho H.S., Cho Y.J.: *A Study of the Thermal Behavior in Resistance Spot Welds*. Welding Journal Research Supplement, 1989, no. 6, pp. 236-244.

[4] Dickinson D., Tsai C., Jammal O.: *Modeling of Resistance Spot Weld Nugget Growth – Applications for the Automotive Industry*. SAE Technical Paper 900738, 1990.
http://dx.doi.org/10.4271/900738

[5] Zhang W., Hallberg H., Bay N.: *Finite Element Modeling of Spot Welding Similar and Dissimilar Metals*. 7th Int. Conf. on Computer Technology in Welding, San Francisco, USA, 1997, pp. 364-373.

[6] Zhang W., Kristensen L.: *Finite Element Modeling of Resistance Spot and Projection Welding Processes*. The 9th Int. Conf. on Computer Technology in Welding, Detroit, Michigan, 1999, pp. 15-23.

[7] Zhang W.: *Design and Implementation of Software for Resistance Welding Process Simulations*. SAE Technical Paper 2003-01-0978, 2003
http://dx.doi.org/10.4271/2003-01-0978

[8] Zhang W.: *New Developments and Challenges in Simulation and Optimization of Resistance Welding*. Proceedings of the 4th International Seminar on Advances in Resistance Welding. 15 November 2006, Wels, Austria, pp. 101-114.

[9] Zhang W.: *Recent Developments and Future Outlook for Simulation and Optimization of Resistance Spot Welding Processes*. Proceedings of the 5th International Seminar on Advances in Resistance Welding, 24-26 September 2008, Toronto, Canada, pp. 269-276.

[10] http://www.swantec.com

[11] Mikno Z., Bartnik Z., Derlukiewicz W., Kowieski Sz.: *Zgrzewanie garbowe w obliczeniach metodą elementów skończonych*. Przegląd Spawalnictwa, 2013, no. 11, pp. 64-70.

[12] Mikno Z., Bartnik Z.: *Zgrzewanie rezystancyjne doczołowe zwarciowe w obliczeniach MES materiałów jednoimiennych (part 01)*. Przegląd Spawalnictwa, 2015, no. 3, pp.14-21.

[13] Mikno Z., Bartnik Z.: *Heating of electrodes during spot resistance welding in FEM calculations*. Archives of Civil and Mechanical Engineering, 2016, vol 16, no. 1, pp. 86-100.
http://dx.doi.org/10.1016/j.acme.2015.09.005

[14] Nielsen C. V., Friis K. S., Zhang W., Bay N.: *Three-Sheet Spot Welding of Advanced High-Strength Steels*. Welding Journal Research Supplement, 2011, vol. 90 (2), pp. 32-40.

[15] Bennedbaek Rune A.K., Nielsen Chris V., Zhang W.: *Latest Developments in Simulation*

and Optimization of Resistance Welding Processes. Biuletyn Instytutu Spawalnictwa, 2015, nr 6, pp. 31-37
http://dx.doi.org/10.17729/ebis.2016.5/4

[16] Blondeau R., Maynier P., Dollet J., Vieillard-Baron B.: *Prévision de la dureté de la résistance et de la limite d'elasticité des aciers au carbone et faiblement alliés d'après leur composition et leur traitement thermique.* Mémoires Scientifiques, Revue Métallurgie, 1975, pp. 759-769.

[17] Maynier P., Jungmann B., Dollet J.: *Creusot-Loire system for the prediction of the mechanical properties of low alloy steel products.* Hardenability Concepts with Applications to Steels. The Metallurgical Society of AIME Heat Treatment Committee American Society for Metals Activity on Phase Transformations, 1978, pp. 518-545.

[18] Nielsen C.V., Bennedbæk R.A.K., Larsen M.B., Bay N., Chergui A., Zhang W., Martins P.A.F.: *Experimental and Simulated Strength of Spot Welds*. The 8th International Seminar on Advances in Resistance Welding, Baveno, Italy, 2014, pp. 161-172.

[19] Nielsen C.V., Martins P.A.F., Zhang W., Bay N.: *Numerical methods in simulation of resistance welding.* VI International Conference on Computational Methods for Coupled Problems in Science and Engineering, 2015, pp. 322-333.

[20] Papkala H.: *Zgrzewanie oporowe metali.* Wydawnictwo KaBe, Krosno, 2003.

[21] Papkala H.: Wytyczne doboru właściwej technologii zgrzewania punktowego, garbowego i liniowego blach w oparciu o własności fizyczne metali. Instytut Spawalnictwa Gliwice, 1990.

[22] Pilarczyk J. (ed.): Poradnik Inżyniera, Spawalnictwo. vol 1, 2, WNT Warszawa 2005.

[23] Li Y. B., Wang, B., Shen Q., Lou M., Zhang H.: *Shunting effect in resistance spot welding steels. Part 2: theoretical analysis.* Welding Journal, 2013, pp. 231-238.

[24] Mikno Z., Kowieski Sz.: International Project, 6th Framework Programme: *FleXible Production Experts for reconfigurable assembly technology – XPRESS* (2007-2011).

[25] Mikno Z., Kowieski Sz.: Invertigation project no. N N501 196940: *Numeryczne i eksperymentalne badania porównawcze zgrzewania garbowego z zastosowaniem pneumatycznego i serwomechanicznego docisku elektrod* (2011-2013).

[26] Mikno Z., Kowieski Sz.: Investigation Project INWELD under the 3rd Contest of Applied Research Programme: *Opracowanie innowacyjnej wysokosprawnej zgrzewarki kompaktowej o podwyższonej częstotliwości*, PBS3/B4/12/2015, 2015-2017.

[27] Mikno Z., Kowieski Sz.: Investigation Project under TANGO 1 Competition: *Innowacyjna metoda sterowania serwomechanicznym systemem docisku w technikach łączenia cienkościennych elementów metalowych*, TANGO1/267374/NCBR/2015, 2015-2017.

Monika Restecka, Robert Jachym

IT Systems Used for Welding Process Simulations and Simulators of Thermal-Strain Cycles

Abstract: The first part of the article presents an overview of software programmes assisting welding-related engineering works as well as discusses possibilities and advantages related to the use of such programmes. Software programmes available today enable, among other things, the monitoring of welding processes, calculations of temperature distribution, the determination of mechanical and plastic properties, simulations of distributions of residual stresses as well as simulations of transformations triggered by welding thermal cycles. The second part of the article is dedicated to simulators enabling physical simulations of welding processes as well as describes principles of simulations tests and presents advantages related to the use of this technique.

Keywords: welding-related software, monitoring of welding processes, welding simulations,

Introduction

The appropriate selection of a welding procedure constitutes a key factor affecting the quality of manufacturing processes used when making any welded structure. In order to properly adjust welding process parameters, it is necessary to perform specific tests and examinations, the results of which can be used in practice. Some of these tests are relatively simple and inexpensive; others can turn out costly and time-consuming. For this reason, tests concerning welding procedures are increasingly based on the modelling of processes. The purpose of modelling is to reduce costs and minimise the risk of an error which may occur during actual welding tests [7].

Undesirable results of welding processes are residual stresses and welding strains which, when significantly exceeded, can lead to the rejection of a given structure as its dimensions and shape fail to satisfy design assumptions. Measuring the values of stresses present in welded structures is a complicated process requiring appropriate skills and equipment. In addition, welding strains are strictly related to an adopted welding procedure. When designing, it is necessary to anticipate and prevent the possible formation of strains. There is demand for complex and accurate tools for simulating welding processes and enabling calculations of temperature distribution as well as the distribution of residual stresses present in elements.

mgr inż. Monika Restecka (MSc Eng.) – Instytut Spawalnictwa, Marketing and Scientific Information Department; dr inż. Robert Jachym (PhD (DSc) Eng.) – Instytut Spawalnictwa, Testing of Materials Weldability and Welded Constructions Department

Tools in demand should also be able to simulate transformations triggered by welding thermal cycles, identify microstructural changes as well as determine plastic and mechanical properties. In some cases, the above named simulations utilise IT systems. Recent years have also seen the growing popularity of physical simulations used in welding tests, heat treatment, hot plastic working and even in relation to the continuous casting of steel. A physical simulation consists in representing a given technological process in a relatively small-sized material specimen. In relation to proper simulation, it is important that all major factors characterising processes (i.e. temperature, strains and stresses with appropriate gradients) should be represented in real time, i.e. at the time of the process. The simulations mentioned above are performed using simulators of thermal-strain cycles [4, 7, 9].

CAE Software

Cae (Computer Aided Engineering) software includes a group of programmes assisting engineering works at the first stages of product development, i.e. during design and structural works. Such programmes can work independently or be supported by cad software programmes (enabling engineering analyses of designed elements). Without the numerical modelling of geometrical, material and dynamic features, the adjustment of optimum parameters related to a given method could be far more difficult and, in some cases, even impossible. The accuracy of individual analyses directly affects the quality of welds. Sadly, the above named programmes can only be used for making prototypes. When using cae software, it is very important to properly verify a model created against an actual element, which entails the necessity of updating relevant information and optimising the structure. The cae-related principle of operation can be described as composed of three stages, i.e. analysis, calculations and the interpretation of obtained results. Cae

programmes can be used to perform kinematic and dynamic analysis of mechanisms, thermal and flow analysis involving the Finite Element Method (fem) and dynamic and static analysis of components (also supported by fem). Additional advantages of cae include the possibility of performing simulations as regards the making of structures and simulations of mechanical phenomena [8, 9].

Examples of IT Systems Used for Simulations of Welding Processes

The use of cae programmes makes it possible to simulate almost any technological process, including welding. Welding is a complex process, in which the quality of obtained joints is not easy to verify. Quite often, quality-related requirements are high. In such cases, the use of simulation in the virtual environment significantly reduces production costs. This fact is one of the main reasons for the growing popularity of numerical methods in recent years. In some cases, simulations may even replace experimental tests, yet simulation results do happen to be encumbered with errors. This is so because actual production conditions often differ from virtual ones and differences related to, e.g., physical phenomena, not always fully predictable during welding, are too large. In order to more precisely take into consideration all factors, it is necessary to perform simulations in several iterations. In this way, it is possible to reduce the occurrence of potential errors and differences between a model created in the programme environment and an actual element. Presented below are examples of cae systems used when simulating welding processes [9].

Welding Simulation Suite

Welding Simulation Suite (Fig. 1) developed by Esi Group is a package composed of programmes calculating the effect of heat on the structure during and at the end of a simulated welding process. Simulations take into consideration changes in

shapes, thermal strains, hardness, phase composition as well as plastic stresses and strains. A factor distinguishing the package is the possibility of simulating multi-run welding and pressure welding. Software programmes making up the package are the following [12]:

– Visual-weld – programme used in the Visual environment, enabling simulations of single and multi-run welding processes involving various types of materials, including steel, aluminium as well as other metals and alloys,

– Weld Planner – programme mainly used for simulating the welding of large-sized elements. The programme enables performing very fast analyses utilising displacement engineering based on simulations of strains. Time required to perform such analyses may amount to a day,

– Pam-assembly – software programme, similar to Weld Planner, dedicated to simulating the welding of large-sized elements using the local-global approach. The programme is based on models calculated using Sysweld and utilises such models to calculate structural strains taking into consideration physical phenomena.
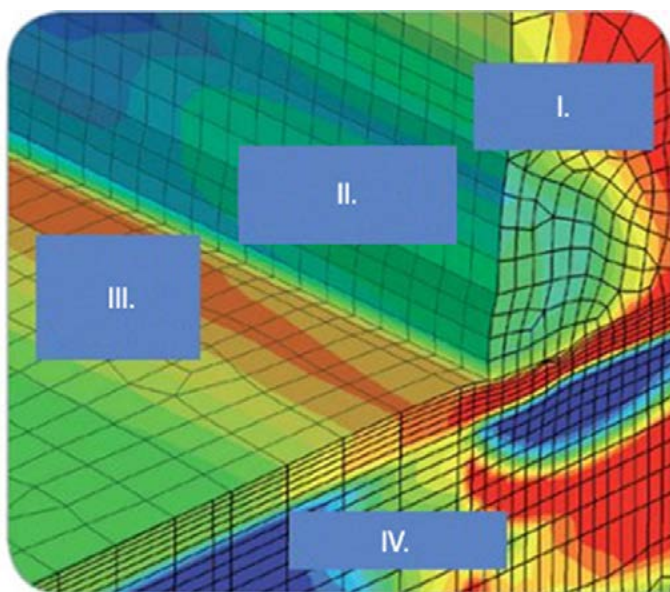
Fig. 1. Exemplary simulations of welding processes using FEM of an element made of various materials (I – element made of nickel alloy Inconel, II – Inconel type filler metal, III – layer of the plated coating made of stainless austenitic steel, IV – structural steel) [12]

SYSWELD

Another element of the Welding Simulation Suite package is Sysweld, an advanced programme for simulating a range of welding processes, including the three-dimensional simulation of welding procedures and of the heat treatment of metals. The software enables the user to perform thermo-metallurgical, electrokinetic-thermo-metallurgical, diffusive and many other analyses. Results of analyses and calculations enable, among others, determining the effect of a selected heat treatment, material, hardening process conditions etc. Calculations performed by the system utilise the Finite Element Method. Sysweld is available in two basic versions:

– heat treatment module (version contains issues related to hardening, tempering and chemical processing, i.e. nitriding and carburising),
– welding module (version contains all principal welding methods).

In order to minimise strains, by selecting an appropriate welding procedure, the software can be used for the optimisation of welding processes. In addition, the programme can import data from CAD systems, which quickens analyses. Although a major disadvantage of the software is its high price, Sysweld remains one of the best available tools for forecasting welding stresses and strains [9, 13].

ANSYS

Ansys is one of the most popular systems used in widely defined strength, thermal and electromagnetic analyses as well as in analyses of fluid mechanics. The software enables the modelling and simulations related to structural and fluid mechanics as well as allied simulations. The programme can be used to perform linear and non-linear calculations and optimisation. The Finite Element Method is used when modelling problems concerning statics, dynamics, fields of temperature, mechanics of fluids, electromagnetic fields, diffusion electrostatics and piezoelectricity. Figure 2 presents the exemplary

visualisation of test results utilising the Ansys software programme [1, 9].

Fig. 2. Exemplary simulation result obtained using Ansys [14]

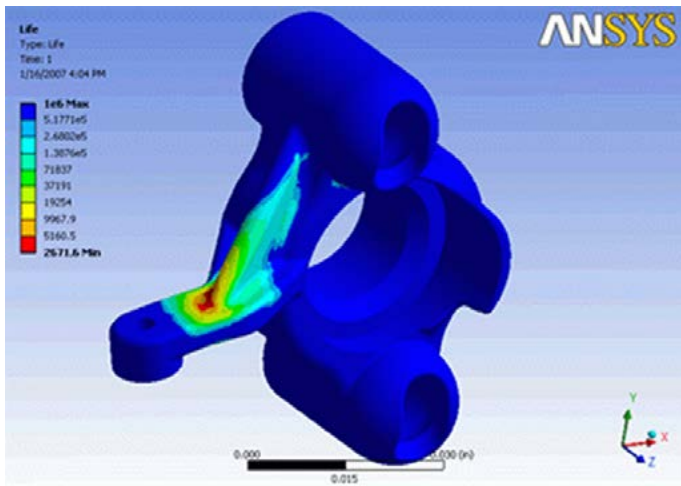Although Ansys does not have an environment dedicated to the modelling and simulation of welded joints, the programme enables the development of models taking into consideration thermal and mechanical processes. Because of this functionality, in industry, Ansys is used for simulating welding processes. One of the examples of such an application includes simulations performed when manufacturing the Audi A8 [1, 9].

ABAQUS

The software programme is used for machinery and structural strength-related calculations. Among other things, the programme enables creating models assisting design and manufacturing. It is also possible to simulate the non-linear problems related to the mechanics of solids and fluids. A model to be simulated can be defined from scratch, e.g. using the Femap programme, dedicated to modelling any complicated structure with any number of details and any level of detail, also including boundary and force conditions (if any). A model prepared in the above-presented manner can be

imported to the Abaqus software programme. Related analyses are based on thermo-mechanical procedures (Fig. 3). The ability to predict stresses generated in the material during welding enables forecasting the ultimate shape of the product after the completion of the process as well as makes it possible to assess the effect of stresses on the structure [7].

To this end, it is necessary to perform thermal analysis combined with stress analysis. Similar to other applications, it takes considerable time to become familiar with the software programme. In addition, entering data and the simulation process itself are also time-consuming. However, as a result of the increased accuracy of the model and because of the appropriate distribution of the model into finite elements, the accuracy of obtained results is high [7].

MSC MARC

The Msc Marc software programme is used for performing effective simulations of welding processes. The programme requires the use of specialist user procedures. The modelling of a heat source can be performed by using the Uwedflux module. Welding processes can be modelled for flat problems (2D), plates, axial symmetry and 3D problems. The programme enables performing thermal and thermo-mechanical analyses. The possibility of modifying the solver by entering user procedures makes the Msc Marc programme a tool characterised
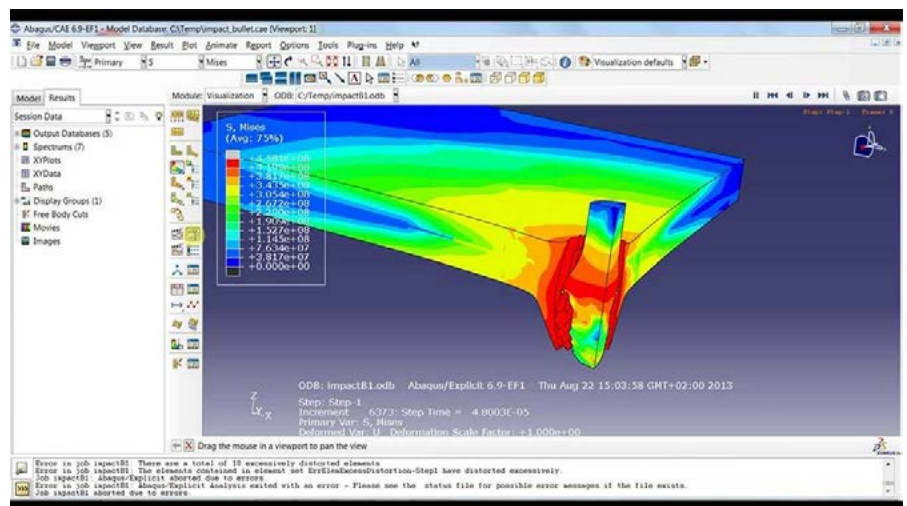

Fig. 3. Window of the Abaqus software programme [7]

by extensive computational possibilities. The software programme also enables performing verification calculations and simulations of complex non-linear problems, e.g. multiple fillet welds. It should be noted that Msc Marc requires considerable computational powers [5].

Simulators of Thermal-Strain Cycles

The use of simulation in tests of technological processes date back to 1949, i.e. the construction of the first simulator of thermal cycles used for current flow-based resistance heating of specimens [6]. The first simulator of thermal-strain cycles was built by the American company Duffers Scientific Inc. (presently Dynamic Systems Inc.). The device was equipped with a pneumatic system of load application. After subsequent modifications the system was provided with a hydraulic servomechanical system making it possible to perform complex thermomechanical tests. Today, Dynamic Systems Inc. produce computer-controlled complex simulators named Gleeble, used in various areas of research including welding engineering, materials engineering, hot plastic working and continuous casting of metals.

Instytut Spawalnictwa also developed (in the 1960s) a simulator of welding thermal cycles based on the resistance heating of a specimen. In the years to come, the simulator was gradually modified and improved (Fig. 4).

Structural changes taking place in the Heat Affected Zone (HAZ) significantly affect the properties of the above named welded joint area, particularly its hardness and related formability, toughness (characterising brittle crack resistance) and susceptibility to hot, cold and annealing crack formation. The manner in which steel responds to a welding thermal cycle constitutes an important factor affecting the steel weldability. In order to test the effect of welding thermal cycles on structural transformations and resultant properties, small specimens are subjected to thermal cycles simulating courses of temperature changes in various HAZ

areas (Fig. 5). Such tests are performed using dedicated devices, i.e. simulators of thermal-strain cycles [2].

Worldwide-manufactured simulators of thermal-strain cycles are characterised by various modes of the heating (induction, resistance) and tensioning of specimens (hydraulic, magnetic or mechanical systems) (Table 1).

Simulator of Thermal-Strain Cycles: Gleeble 3500

Instytut Spawalnictwa has multi-annual experience of using the above-presented simulation techniques in terms of weldability testing. Recently, Instytut's laboratories have acquired a Gleeble 3500 (DSI) (Fig. 6) modern simulator

Fig. 4. Main view of the simulator of thermal-strain cycles produced by Instytut Spawalnictwa (version from 1996)
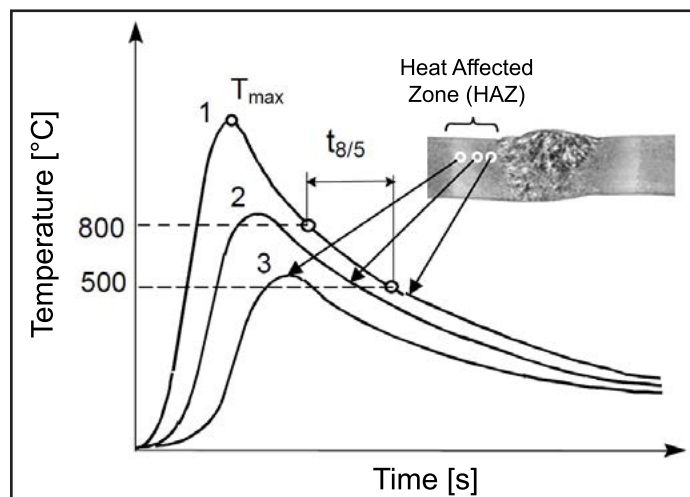
Fig. 5. Welding thermal cycles at various distances from the weld fusion zone [2]

Table 1. Selected specifications of Gleeble, Thermorestor, Smitweld and Instytut Spawalnictwa's simulators of thermal-strain cycles [3, 10]

Name	Specimen heating mode	Specimen cooling mode	Technical possibilities of control
Gleeble	Joule heat	Controlled cooling in jaws cooled by water	$T = f(t)$ $P = f(t)$ $P = f(\varepsilon)$
Thermorestor	induction	Cooling gas (Ar, He) injection	$T = f(t)$ $P = f(t)$ $P = f(\varepsilon)$
Smitweld	Joule heat	Controlled cooling in jaws cooled by water	$T = f(t)$ $P = f(t)$
Simulator IS (version from 1996)	Joule heat	Controlled cooling in jaws cooled by water	$T = f(t)$ $P = f(t)$ $P = f(\varepsilon)$

Designations: P – tensile force, kN; ε – strain, %; t – testing time, s;

for physical simulations of joining processes, replacing the previously used simulator made by Instytut Spawalnictwa. The simulator enables the modelling of thermo-mechanical conditions occurring in the most unfavourable area of a welded joint, i.e. HAZ. The primary specifications of the device are the following:

– hydraulic system for subjecting specimens to stresses and strains,
– maximum load force of 98 kN,
– maximum rate of moving jaw displacement of 1 m/second,
– maximum cycle temperature:
  ∘ 1350°C – Ni-NiCr thermocouple,
  ∘ 1750°C – Pt-PtRh thermocouple.

Among other things, the device makes it possible to simulate welding processes, test mechanical properties of steels at higher temperatures, simulate the effect of welding thermal cycles on the microstructure and properties of steels (HV, KV) and determine the susceptibility of materials to hot, cold and annealing cracking. The device has also been equipped with a specially designed additional working chamber making it possible to perform tests focused on resistance to cold cracking under hydrogen. During tests, specimens can be subjected to any thermo-mechanical conditions and, simultaneously, to saturation with hydrogen.

Fig. 6. Gleeble 3500 series simulator for physical simulations of welding processes: a) main view, b) working chamber

Summary

The quality of welding processes is of crucial importance. The key factor affecting the quality of processes used when making welded structures is the appropriate selection of the welding procedure. In order to properly adjust welding process parameters, it is necessary to perf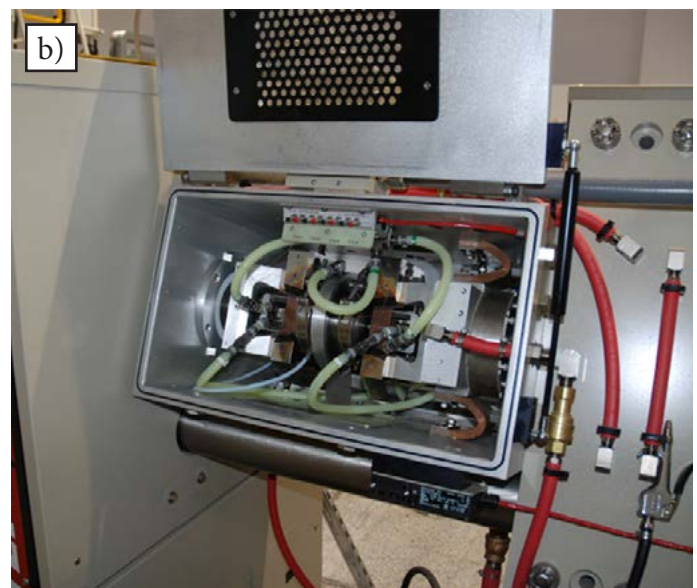orm specific tests and examinations, results of which can be put in practice. To this end, it is possible to use a wide range of software programmes enabling the monitoring of welding processes, calculations of temperature distribution, the determination of microstructural transformations, the identification of plastic and mechanical properties, simulations of distributions of residual stresses in elements, and simulations of transformations induced by welding thermal cycles. The adjustment of appropriate parameters is also possible by using physical simulations of welding processes performed by simulators of thermal and strain cycles; the simulators are becoming increasingly popular in tests focused on the weldability of steels. In specimens characterised by relatively small volumes, the above named simulations enable the formation of areas having homogenous microstructures and corresponding to particular areas in the HAZ of welded joints, thus making it possible to perform a variety of tests. Based on obtained results, it is possible to forecast the effect of welding conditions on HAZ properties without performing laborious and expensive tests involving actual welded joints. The possibility of subjecting specimens to stresses and strains at any moment of the thermal cycle makes the simulator a very useful tool when testing steels for their susceptibility to developing various cracks.

References

[1] Akaike S.: *Denso Corporation standarizes on Ansys structural software to expedite global product development*. Ansys Advantage, vol. 9, 2015.

[2] Brózda J.: *Stale konstrukcyjne i ich spawalność*. Instytut Spawalnictwa, Gliwice, 2009.

[3] Brózda J., Malczewski K., Zeman M.: *Symulator cykli cieplnych i odkształceniowych i jego wykorzystanie w badaniach nad spawalnością stali*. 3rd Scientific-Technical Seminar "Badania materiałowe na potrzeby elektrowni i przemysłu energetycznego", Zakopane, 19-21 June 1996 r.

[4] Ferguson H.S.: *Fundamentals of Physical Simulation*. [in]: Proceedings of the International Symposium on Physical Simulation, TU Delft, The Netherlands, 1992, pp. 1-21.

[5] Flis L.: *Wykorzystanie Msc Marc/Mentat do symulowania spawania cienkich płyt*. Zeszyty Naukowe Akademii Marynarki Wojennej, 2006.

[6] Nippes E.F., Savage W. F.: *Tests of Specimens Simulating Weld Heat-Affected Zones*. Welding Journal, 28 (1949), Res Suppl, pp. 599-616.

[7] Pakos R., Szymczak M.: *Przegląd programów komputerowych do przewidywania odkształceń i symulacji procesów spawalniczych na wczesnych etapach produkcji*. Przegląd Spawalnictwa, 2010, no. 3.

[8] Ralston D., Munton T.: *Computer Integrated Manufacturing*. Computer–Aided Engineering Journal, 2009, vol. 4, no. 4, pp. 167-174
http://dx.doi.org/10.1049/cae.1987.0039

[9] Restecka M.: *IT Systems in Aid of Welding Processes*. Biuletyn Instytutu Spawalnictwa, 2015, no. 3, pp. 6-20
http://dx.doi.org/10.17729/ebis.2015.3/1

[10] Samardžić I., Stoić A., Kozak D., Kladaric I., Dunđer M.: *Application of Weld Thermal Cycle Simulator in Manufacturing Engineering*. Journal of Manufacturing and Industrial Engineering, 2013, vol 12, no. 1-2, pp. 7-11.
http://dx.doi.org/10.12776/mie.v12i1-2.177

[11] Stachów J.: *Przełomowy rok w branży motoryzacyjnej*. KS Automotive, 2013.

[12] http://www.cim-mes.com.pl

[13] http://www.e-spawalnik.pl

[14] http://www.directindustry.com

Eugeniusz Turyk

Qualifying the Technology of the Aluminothermic Welding of Tramway Rails on the Basis of Quality Assurance System Requirements in Welding Engineering

---

Abstract: The article discusses the issue of demonstrating the correctness of a technology dedicated to the aluminothermic welding of tramway rails, recommends that the technology be qualified in accordance with standard Pn-en iso 15613:2006 concerning the pre-production testing of technologies used when welding atypical joints, proposes the scope of qualification tests and presents test results concerning defective welded joints.

Keywords: aluminothermic welding, welding of tramway rails, atypical joints

---

Introduction

According to Iso 9000 series standards, welding is regarded as a special process, the control of which significantly affects product quality and the results of which cannot be entirely verified by subsequent tests, inspections or examinations [1]. Welding-related quality assurance is addressed by the Pn-en iso 3834 series of standards, supplementing the Iso 9000 series of standards or used as the basis for documenting quality systems including elements directly related to welding processes. Welding is used when making jointless railway or tramway tracks, i.e. tracks where rails are joined permanently using mma welding, pressure welding or aluminothermic welding.

Quality assurance system requirements related to welding engineering, including the aluminothermic welding of railway rails regarded as a special process are addressed by a number of publications, e.g. [2, 3]. In railway

engineering, the aluminothermic welding of rails is governed by standards related to the approval of aluminothermic welding processes (Pn-en 14730-1+A1:2010 [4]), qualifications of welders performing aluminothermic welding as well as the approval of contractors and the acceptance of welds (Pn-en 14730-2:2006 [5]). Requirements concerning rail welding technologies and tests of welded joints contain a number of documents, including specifications related to the aluminothermic welding of railway rails [6] and defectoscopic tests [7] developed by the Polish Railways, *Technical Conditions of the Making and Acceptance of Rail Joints Welded Using the SoWoS-P Method* developed by the Rolf Plötz company [8] and DB Rail 824 series guidelines concerning the making of railway tracks [9, 10].

The documents named above concern the joining of railway rails, different from tramway rails in terms of shapes. There are no regulations

---

dr hab. inż. Eugeniusz Turyk (PhD (DSc) hab. Eng.), Professor extraordinary at Instytut Spawalnictwa; Welding Technologies Department

concerning the qualification of the alumino-
thermic welding of tramway rails as in the case
described in publications [4, 6]. In addition,
requirements concerning the qualification of
the aluminothermic welding of tramway rails
are not always defined by the customer. How-
ever, due to the responsibility of rail joints it
is necessary that the above-named technolo-
gy be qualified (or in other words approved,
accepted or verified) by the manufacturer. For
this reason, the article discusses the possibili-
ty of qualifying the aluminothermic welding
of tramway rails on the basis of existing weld-
ing-related standards.

Qualifying the Technology of the Aluminothermic Welding of Tramway Rails

In welding procedure specifications, contrac-
tors performing the aluminothermic welding of
tramway rails refer to the SoWoS welding meth-
od or the Srz LP method used when welding
tram dock rails [11]. An exemplary cross-sec-
tion of a 60R2 tramway rail and an alumino-
thermic welded joint are presented in Figure 1
and 2.

Defects troubling the operation of tracks re-
lated to improperly performed aluminothermic
welding include horizontal cracks located in the
rail web (Fig. 3) and transverse cracks located
in a place close to the normal cross-section of
a rail (e.g. a fatigue crack in the vertical plane
of a rail initiated at a gas pore [13÷16]). Cracks
pose hazards to safe transport, require the clo-
sure of a track, the removal of a rail fragment
containing a defective joint and the placement
of a new rail fragment.

Aluminothermic welding-related potential
reasons for crack generation include unfavour-
able stresses (cracks occur in the zone of the
highest tensile welding stresses in the rail web;
Fig. 4) [17-19] as well as the failure to satisfy the
technological conditions of welding processes:
– overly short heating time favouring weld po-
  rosity formation [19] (porosity mentioned

Fig. 1. Shape and primary dimensions of a cross-section
of the 60R2 dock rail [12]
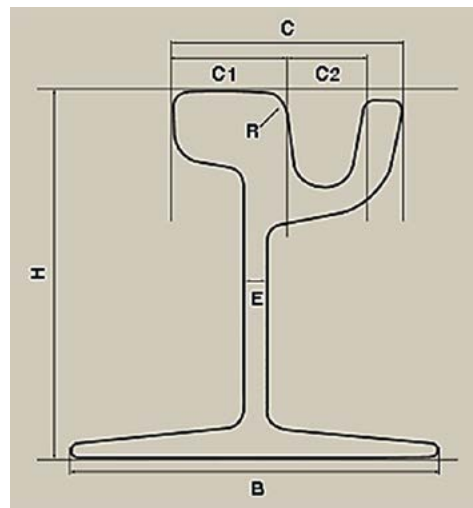
H = 180 mm
B = 180 mm
C = 113 mm
C1 = 55,8 mm
C2 = 36,3 mm
E = 12 mm
R = 13 mm

Fig. 2. Aluminothermic welded joints of 60R2 rails
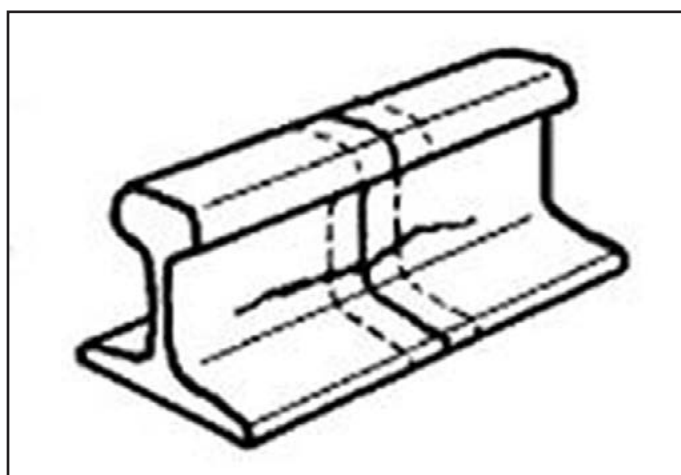
Fig. 3. Schematically presented rail web crack
in the welded joint area [13, 14]

in the publication was referred to as micro-
-shrinkages formed in welds),
– overly low temperature of heating applied
  to rail ends [20],
– asymmetric (non-uniform) heating of rail
  ends,
– overly short gap between rails being joined
  [20].

Fig. 4. Distribution of stresses in a aluminothermic-
-welded joint of railway rails [17, 19]

In order for the manufacturer to demonstrate the correctness of an aluminothermic welding technology applied when joining tramway rails, it is necessary to qualify the above-named technology. In accordance with requirements concerning quality assurance in welding engineering (entire or standard quality-related requirements according to item 10.3 of Pn-en iso 3834-2 and Pn-en iso 3834-3 respectively [21, 22]), welding technologies should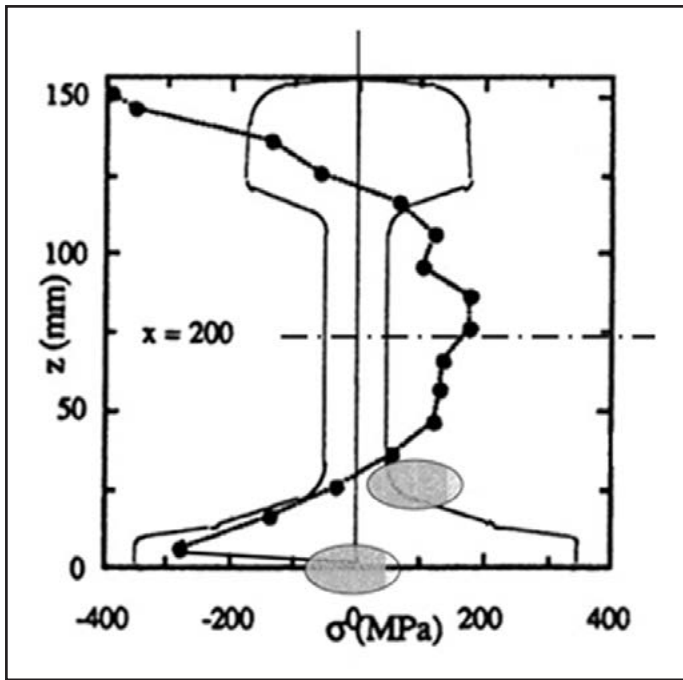 be qualified before the commencement of production. Presently, as regards aluminothermic welding, there are no iso documents necessary to confirm conformity with the above-presented quality requirements (Pn-en iso 3834-5, Table 10 *Other fusion welding processes* [23]). Hence the question, whether due to the lack of special standards similar to Pn-en 14730-1 as well as because of the lack of regulations concerning the welding of tramway rails, the contractor has the possibility of demonstrating the correctness of the aluminothermic welding technology applied for the joining of tramway rails by an independent certification body, and if so, on what basis.

On the basis of the overview of possible variants concerning the qualification of welding technologies it is possible to propose the qualification of a technology used for the aluminothermic welding of tramway rails according to Pn-en iso 15613:2006 [24] concerning the so-called pre-production testing of technologies used for welding atypical joints including additional requirements (if any) specified by the investor or inspection personnel (according to Pn-en iso 3834-2, item 10.3 stating that *Qualification methods should be consistent with related product requirements or specification arrangements*). The process of welding procedure qualification includes four major stages, i.e. the establishment of the scope and conditions of qualification, the making of a test joint, the examination of a test joint and the development of qualification documents [25, 26].

Test joints should be welded by a welder holding a valid licence to perform aluminothermic welding using a method subject to qualification. Both the welding and testing of test joints should be performed in the presence of a so-called examiner, i.e. the representative of a certification body (so-called examination body) performing the process of welding procedure qualification (analogous requirement is formulated in standard Pn-en iso 15614-1 concerning the qualification of a technology used for the arc welding of steel). Test joint examinations should include at least:

– non-destructive tests: visual tests and ultrasonic tests,
– destructive tests: macroscopic tests, hardness tests, microscopic tests, the chemical analysis of weld metal in the zone of the rail head, web and foot as well as the chemical analysis of rail material. The scope of destructive tests can also include transverse tensile tests of welded joints performed on specimens sampled from the foot, web and head as well as impact strength tests of the weld and heat affected zone.

The acceptance criteria concerning test results should be established before the commencement of the process of welding procedure

qualification. In relation to non-destructive tests it is possible to rely on requirements of Polish Railways PKP [7] and on the technical conditions related to the making and acceptance of rail joints [8]. In terms of macroscopic tests it should be assumed that cracks and incomplete fusions are unacceptable and it is necessary to specify the acceptable size and density of porosity and solid inclusions. The acceptance criteria concerning test results related to mechanical properties can be based on the requirements of PN-EN ISO 15614-1.

An acceptable test result enables the examination body to provide the manufacturer with a Welding Procedure Qualification Record (WPQR) based on a pre-production test according to PN-EN ISO 15613:2006. The record specifies the scope of qualification, conditions concerning the making of a test joint and test results. If a test result is unacceptable, the examination body provides the manufacturer with a report concerning the examination of a test joint. The report presents the conditions related to the making of the test joint and the results of performed tests and well as test reports (if any). The above named information enables the manufacturer to take corrective and preventive actions aimed to assure the correctness of the aluminothermic welding process and the making of a test joint satisfying qualification-related requirements.

Presented below are examples of joints failing to meet qualification requirements. The failure to satisfy the above named requirements was confirmed by tests performed on rail fragments containing fatigue cracks.

Examples of Welding Imperfections in Aluminothermic Welded Joints of Tramway Rails

In order to determine possible reasons for fatigue cracks of aluminothermic welded joints of tramway rails it was necessary to perform tests of two joints containing cracks passing horizontally through the weld and the rail web, at the half of the rail web height. The characteristic forms of the cracks in joints S1 and S2 are presented in Figures 5 and 6.
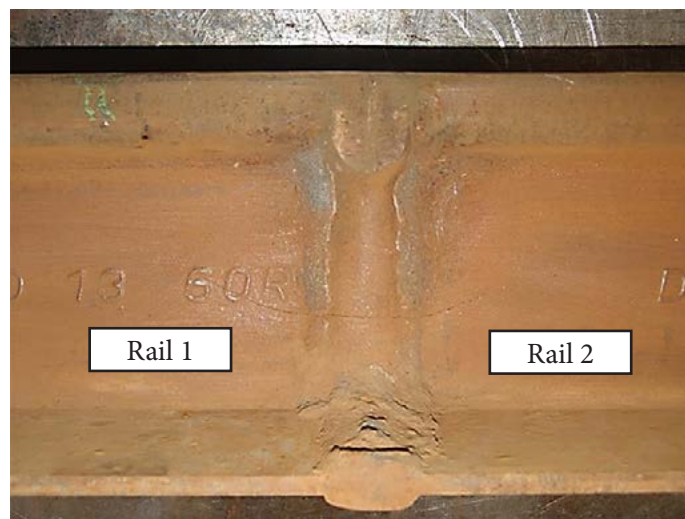
Fig. 5. Fatigue crack in joint S1 of rail 1 and 2
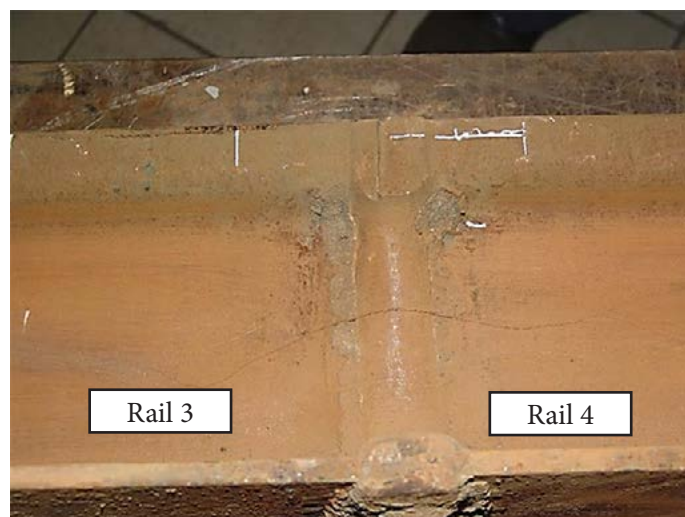
Fig. 6. Fatigue crack in joint S2 of rail 3 and 4

The tests of rails nos. 1÷4 revealed that the chemical composition, tensile strength R_m and elongation strength A_5 of the material of the rails subjected to the tests satisfied the requirements concerning steel grade R260 according to standard PN-EN 14811+A1:2010. In turn, the chemical composition of the welds of joints S1 and S2 satisfied the requirements of standard PN-EN 14730-1+A1:2010, Table 7.

The macroscopic metallographic tests did not reveal the presence of welding imperfections such as local lacks of penetration and solid inclusions in the joints.

The heat affected zone of the weld made using aluminothermic welding did not contain

the unfavourable martensitic structure; the HAZ hardness did not exceed 325 HV.

The metal of the welds in joints S1 and S2, in the crack zone, contained welding imperfections in the form of localised porosity (Fig. 7, 8) caused by the excessively fast cooling of the weld metal precluding its entire degassing.

The weld of joint S1, in the rail web area, contained a welding imperfection in the form of a microcrack along grind boundaries (Fig. 9).

Cracking in welds results from a strain which the metal of the weld is unable to transfer because of its limited ductility. Microcracks formed during welding are caused by films of fluids (low-melting eutectics having a solidification point significantly lower than that of iron) formed during solidification and incapable of transmitting stresses connected with the shrinkage of the weld during its cooling and solidification [27]. Similar to gas pores, microcracks of this type (welding imperfection 1001 according to Pn-en iso 6520-1:2009 [28]) may initiate fatigue cracking.

If the above named welding imperfections are present in a test joint performed during the process of welding procedure qualification, the contractor has the possibility of analysing and eliminating the reasons for the formation of such imperfections. Porosity (Fig. 7, 8) and microcracks in the weld (Fig. 9) may be caused by an overly short time during which rail ends are subjected to heating and an excessively fast cooling rate following the formation of a joint. This conclusion was confirmed by the results of works described in publication [19]. The elimination of the above named reasons should enable making another test joint free from unacceptable welding imperfections as well as result in the confirmation of the correctness of the aluminothermic welding of tramway rails performed by the contractor in a related Welding Procedure Qualification Record (WPQR).

Summary

In addition to providing qualified welding and coordinating personnel, supervising base materials and filler metal as well as coordinating and controlling the welding process itself, the coordination of the aluminothermic welding of tramway rails should also include the qualification of the process aimed to demonstrate the correctness of the welding procedure applied by the contractor.

The qualification of a technology used for the aluminothermic welding of tramway rails could be based on standard Pn-en iso 15613:2006 concerning the pre-production testing of technologies used for welding atypical joints, including additional requirements (if any) formulated by the investor or inspection personnel.

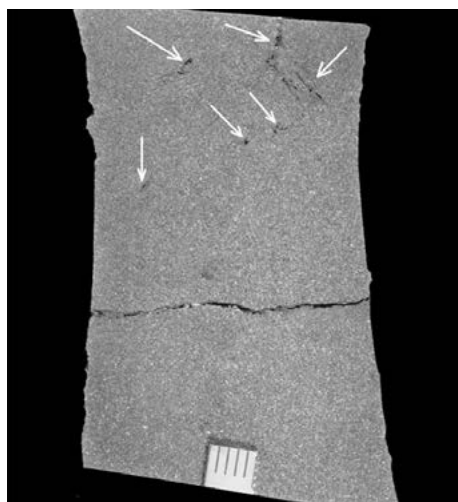Fig. 7. Macrostructure of the weld of joint S1 in the crack zone. The arrows indicate the location of gas pores in the weld
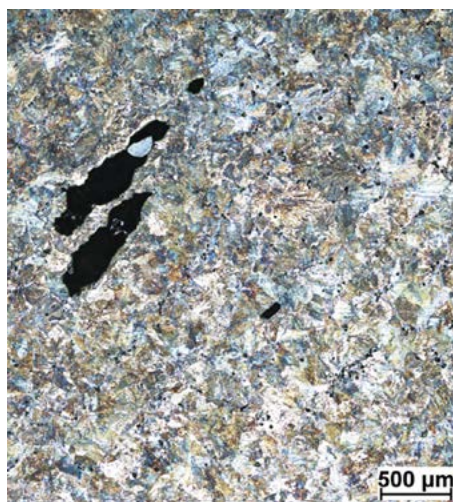
Fig. 8. Microstructure of the weld of joint S1 in the crack zone – main view (mag. 50x); visible porosity in the weld material
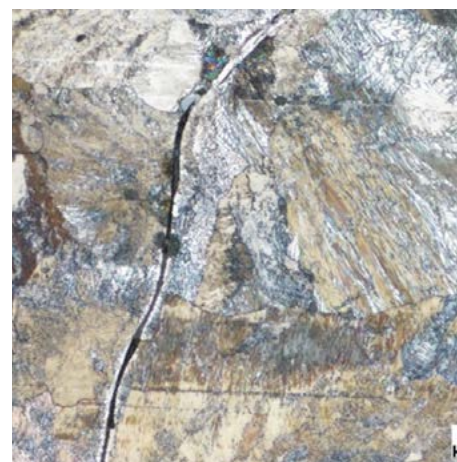
Fig. 9. Microstructure of the weld of joint S1 in the crack zone – microcrack along grain boundaries at a significant distant from the main crack (mag. 500x); etchant: $FeCl_3$

References

[1] Szczok E.: *Zapewnienie jakości w spawalnictwie.* [in]: J. Pilarczyk (ed.): *Poradnik Inżyniera. Spawalnictwo.* vol. 1. Wyd. Wnt, Warszawa, 2014, pp. 699-756

[2] Wiśniewski G.: *Systemy zarządzania jakością w procesach spawania. Kwalifikowanie personelu wykonującego i nadzoru zgodnie z EN 14730-2. Harmonizacja kwalifikowania spawaczy złączy termitowych szyn.* Proceedings of III National Scientific-Technical Conference „Spawalnictwo dróg szynowych oraz materiały, wykonawstwo, odbiory". Warszawa – Bochnia, 2007 r. [online], access date: 15.05.2016, *http://spawalnictwoszyn.pl/wp-content/uploads/2014/08/wisniewski_07.pdf*

[3] Jasiński I.: *Wybrane aspekty dziedziny spawalnictwa.* IV National Scientific-Technical Conference „Spawalnictwo Dróg Szynowych, Bochnia, 2011, Sitk RP. [online], access date: 15.05.2016 r., *http://spawalnictwoszyn.pl/download/pobieranie/o-konferencji/bochnia-2010/j_jasiski.pdf*

[4] Pn-en 14730-1+A1:2010: Railway applications. Track. Aluminothermic welding of rails. Part 1: Approval of welding processes

[5] Pn-en 14730-2:2006: Railway applications. Track. Aluminothermic welding of rails. Part 2: Qualifications of aluminothermic welders, approval of contractors and acceptance of welds

[6] Instruction of aluminothermic welding of railway tracks. Id-5. Attachment to the Directive of PKP Polskie Linie Kolejowe S.A. Management no. 4/2005, 10 March 2005

[7] Instrukcja badań defektoskopowych szyn, spoin i zgrzein w torach kolejowych Id-10 (D-16). PKP S.A., Warszawa, 2005.

[8] Pałka M.: *Warunki techniczne wykonania i odbioru złączy szynowych 49E1, 60E1 spawanych termitowo, metodą SoWoS-P.* Railtech Plötz. Wyd. Rolf Plötz Poland Ltd., Goczałkowice-Zdrój.

[9] DB Rail 824 Wykonawstwo dróg szynowych.

[10] Wolański Z.: *Certyfikacja zakładów wykonujących prace spawalnicze w zakresie nawierzchni kolejowych w Niemczech.* Proceedings of III National Scientific-Technical Conference „Spawalnictwo dróg szynowych - jakość, niezawodność, bezpieczeństwo", Bochnia, 2010 r., [online], access date: 15.05.2016, *http://spawalnictwoszyn.pl/wp-content/uploads/2014/08/z_wolaski.pdf*

[11] Junghähnel W.D.: *Technologie spawania Thermit®.* Elektro-Thermit GmbH. Kraków, 2013 r., [online], access date: 15.05.2016, *http://spawalnictwoszyn.pl/wp-content/uploads/2014/08/elektro_thermit_3_2013.pdf*

[12] Pn-en 14811+A1:2010: *Railway applications – Track – Special purpose rail – Grooved and associated construction.*

[13] Katalog wad w szynach. PKP Polskie Linie Kolejowe S.A., Warszawa, 2005.

[14] Makuch J.: *Wady w szynach.* Lecture 5. Wrocław University of Technology, 2014, [online], access date: 15.05.2016, *http://www.zits.pwr.wroc.pl/makuch/tinds_w5.pdf*

[15] *Defekty relsow. Klassifikacija, katalog i parametry defektnych i ostrodefektnych relsow.* OAO Rossijskie Żeleznye Dorogi. Moscow, 2014, [online], access date: 15.05.2016, *http://epk-rzd.ru/defektyi-relsov-klassifikatsiya-katalog-i-parametryi-defektnyih-i-ostrodefektnyih-relsov.html*

[16] Katalog defektow rel'sow NTD/CP-2-93. [online], access date: 15.05.2016, *ipk.stu.ru/userfiles/files/НТД+ЦП+2+93.doc*

[17] Lawrence F.V., Chen Y-R., Cyre J.P.: *Improving the Fatigue Resistance of Thermite Railroad Rail Weldments.* [online], access date: 15.05.2016, *http://fcp.mechse.illinois.edu/files/2014/07/Lawrence-presentation.pdf*

[18] Mutton P.J., Alvarez E.F.: *Failure modes in aluminothermic rail welds under high axle load conditions.* Engineering Failure Analysis, 2004, vol. 11, no. 2, pp. 151-166. *http://dx.doi.org/10.1016/j.engfailanal.2003.05.003*

[19] Wielgosz R., Parzych S., Rec T.: *Pęknięcia w złączach szynowych spawanych termitem.*

V National Technical Conference „Spawalnictwo dróg szynowych". Cracow, 2013 r. [online], access date: 15.05.2016, *http://spawalnictwo-szyn.pl/wp-content/uploads/2014/08/wiel-gosz_2013.pdf*

[20]   Naumenko W.S., Worobjew A.A.: *Termitnaja swarka rel'sow*. Wyd. Strojizdat, Moscow, 1969.

[21] Pn-en iso 3834-2:2007: *Quality requirements for fusion welding of metallic materials – Part 2: Comprehensive quality requiremens*

[22]   Pn-en iso 3834-3:2007 *Quality requirements for fusion welding of metallic materials – Part 3: Standard quality requiremens*

[23] Pn-en iso 3834-5:2015-08: *Quality requirements for fusion welding of metallic materials – Part 5: Documents with which it is necessary to conform to claim conformity to the quality requirements of Iso 3834-2, Iso 3834-3 or Iso 3834-4*

[24]   Pn-en iso 15613:2006: *Specification and qualification of welding procedures for metallic materials. Qualification based on pre-production welding test*

[25] Pn-en iso 15607:2007: *Specification And Qualification Of Welding Procedures For Metallic Materials – General Rules*

[26]   Kuzio T.: *Kwalifikowanie technologii spawalniczych przez Instytut Spawalnictwa*. Biuletyn Instytutu Spawalnictwa, 2007, no. 2.

[27]   Pilarczyk J.: *Metalurgia spawania*. [in]: J. Pilarczyk (ed.): *Poradnik Inżyniera. Spawalnictwo*. vol. 1, 2003, chapter 4. Wyd. WNT, Warsaw, 2014, pp. 88-112

[28]   Pn-en iso 6520-1:2009: *Welding and allied processes – Classification of geometric imperfections in metallic materials – Part 1: Fusion welding*

Maciej Różański, Sebastian Stano, Adam Grajcar

Laser Welding and Heat Treatment of Steel 0H15N7M2J

Abstract: The article presents the results of tests concerning the mechanical and structural properties of single-spot and twin-spot laser beam welded joints made of a steel strip, the chemical composition of which corresponds to that of steel 0H15N7M2J. In addition, the article presents the comparison concerning the geometry of joints made using the single and twin-spot laser beam. The test joints were subjected to heat treatment involving austenitisation, cold treatment and ageing. The study also involved the comparison of the mechanical and structural properties of the joints subjected and those not subjected to the above named heat treatment.

Keywords: laser welding, steel 0H15N7M2J, welding tests, joint properties

Introduction

Precipitation hardened corrosion resistant martensitic steels, often referred to in scientific publications as controlled transformation steels, combine good strength characteristic of martensitic structures with good ductility, usually characteristic of austenitic steels. One of such steels is steel 0H15N7M2J according to Pn-en 10088-2:2005, characterised by high fatigue strength, excellent corrosion resistance, plastic workability and small strains accompanying heat treatment. In the supersaturated state, the steel structure is austenitic. Only after long cold treatment at a temperature below 78°C is it possible to obtain a martensitic-austenitic structure. Further hardening of the steel is obtained through ageing at a temperature ensuring the dispersive precipitation of intermetallic phases in the matrix, leading to the significant increase in mechanical properties.

The above-presented steel is used when making sheets/plates, rods and wires, out of which high strength corrosion resistant elements are manufactured [1-4].

Laser welding is the process of joining metals, during which heat necessary for melting a given material is obtained by absorbing the monochromatic electromagnetic wave. The possibility of obtaining considerable power density at an area where a laser beam is focused (high laser beam power over a very small area) is responsible for the fact that welds obtained through keyhole welding are relatively narrow and deep, whereas the area of the heat affected zone (HAZ) is very limited. Very high metal heating and melting rates as well as equally fast cooling are responsible for the fact that both the weld and the HAZ do not reveal any significant grain growth and structural changes may significantly differ from those occurring during

dr inż. Maciej Różański (PhD (DSc) Eng.); dr inż. Sebastian Stano (PhD (DSc) Eng.) – Instytut Spawalnictwa, Welding Technologies Department; dr hab. inż. Adam Grajcar (PhD (DSc) Hab. Eng.) – Silesian University of Technology; Division of Constructional and Special Materials

arc welding processes. In some cases, it is convenient to split the laser beam into two component beams focused at two different points (bifocal welding). Depending on the distance between each other, the beams can form a common wider gasodynamic channel or two separate channels, thus affecting the solidification of metal and structural changes, if any. The focusing of the beam at two points in the tandem system reduces the cooling rate of elements during welding, may reduce welding stresses, and, in cases of materials susceptible to hardening, could temper the martensitic structure or prevent entire hardening [5-7].

The work involved tests concerning the effect of single-spot and twin-spot laser beam welding on the structure and mechanical properties obtained directly after welding and after treatment involving hardening, cold treatment and ageing.

Test Materials

The tests concerned the effect of laser welding parameters on the properties of joints made of precipitation hardened martensitic-austenitic steel 0H15N7M2J. The test joints were made using 0.8 mm thick, 65 mm wide and 100 mm long strips of the steel in the supersaturated state.

The tests also involved the verification of chemical composition using spark source optical emission spectrometry and a Q4 TASMAN spectrometer manufactured by Bruker. The chemical composition test results are presented in Table 1. In addition, the tests concerned the mechanical properties of the strip used. The results of the above named tests are presented in Table 2.

Test Joints

The welding tests involving the above named steel were performed using the keyhole welding technique, a solid state laser, integrated with a robotic system for laser processing, installed at Instytut Spawalnictwa in Gliwice (Fig. 1). The welding station was equipped as follows:

– Laser TruDisk 12002 – a Yb:YAG solid-state laser (Trumpf) having a maximum power of 12 kW and laser beam quality designated by the parameter of $B_{PP} \leq 8$ mm·mrad (Fig. 1a)

– CFO head (Trumpf) used for single-spot laser welding (Fig. 1b). The head was connected to the laser source using an optical fibre having a diameter of 200 μm and a focusing lens having a focal length of $f_{og} = 300$ mm. The diameter of the laser beam focus amounted to 300 μm.

– D70 head (Trumpf) provided with a system enabling the twin-spot focusing of a laser beam (Fig. 1c); the head was connected to the laser source using an optical fibre having a diameter of 600 μm and a focusing lens having a focal length of $f_{og} = 200$ mm; the diameter of a single laser beam focus amounted to 600 μm.

The distribution of power density (laser beam power distribution) between two focuses was

Table 1. Chemical composition of the steel used in the tests – chemical analysis result

Steel designation	Chemical composition, % by weight								
	C	Si	Mn	Cr	Mo	Ni	Cu	Co	Al
0H15N7M2J	0.024	0.16	1.41	17.14	2.14	9.1	0.22	0.084	0.89

Table 2. Mechanical properties of the strip in the supersaturated state corresponding in terms of chemical composition to steel 0H15N7M2J

Designation of tested steel equivalent	Tensile strength Rm, MPa	Yield point Re, MPa	Elongation A5, %
0H15N7M2J	1030	804	23,9

Note: values averaged from three measurements

monitored using a UFF100 laser beam analyser manufactured by Prometec (Fig. 1c). The shielding gas (Ar) was blown via a side nozzle at a flow rate of 12 l/min.

As regards the D70 head, the twin-spot laser beam is obtained by placing a special optical module across the laser beam, thus splitting the beam and changing its trajectory. Afterwards, the beam is focused on two spots by standard focusing lenses, as in classical laser welding. The distance between the focuses of the laser beam is affected by the inclination of the optical module plane. The laser beam power distribution is influenced by the position of the optical module in relation to the laser beam. The maximum distance between the beam focuses adopted when making the test joints amounted to 4 mm, i.e. the maximum distance available for the head used in the tests (D70). It was assumed that the tests would be performed with a beam power distribution of 50:50 and 60:40 (the first value defines the percentage fraction of beam power in the pilot focusing point of the tandem system). The change in power density distribution consisted in the manual change in the position of the optical module in relation to the laser beam. Each change in the above named position entailed a change in power distribution between individual focuses and in each case was verified by measuring density distribution between the two focuses. In the tests, the verification of the actual power density distribution was performed using the UFF100 laser beam analyser manufactured by Prometec. The graphic representation concerning the results of the measurement related to the power distribution of the twin-spot laser beam is shown in Figure 2.
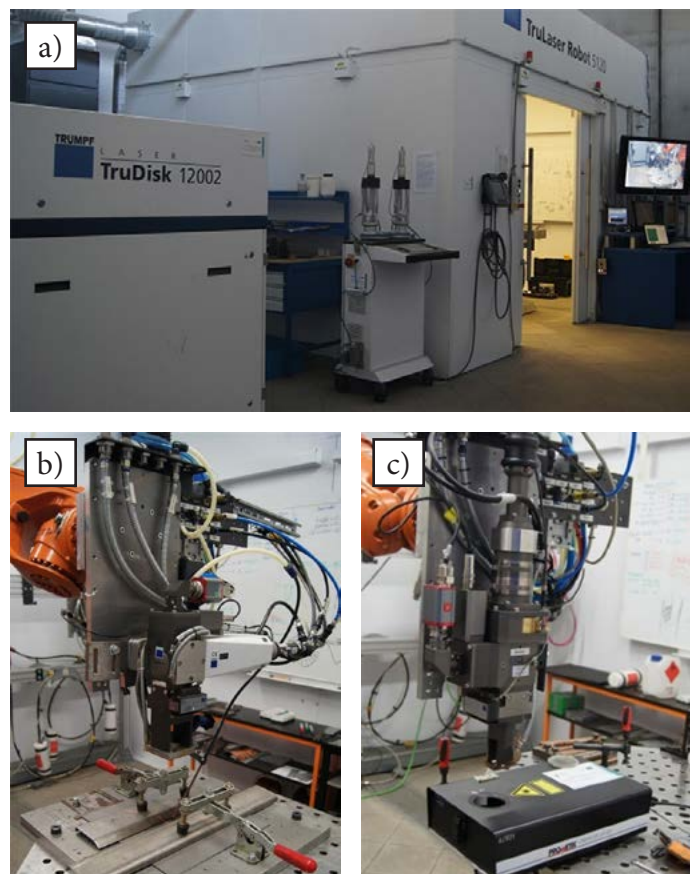
Fig. 1. TruDisk 12002 disc laser integrated with the robotic station. Main view (a), CFO head for keyhole welding (b), D70 head with the bifocal system fixed to the wrist of the industrial robot and the UFF100 laser beam analyser (c)

Assumed distribution of twin-spot laser beam power	Distribution of power density between individual focuses, 4 mm away from each other, position f = 0 mm (direction of welding along y-axis)	
50:50%		
60:40%		
Note: location of the focus on the surface of workpieces - f = 0 mm.		

Fig. 2. Graphic presentation of twin-spot laser beam power distribution, performed using a UFF100 device manufactured by Prometec

In order to determine the effect of single and twin-spot laser welding parameters on the mechanical properties and the structure of 0.8 mm thick butt joints made of steel 0H15N7M2J, it was necessary to make test joints using various sets of process parameters. The initial tests enabled the selection of 3 sets of single-spot laser welding parameters (Table 3) and 4 sets of twin-spot laser welding parameters (Table 4). Parameters were selected in a manner ensuring the obtainment of the proper quality of joints (according to adopted parameters), i.e. with the penetration across the entire thickness of the base material and without spatters, burn-throughs, undercuts etc.

Visual Tests

The making of the test joints was followed by their visual inspection performed in accordance with standard Pn-en iso 17637:2011e *Non-destructive tests of welds. Visual testing of fusion-welded joints.* The tests aimed to determine the correctness of weld geometry and to enable the selection of joints for further tests by eliminating those failing to meet the requirements of quality level B according to Pn-en iso 13919-1 *Welding. Electron and laser beam welded joints. Guidance on quality levels for imperfections. Steel.*

Table 3. Parameters of the single-spot laser beam welding of 0.8 mm thick sheets made of steel 0H15N7M2J

Specimen no.	11	12	13
Beam power, kW	1.5	2.5	4.5
Welding rate, cm/min	350	780	1500
Linear energy, kJ/mm	0.0257	0.0187	0.0180

Table 4. Parameters of the twin-spot laser beam welding of 0.8 mm thick sheets made of steel 0H15N7M2J

Specimen no.	21	22	23	24
Beam power, kW	4	4	3	3
Welding rate, cm/min	1080	1080	840	840
Beam power distribution,%	50:50	60:40	50:50	60:40
Linear energy, kJ/mm	0.039	0.039	0.035	0.035

Joints nos. 11 and 12 (welding parameters - Table 3) revealed the entire penetration across the thickness of the base material; the geometry of the weld face and of the weld root was unchanged along the entire length. Joint no. 13 revealed local burn-throughs and spatters in the welded joint area. Despite the foregoing, the latter joint was also selected for macro and 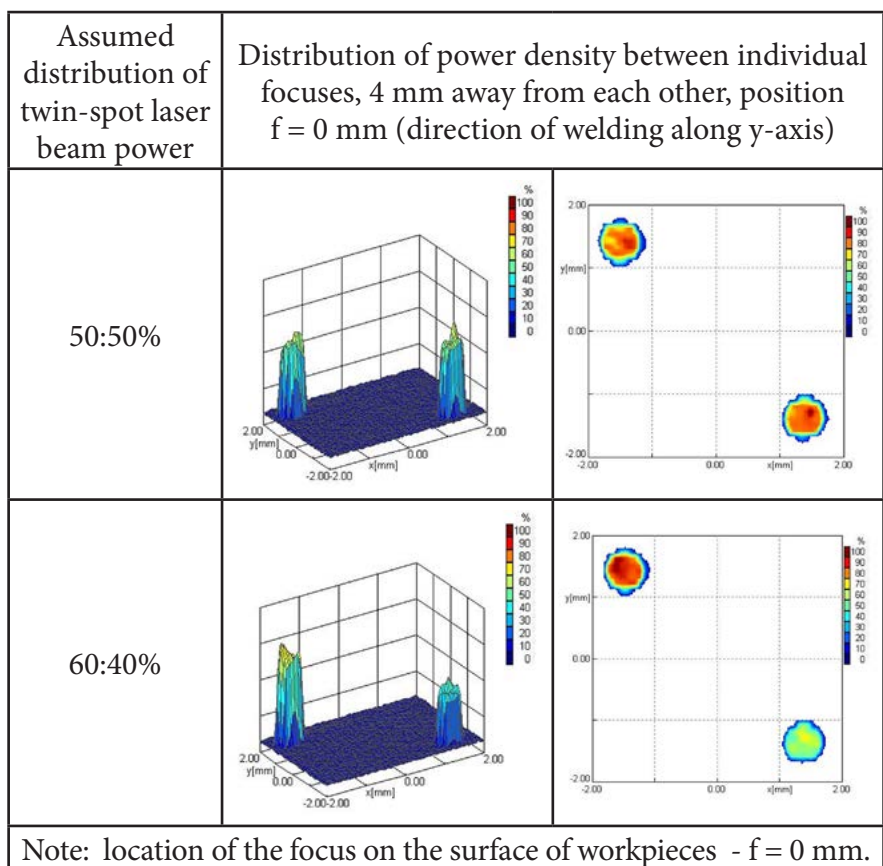microscopic metallographic tests as well as for cross-sectional hardness measurements. All of the twin-spot laser beam welded joints (Table 4) revealed the entire penetration of the base material and the unchanged and proper geometry of the weld face and weld root along the entire length of the joint. All of the joints revealed the depletion of weld metal, which was probably caused by the evaporation of steel components characterised by high vapour pressure at welding temperature. Because of the thickness of the sheets being welded (0.8 mm), the visual inspection concerning the depletion of weld metal and the measurement of possible dimensions of characteristic welding imperfections, such as undercuts or the incomplete filling of the weld groove and qualifying such observed imperfections as representing a given quality level according to standard Pn-en iso 13919-1 was very difficult. The assessment of the quality of the joints was possible only after performing macroscopic metallographic tests.

Heat Treatment of Laser Welded Joints Made of Steel 0H15N7M2J

The obtainment of appropriately high mechanical properties of precipitation hardened high-alloy austenitic steels is ensured by properly performed heat treatments. As regards the tested high-alloy steel corresponding, in terms of the chemical composition, to steel 0H15N7M2J, in accordance with the steel data sheet, the process of heat treatment consisted in 1-hour long austenitisation at a temperature 950°c, cooling in oil, 1-hour long cold treatment at a temperature of -80°c and 3-hour long

ageing at a temperature of 510°C. As regards the single-spot laser beam welded joints, the heat treatment involved joints nos. 11, 12 and 13 (welding parameters – Table 3). In terms of the twin-spot laser beam welded joints, the heat treatment involved all of the welded joints (welding parameters – Table 4).

The process of heat treatment was performed in the laboratory of Testing of Materials Weldability and Welded Constructions Department at Instytut Spawalnictwa. The heat treatment process is presented in Figure 3.
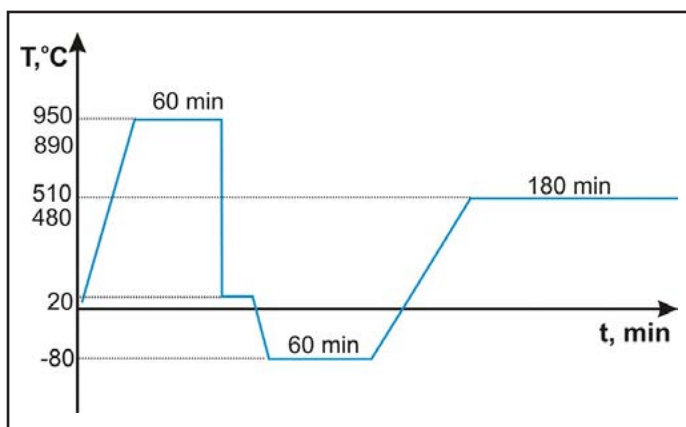
Fig. 3. Scheme of the temperature-time parameters used during the heart treatment of steel 0H15N7M2J

Metallographic Tests

Macroscopic Metallographic Tests

The structure of the welded joints made of steel 0H15N2M2J was revealed by electrolytic etching. The macroscopic metallographic tests were performed using a Nikon Eclipse MA200 light microscope. The macroscopic metallographic tests were performed using all of the selected sets of parameters. The macrostructures of the single-spot laser beam welded joint made of steel 0H15N7M2J are presented in Figure 4, whereas those of the twin-spot laser beam welded joint are presented in Figure 5.

As regards the single-spot laser beam welded joints, the decrease in welding linear energy from 0.0257 kJ/cm to approximately 0.0180 kJ/cm only slightly affected the width of the weld. In turn, the geometry of the welded joints was

Welding linear energy – 0.0257 kJ/cm – specimen no. 11

Welding linear energy – 0.0187 kJ/cm – specimen no. 12

Welding linear energy – 0,0180 kJ/cm - specimen no. 13

Fig. 4. Macrostructure of the single-spot laser beam welded joints made of steel 0H15N7M2J using a linear energy of 0.0257 kJ/cm – specimen no. 11 (a), 0.0187 kJ/cm – specimen no. 12 (b) and 0.0180 kJ/cm – specimen no. 13 (c)

significantly influenced by the welding rate. In the case of the welded joint made using a welding rate of 350 cm/min (Fig. 4a) and 780 cm/min (Fig. 4b), the welds revealed almost parallel fusion lines, which reduced stresses in the weld and minimised the angular strain of the joint. After increasing a welding rate to 1500 cm/min (Fig. 4c), the weld geometry changed significantly; the volume of the crystallising metal of the weld above its neutral axis was significantly greater than the volume of the weld metal below the axis. The areas of the single-spot laser beam welded joints subjected to the macrostructural tests did not reveal welding imperfections disqualifying the joints as made improperly.

The twin-spot laser beam welded joints made of steel 0H15N7M2J did not reveal the significant
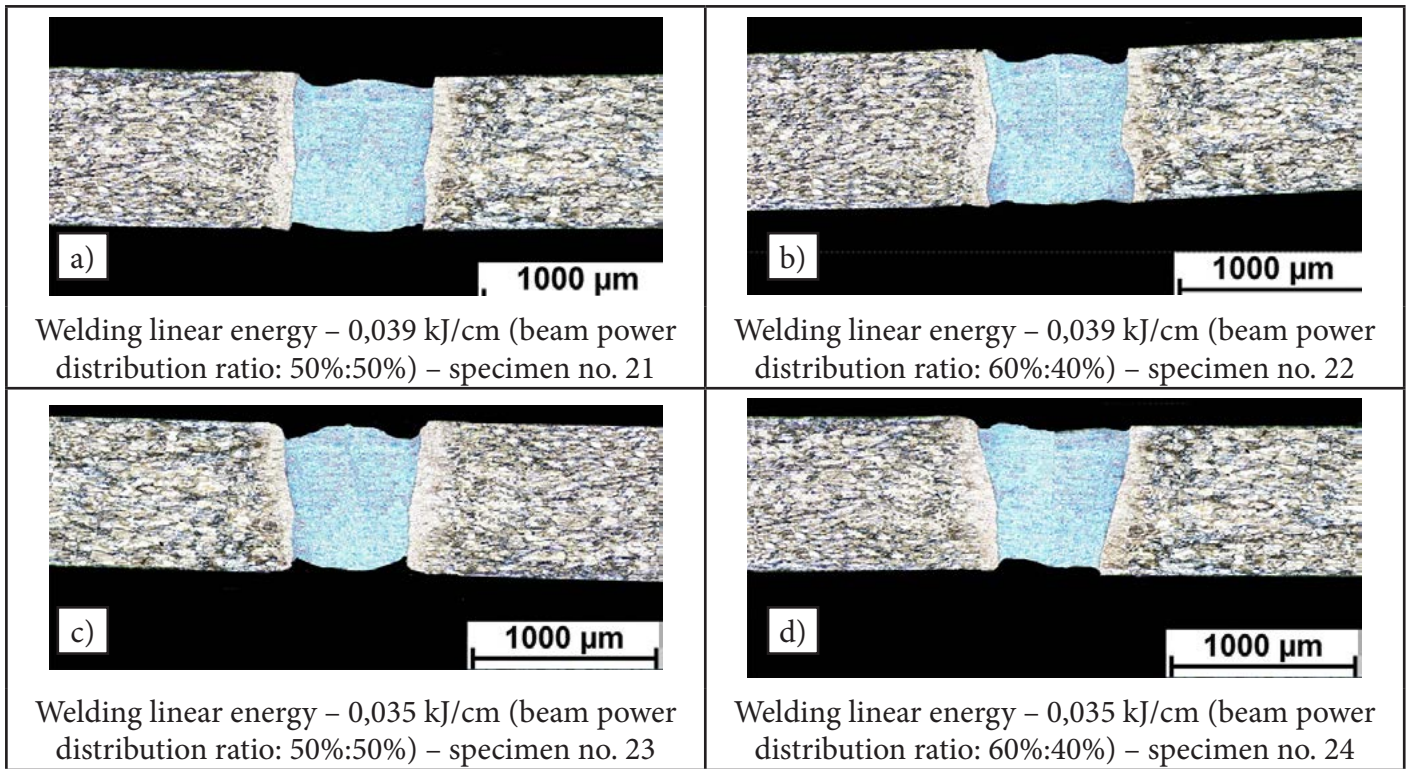
Fig. 5. Macrostructure of the twin-spot laser beam welded joints made of steel 0H15N7M2J using a linear energy of 0.039 kJ/cm with the beam power distribution ratio of 50%:50% - specimen no. 21 (a), using a linear energy of 0.039 kJ/cm with the beam power distribution ratio of 60%:40% - specimen no. 22 (b), using a linear energy of 0.035 kJ/cm with the beam power distribution ratio of 50%:50% - specimen no. 23 (c) and using a linear energy of 0.035 kJ/cm with the beam power distributu ratio of 60%:40% - specimen no. 24 (d)
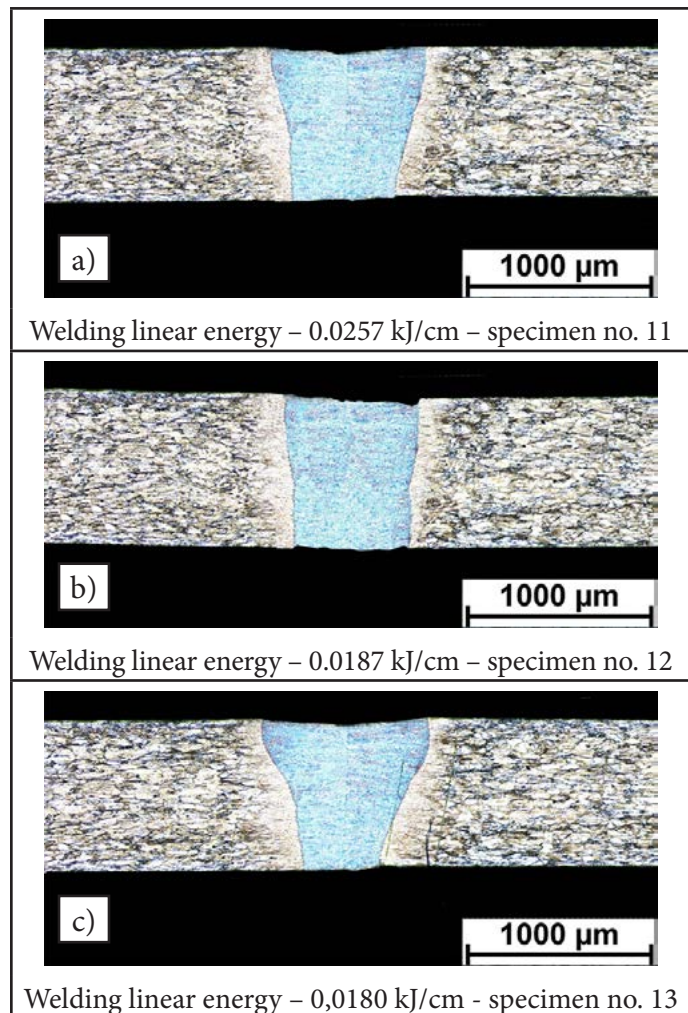
effect of the laser beam power distribution (between the focuses) on the joint geometry. However, in each case (Fig. 5a-d), numerous welding imperfections (undercuts) were observed; the imperfections were restricted within quality level B according to standard Pn-en iso 13919-1. In addition, the twin-spot laser beam welded joints revealed a decrease in the active cross-section of the joint caused by the depletion of the weld metal. It should be emphasized that the significant depletion of the weld metal, decreasing the active cross-section of the joint, undoubtedly reduced its strength.

Microscopic Metallographic Tests

Similar to the macroscopic tests, the microscopic metallographic tests of the welded joints were performed using a Nikon Eclipse MA200 metallographic light microscope. The microstructural observations involved the base material and the welded joint, i.e. the weld and the heat affected zone. The tests were performed on the joints made using the single-spot laser

beam having a linear energy of 0.018 kJ/cm in the state before and after the heat treatment. The test results are presented in Figure 6 and 7.

As regards the welded joint made of steel 0H15N7M2J in the pre-heat-treatment state, the weld material was the dendritic mixture of austenite with ferrite delta (Fig. 6c). In turn, the base material structure contained strain-induced austenite with numerous slide lines, strain bands and some amounts of martensite (Fig. 6b). The strain effects were not visible or only slightly visible in the heat affected zone; the content of martensite was close to 0, the slide lines and bands were hardly visible (Fig. 6d). The structure of the base material contained few coagulated precipitates (Fig. 6d), affecting the steel hardening to a very little degree.

The heat treatment of the welded joint significantly changed the microstructure of the joints and of the base material. The base material microstructure was almost entirely composed of austenite; the chemical composition might also include some amount of ferrite delta) (Fig.

7b). The base material contained numerous dispersive precipitates. Taking into consideration the chemical composition of the steel and the effect of the heat treatment, it could be supposed that precipitated particles were $M_{23}C_6$ carbides and intermetallic phases such as Ni_3Mo, Fe_2Mo, $(Fe,Ni)_2Mo$, Ni_3Al and $NiAl$. The supposition needs to be fully confirmed using more detailed X-ray tests as well as the accurate analysis of the chemical composition of precipitates using energy dispersive spectrometry (EDS). The structure of the weld subjected to the heat treatment was the mixture of martensite (formed after cold treatment) as well as ferrite delta and other precipitates. The detailed analysis of the above named precipitates will be the subject of further studies (Fig. 7c). In addition, the fusion line (Fig. 7d) contained chain-like precipitates of hardening phases. Such an arrangement of hard phases can significantly reduce joint plasticity and even lead to joint brittleness.

Tensile Tests

The tensile tests involved the single-spot laser beam welded joint made using the set of parameters no. 12 in Table 3 and the twin-spot laser beam welded joint made using the set of parameters no. 22 in Table 4. The tensile tests involved both the specimens directly after welding (not subjected to the heat treatment) and those subjected to the heat treatment. The tensile tests were performed using a testing machine (model 4210) manufactured by Instron.

Fig. 6. Macro and microstructure of the joint made of steel 0H15N7M2J using a linear energy of 0.0180 kJ/cm in the state before and after the heat treatment: joint macrostructure (a), base material microstructure (b), weld (c) fusion line and HAZ (d)
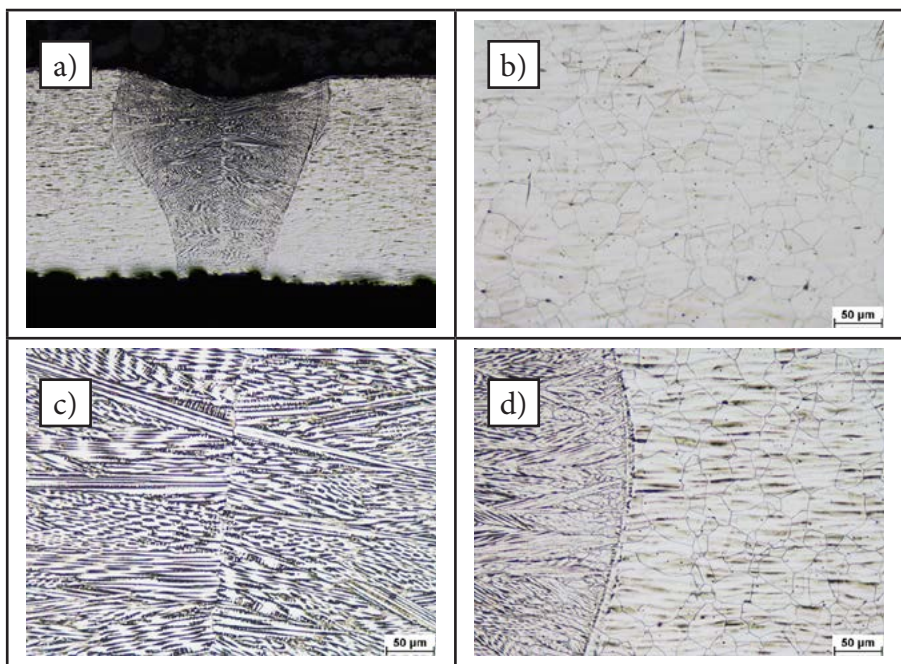
Fig. 7. Macro and microstructure of the single-spot laser beam welded joint made of steel 0H15N7M2J using a linear energy of 0.0180 kJ/cm in the state after the heat treatment: joint macrostructure (a), base material microstructure (b), weld (c) fusion line and HAZ (d)

Specimens for the tensile tests were prepared in accordance with the requirements specified in standard PN-EN ISO 4163:2013. Each of the joints was subjected to 3 tensile tests. The tensile test results are presented in Table 5 and Figure 8.

The tensile test results revealed that both as regards the single and twin-spot laser beam
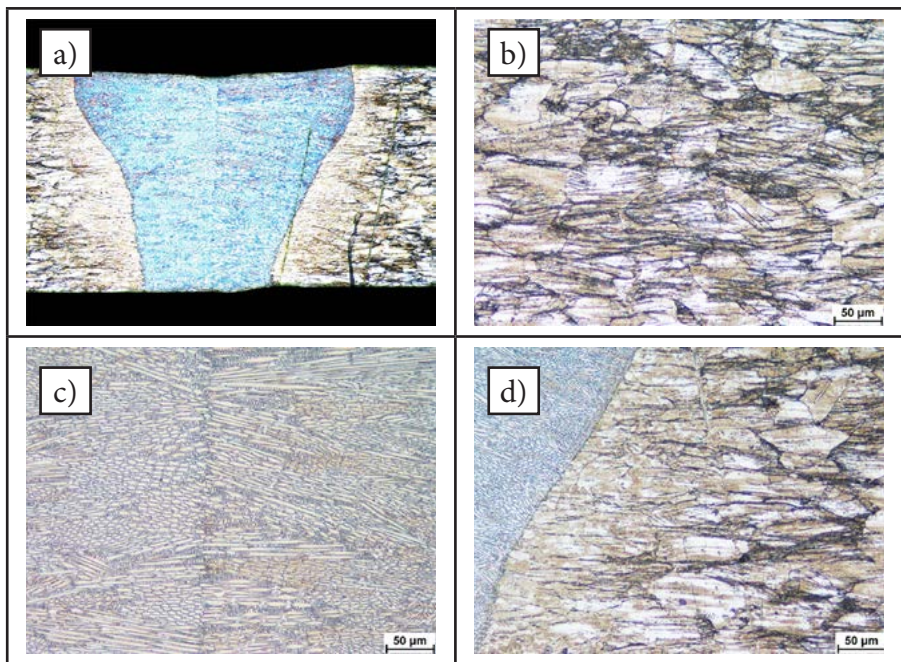
Table 5. Tensile test results related to the joints made of steel 0H15N7M2J, laser welded using the single-spot (no. 12) and twin-spot beam (no. 22)

Specimen (Table 3 and 4)	Heat Treatment	Tensile strength, R_m MPa			Average, R_m MPa	Standard deviation MPa
		1	2	3		
12	No	610	562	584	585	24.1
12	Yes	984	1027	999	1003	21.8
22	No	541	572	529	547	22.2
22	Yes	978	953	942	958	18.4

Note: In each case, the specimen ruptured in the weld
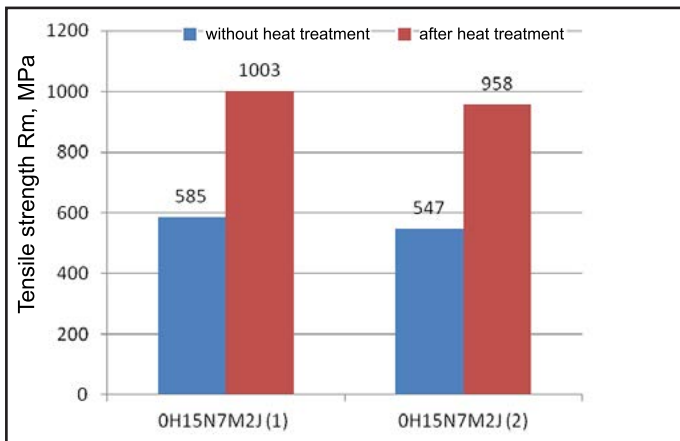
Fig. 8. Tensile strength of the single-spot (1) and twin-spot (2) laser beam welded joints made of steel 0H15N-7M2J not subjected and subjected to the heat treatment
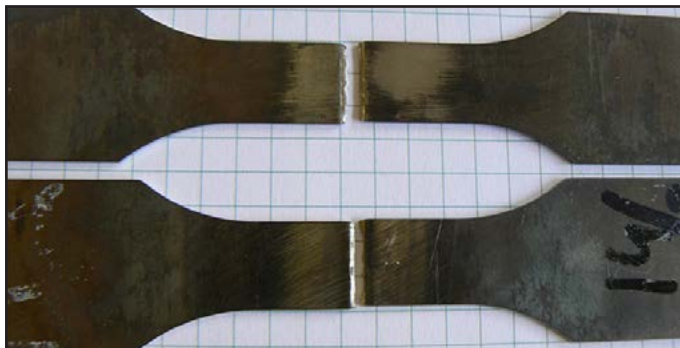
Fig. 9. Photographs of the exemplary laser-beam welded specimen after the tensile strength test – rupture in the weld

welded joints, the test specimens ruptured in the weld (Fig. 9), which means that in each case the strength of the welded joint was lower than that of the base material, both as regards the joints subjected to the heat treatment and those which remained in the state directly following the welding process. The tensile strength of the single-spot laser beam welded joints directly after welding amounted to 585 MPa, constituting approximately 56% of the base material hardness (Table 2, Table 5). The tensile strength of

the same joints subjected to the heat treatment amounted to 1003 MPa, constituting approximately 97% of the base material hardness. In turn, the tensile strength of the twin-spot laser beam welded joint not subjected to additional heat treatment amounted to 547 MPa, constituting approximately 53% of the base material hardness, whereas the tensile strength of the twin-spot laser beam welded joint subjected to the heat treatment amounted to 958 MPa, constituting approximately 93% of the base material hardness. Therefore, it can be assumed that it is possible to make a weld characterised by tensile strength similar to that of the base material. It should be noted that the weld geometry always constitutes a geometrical notch (depletion of metal on the weld face side) leading to the accumulation of stressed in the transition area between the weld face and the base material.

Cross-Sectional Hardness Measurements of Welded Joints

Cross-sectional hardness measurements of the welded joints were performed by means of a Kb50bvz-fa testing machine manufactured by KB Prüftechnik, using an indenter load of 9.81 N (hv1). Hardness was measured in both directions from the weld axis. The distance between measurement points amounted to 0.2 mm and the measurement line was located in the middle of the weld thickness. Hardness tests only involved the single-spot laser beam welded joints in relation to each set of welding parameters used. Hardness tests involved both the joints subjected and not subjected to the

heat treatment. The primary objective concerning cross-sectional hardness measurements of the welded joints was to determine the effect of the welding process on changes in the hardness of the welded joints as well as to identify the effect of the heat treatment and precipitation processes on the hardness increase in the individual areas of the welded joints. Cross-sectional hardness measurements involving the twin-spot laser beam welded joints were omitted as changes in the width of the weld and that of the heat affected zone do not affect hardness. The results of the hardness tests involving the single-spot laser beam welded joints are presented in Figure 10.
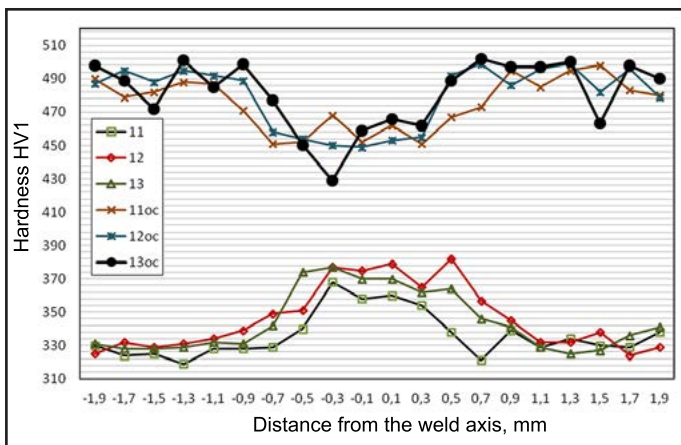
Fig. 10. Results of the cross-sectional hardness measurements of the single-spot laser beam welded joints made of steel 0H15N7M2J before (11-13) and after the heat treatment (11oc-13oc)

The cross-sectional hardness measurement of the single-spot laser beam welded joints made of steel 0H15N7M2J revealed that the process of welding increased the hardness of the weld metal if compared with that of the base material. The hardness of the base material amounted to 315-343 HV1 and increased in the weld metal to approximately 360-375 HV1, where the direct effect of welding linear energy on the increase in the weld metal hardness was not observed. The significant increase in the hardness of both the base material and the weld was caused by the heat treatment. After the heat treatment, the hardness of the base

material increased to 470-505 HV1, i.e. by more than 150 HV1. This could be attributed to the precipitation process taking place during ageing and the precipitation of numerous hardening phases, the identification of which will be possible after the use of X-ray and microscopic techniques of greater resolution. The hardness of the weld increased to a lesser degree, i.e. to 430-470 HV1, by approximately 100 HV1 in relation to the hardness of the welded joint preceding the heat treatment.

Conclusions

1. Single and twin-spot laser beam welding enables the obtainment of high-quality joints of thin-walled elements made of steel 0H15N7M2J.

2. The heat treatment of laser welded joints made of steel 0H15N7M2J leads to the precipitation of dispersive phases in the austenitic matrix.

3. The tensile strength of the single and twin-spot laser beam welded joints not subjected to further heat treatment amounts to 585 MPa and 547 MPa respectively, i.e. 53% and 56% of the base material in the as-delivered state. The heat treatment of the joints increases the tensile strength to a tensile strength value close to that of the base material, i.e. to 1003 MPa and 958 MPa respectively, constituting 97% and 93% of the base material tensile strength. Such significant hardening is caused by the occurrence of precipitation phenomena.

4. The heat treatment of laser welded joints made of steel 0H15N7M2J increases the hardness of the base material from approximately 300 HV1 to approximately 500 HV1 and that of the weld from approximately 370 HV1 to approximately 450 HV1, which can be attributed to the effect of precipitation hardening.

5. Single-spot laser beam welding causes the less intense evaporation of the weld metal than that accompanying twin-spot laser beam welding.

References

[1] Blicharski M.: *Inżynieria materiałowa. Stal.* WNT, Warszawa, 2004.

[2] Pawlak S.J.: *Austenite stability in the high strength metastable stainless steel.* Journal of Achievements in Materials and Manufacturing Engineering, 2007, vol. 22, issue 2.

[3] *Charakterystyki stali seria E*, vol. II. Instytut Metalurgii Żelaza im. S. Staszica w Gliwicach

[4] Ozgowicz W., Kurc-Lisiecka A., Grajcar A.: *Corrosion behaviour of cold-deformed austenitic alloys.* [in]: Valdez Salas B., Schorr M. (eds.): *Environmental and industrial corrosion – practical and theoretical aspects* InTech, Rijeka, 2012, chapter 4, pp. 79-107

[5] Banasik M., Stano S., Polak J.: *Possibility of using Nd:YAG laser for precise joining of thin-walled elements of structures on the example of the flow sensor pitot probe.* Welding International, 2013, vol. 27, issue 6.
http://dx.doi.org/10.1080/09507116.2011.606139

[6] Pilarczyk J., Stano S., Banasik M., Dworak J.: *Wykorzystanie technik laserowych do spawania elementów o małych wymiarach w Centrum Laserowym Instytutu Spawalnictwa. Problemy Eksploatacji.* Zeszyty Naukowe Instytutu Technologii Eksploatacji – PIB, 2011, no. 4.

[7] Różański M., Grajcar A., Stano S.: *Wpływ energii liniowej spawania wiązką laserową na mikrostrukturę i wybrane właściwości połączeń ze stali* AHSS *na przykładzie* CPW 800. Przegląd Spawalnictwa, 2015, vol. 87, no. 2.

Rafał Kaczmarek, Karol Kaczmarek, Jacek Słania, Ryszard Krawczyk

Performing of Ultrasonic Tests Using the TOFD Technique in View of the Requirements of Related Standards

Abstract: The article concerns the time of flight diffraction testing technique (TOFD), which is, next to the simultaneous TOFD + Phased Array testing, one of the most effective methods of volumetric non-destructive tests. The article discusses the advantages of the TOFD technique as well as the basis of diffraction phenomenon and the formation of imaging signals. In addition, the article presents a TOFD image of a welded joint and describes its characteristic elements. Also, the article discusses the TOFD-related testing standards and analyses their requirements related to welded joints and their acceptance criterion, i.e. the quality level according to PN-EN ISO 5817. The target readers of the article include NDT personnel, inspectors, welding engineers and welding equipment manufacturers wishing to implement an effective tool enabling the detection of welding imperfections.

Keywords: time of flight diffraction, TOFD, non-destructive testing of welds, ultrasonic tests.

Introduction

Increasing requirements in terms of the reliability of welded products and structures require the use of new more advanced testing techniques allowing the verification of quality and workmanship. Modern ultrasonic techniques, such as TOFD, Phased Array and Full Matrix Capture (also known as Total Focusing Method) are becoming increasingly important. Each of the above-presented techniques is at a different stage of development. The TOFD technique, widely used for many years in English-speaking countries, has become internationally standardised, both in terms of workmanship and as regards the assessment of test results. For this reason, the TOFD technique is likely to become increasingly popular in industry. Undoubtedly, factors increasing the application potential of TOFD technique-based tests in Poland include relatively low testing equipment costs, possibility of obtaining funds from the National Centre for Research and Development (within implementations of innovative projects) and the initiation (in 2016) of training courses for operators of TOFD technique-based ultrasonic tests at the Welding Education and Supervision Centre of Instytut Spawalnictwa in Gliwice.

dr inż. Karol Kaczmarek (PhD (DSc) Eng.); dr hab. inż. Jacek Słania (PhD (DSc) hab. Eng.), Professor at IS – Instytut Spawalnictwa, Welding Education and Supervision Centre; mgr inż. Rafał Kaczmarek (MSc Eng.), dr inż. Ryszard Krawczyk (PhD (DSc) Eng.) – Częstochowa University of Technology; Welding Department

The TOFD technique is characterised by a number of advantages justifying its implementation for verifying the quality of welded joints to a significantly greater degree than presently. One of the most important advantages of the method, as regards non-destructive tests, is the very high and repeated detectability, particularly of flat discontinuities. The high TOFD detectability has been verified by results of research programmes aimed to confirm the effectiveness and reliability of TOFD tests. In one of such programmes, performed by the Netherlands Institute of Welding (NIL), TOFD tests were compared with manual ultrasonic tests (UT) and X-ray radiographic (RT-X) and (RT-γ) tests. Both the probability of detection (POD) and the false call rate (FCR), amounting to 82% and 11% accordingly, speak for the use of the TOFD technique. As regards the other volumetric methods, POD and FCR amounted to 52% and 22% for UT, 60% and 11% for RT-γ and 66% and 15% for RT-X accordingly [1].

The valuable and interesting comparison of the TOFD technique possibilities and those of RT-γ also results from experience gained when building pipeline DN1000 [2]. The authors have compared the test results concerning 356 pipeline welds tested using both the TOFD technique and the RT method and the source of Ir192. The total length of imperfections detected using the TOFD technique (in case of the same welds) was almost 3 times greater than that of the imperfections detected using the RT method. The reason for such a large discrepancy of test results was ascribed to the low detectability of flat discontinuities (primarily incomplete fusions) in the radiographic tests. The presence of the above named imperfections was later confirmed (at the repair stage) by magnetic particle tests of weld segments subjected to grinding [2].

The possibilities and advantages of TOFD tests call for the replacement of conventional volumetric tests, where possible, with the TOFD technique. However, in order for this to happen, it is necessary to raise the awareness of NDT personnel as to the use of modern UT methods, and at the same time, allay fears related to the implementation of new and previously rarely used testing techniques (in Poland). This task is by far facilitated by the complete standardisation of TOFD tests as regards the workmanship and the assessment of the quality of joints.

TOFD Technique versus Conventional Ultrasonic Tests Based on the Echo Method

Conventional ultrasonic tests utilise the laws of geometric optics, i.e. reflection law, refraction law and transformation law in relation to the ultrasonic waveform. One of the examples is the echo technique utilising the phenomenon of the directional reflection of an ultrasonic wave. High signal amplitudes are obtained when ultrasonic beams are reflected from flat surfaces (e.g. incomplete fusions) perpendicular to the direction of an ultrasonic beam and from rectangular reflectors (e.g. a crack reaching the surface or incomplete penetrations in the Y-bevelled weld root). In cases of unfavourably oriented discontinuities, an incident beam may be reflected in another direction and not return to the transducer, thus not giving the signal of discontinuity on a defectoscope.

Conventional techniques of ultrasonic tests aim to leave only one type of wave generated in a material subjected to a test. Such a situation occurs in cases of most common tests utilising simple transducers of longitudinal waves and angle transducers of transverse waves. In cases where more than one type of ultrasonic wave is generated, as is the case with angle transducers of transverse waves, the analysis of indications can cause some difficulties as it is not possible to ensure if a signal appearing on the defectoscope screen comes from the primary wave type, e.g. longitudinal wave (in the examples discussed). Such a phenomenon is undesirable as it impedes the interpretation of indications.

Similar to other techniques of ultrasonic tests, the TOFD technique utilises the laws of geometric optics. However, the phenomenon of the generation of diffracted waves on discontinuity edges is of primary importance. Such waves are generated as a result of striking the edge of discontinuity by a high amplitude wave emitted from a transmitter. In accordance with the Huygen's principle, each centre point reached by a wave (including atoms at the top of the centre) becomes the independent source of spherical waves (Fig. 1). Spherical waves have a low amplitude, propagate within the wide range of angles, and their generation only slightly depends on the angle of an incident beam [3]. This may lead to the obtainment of signals of unfavourably oriented discontinuities, the detection of which is problematic using the conventional echo technique, in particular, flat discontinuities such as cracks and incomplete fusions, unacceptable for quality levels B and C according to PN-EN ISO 5817.

Unlike in the ultrasonic echo technique, in TOFD technique-based tests various types of ultrasonic waves, i.e. longitudinal, transverse and surface (Rayleigh) waves, are excited in a material being tested. Signals obtained from each of these waves provide information about the presence of a discontinuity in the material and can be used in analysis. However, the most frequently used are longitudinal waves, propagating (in a material being tested) within the wide ranges of angles, also as lateral waves.

Figure 1 presents the schematic generation of diffracted waves on discontinuity edges. Figure 2 presents the insertion of ultrasonic waves into soda-lime glass using a TOFD transducer [3]. Such a centre (soda-lime glass), because of similar velocities of longitudinal and transverse waves (5800 m/s and 3450 m/s accordingly), well reflects phenomena taking place in steels. Figure 2a presents the front of a longitudinal and transverse wave before reaching a gap. In turn, Figure 2b presents the partial directional reflection of a longitudinal wave from a flat

discontinuity surface along with the transformation of the longitudinal wave into a transverse wave as well as the excitation of, both longitudinal and transverse, diffracted waves at the tops of the gap.
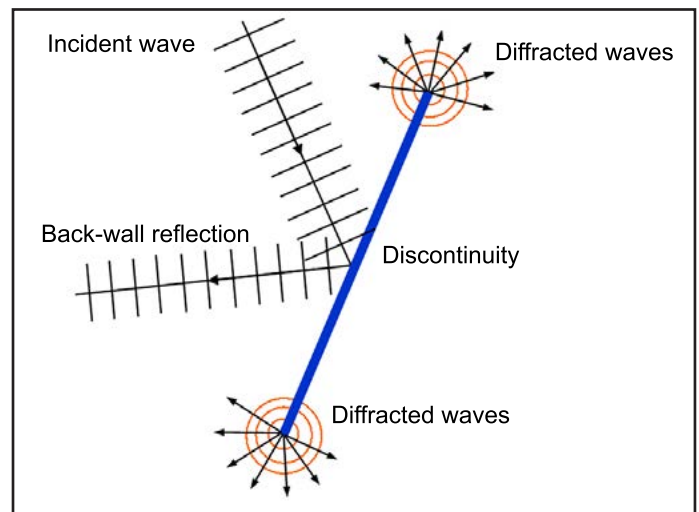
Fig. 1. Schematically presented generation of diffracted waves on discontinuity edges
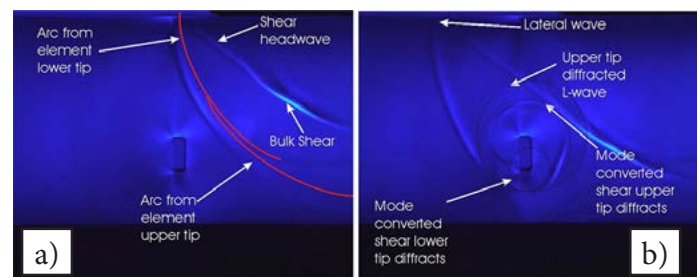
Fig. 2. Generation of diffracted waves on the edges of a gap (1 mm x 3 mm) in soda-lime glass [4]
a) longitudinal wave (red marker) before reaching the gap, b) longitudinal wave after passing the gap, partial reflection and the excitation of diffracted waves (black markers)

Fundamentals of TOFD Tests

As a rule, the TOFD technique is aimed at the reception of imaging (diffraction) signals. Unlike in the echo method, in the TOFD technique the amplitude of signal is not used for assessing the size of analysed material discontinuities. The appropriate setting of defectoscope gain only aims to ensure the obtainment of good quality imaging. The gain should be high enough so that a TOFD image, using the grey scale, could easily represent recorded disturbances. However, the value of gain must not be excessively high, as this could deteriorate the quality of TOFD images. Annex B of standard [5] presents

examples of TOFD images with proper and improper gain values.

Because of the low amplitude of imaging signals, it is necessary to use relatively high gain (usually 80-100 dB). The typical configuration of TOFD transducers consists of two angle transducers of longitudinal waves mounted in a push-pull system at the constant distance from each other (Fig. 3). Such an arrangement of transducers minimises the number of signals coming from the directional reflection of an ultrasonic beam. In practice, only discontinuities parallel to the scanning surface (e.g. laminar imperfections in a sheet) cause the directional reflection of a beam emitted by a transmitting transducer in the direction of a receiving transducer. An angle of the refraction of transducers is restricted within the range of 40° to 70°. In cases of joints having thicknesses restricted within the range of 6-50 mm, the most frequently used angle amounts to 70° or 60°. When testing elements having thicknesses up to 50 mm, without dividing into zones, the beam intersection point corresponds to 2/3 of the thickness of an element subjected to a test. Usually, the TOFD technique involves the use of strongly dampened transducers having a small diameter (usually 3 or 6 mm). A small transducer diameter ensures the generation of a strongly divergent beam in the wedge, which when entering a material being tested, simultaneously generates a longitudinal wave within the wide range of angles as well as transverse and surface waves. The range of transducer frequency is higher in comparison with that used during conventional ultrasonic tests and amounts to 1-15 MHz. In cases of thicknesses up to 50 mm, frequencies amounting to or higher than 3 MHz are used. Recommendations concerning the adjustment of frequency, transducer angles and sizes when performing the TOFD technique-based tests of welded joints are presented in Table 2 of PN-EN ISO 10863 [5].

In typical TOFD tests, the signal of a longitudinal wave is of the greatest importance. The velocity of a longitudinal wave is by twice faster than that of a transverse and surface wave. As a result, a longitudinal wave reaches the receiving transducer and gives an impulse as first. This is important because of practical reasons as the pro,cess of sizing requires the knowledge of wave velocity at which a given signal propagated. Sizing can be performed only using signals which covered the entire distance from the transmitting transducer to the receiving transducer as one wave type as it is only then that the signal velocity, necessary for further calculations, is known. In practice, the sizing of discontinuities does not pose difficulties within such a linearization range, where only signals of one ultrasonic wave type, i.e. longitudinal, are present. As a result, only the fragment of a TOFD image between the lateral wave and longitudinal back-wall reflection can be used for assessing the deposition depth of a discontinuity (Fig. 4). The fragment between the back-wall reflection and the transformed wave are used only for the detection of indications.
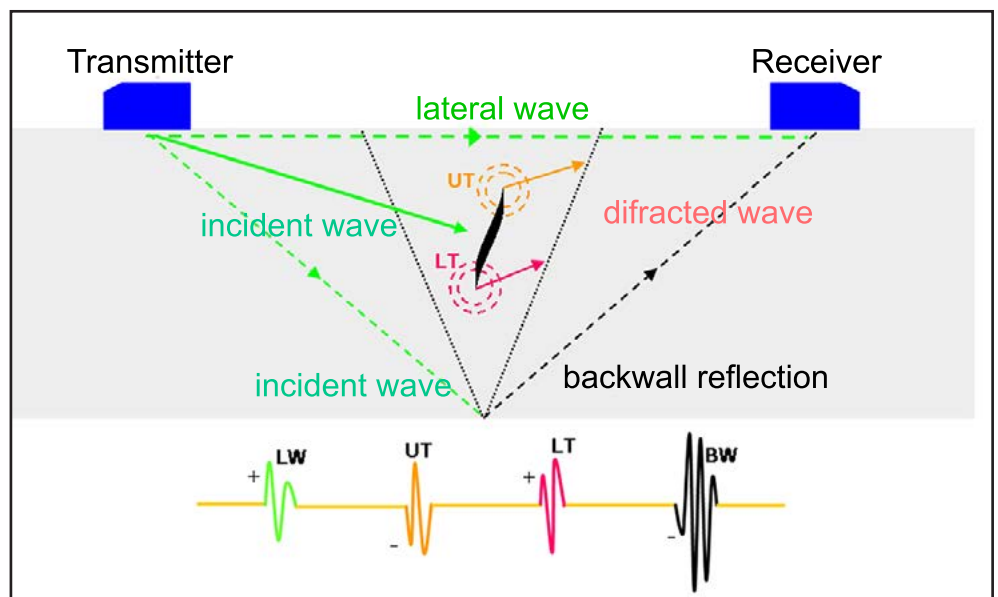

Fig. 3. Scheme of A type image generation during the TOFD technique-based tests

Normally, the TOFD-based tests are performed using a scanner provided with an encoder. The use of an encoder enables the graphic presentation of test results in 2D images, where, depending on the direction of scanner movement in relation to the ultrasonic beam axis, parallel and non-parallel scans can be obtained. Usually, non-parallel scans (in relation to the beam axis) are performed, i.e. where the direction of scanning is parallel to the weld. If it is necessary to obtain further information about the nature, location and space orientation of a discontinuity, it may be useful to make a parallel scan performed in the direction determined by the axes of transducers, usually transversely in relation to the weld axis.

A typical TOFD image contains signals of a subsurface and back-wall reflection, constituting a very comfortable reference point at the stage of TOFD image linearization and the dimensioning of indication depth (Fig. 4). The term of a lateral wave stands for the part of a longitudinal wave beam running directly under the surface, whereas the term of a back-wall reflection stands for the part of a longitudinal wave beam reflected from the opposite surface and entering the receiving transducer. In addition, the range from the back-wall reflection to the transformed wave contains signals which have covered at least some part of the path as a transverse wave. Due to the twice lower velocity of a transverse wave, the above named signals are moved to longer times. Figure 4 presents a TOFD image after the synchronisation of a lateral wave and linearization, obtained when testing a 15 mm MAG welded joint fragment. In addition to the above named constant signals, the TOFD image contains two internal indications of large incomplete side fusions, one indication reaching the surface opposite in relation to the scanning surface (indication of the lack of penetration on 115 mm of the joints) as well as several point indications of short interlayer incomplete fusions.

Standardisation of the TOFD Technique-Based Tests

The oldest standardisation document concerned with the TOFD technique was British standard BS7706. The standard was replaced by European standard EN 583-6, and currently ISO 16828, specifying the fundamentals of the TOFD technique-based tests. Afterwards, standards concerning tests of welded joints were developed, i.e. standard ISO 10863, specifying primary requirements as well as defining test levels and classifying indications and ISO 15626, specifying acceptance levels corresponding to quality levels according to ISO 5817. The last two standards constitute the basis for using the TOFD technique in acceptance tests with the acceptance criterion being a quality level according to ISO 5817. The correlation between quality levels, test levels and acceptance levels in relation to the TOFD technique-based tests is presented in Table 1.

The source of primary guidance on performing tests using the TOFD technique is PN-EN ISO 16828 *Non-destructive testing. Ultrasonic testing. Time-of-flight diffraction technique as a method for detection and*
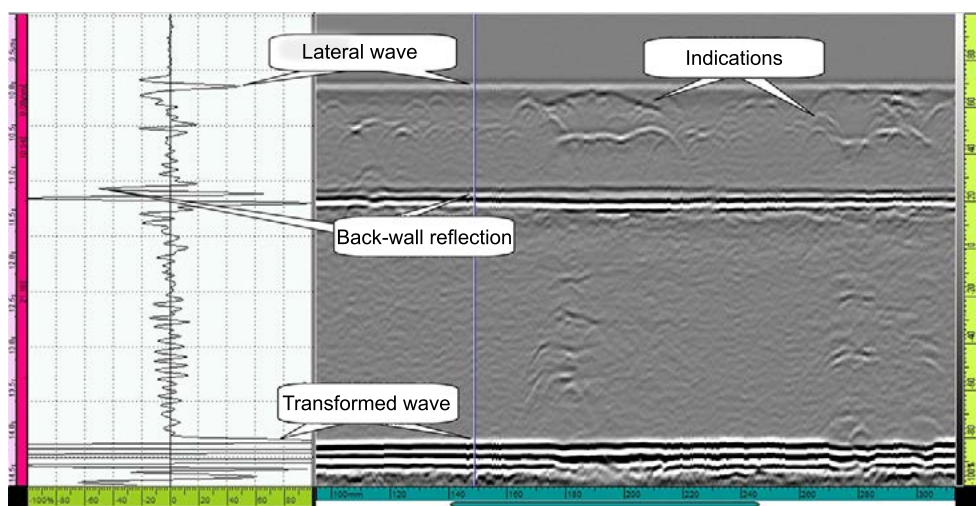

Fig. 4. TOFD image of a welded joint composed of B-scan (right) and A-scan (left); A-scan represents the area marked with the cursor (blue line) in B-scan

Table 1. Welded joint quality levels with corresponding test and acceptance levels when performing the TOFD technique-based tests [6]

Quality level according to ISO 5817	Test level according to ISO 10863	Acceptance level according to ISO 15626
B	C	1
C	at least B	2
D	at least A	3

sizing of discontinuities. Among other things, the standard provides primary definitions, general information concerning the test configuration of TOFD, the interpretation of TOFD images as well as requirements related to equipment and testing personnel. The standard defines the two primary types of TOFD scans, i.e. parallel scans, where the scanner moves in parallel to the axis of ultrasonic beams and a non-parallel scan, where the scanner does not move in parallel to the axis of ultrasonic beams. It should be noted that the non-parallel scan defined above is usually performed (when testing welded joints) along a weld, i.e. parallel to its axis. One might wonder why such an apparently illogical convention has been adopted. This is related to the history of the technique, which was initially used for the sizing of fatigue cracks in elements other than welded products. In such products, the only reference direction for the scanner movement was the orientation of the axis of an inserted ultrasonic beam.

Standard PN-EN ISO 16828 contains guidelines concerning the adjustment of test parameters, in particular, the frequency and size of a transducer, wedge refraction angle, time window settings and techniques used for adjusting the gain of a defectoscope. The standard contains guidance on the interpretation of indications and useful mathematical formulas enabling the calculation of scan resolution, size of dead zone and measurement uncertainty related to the deposition depth of discontinuity edge. It should be noted that standard PN-EN ISO 16828 is not specialised as regards tests of welded joints but only contains general guidance on TOFD tests.

The primary standard concerning tests of welded joints involving the TOFD technique is PN-EN ISO 10863 *Non-destructive testing of welds. Ultrasonic testing. Use of time-of-flight-diffraction technique (TOFD).* The standard defines the primary principles and requirements concerning tests of joints and specifies four test levels, i.e. A, B, C and D. Each subsequent test level from A to D requires better documented confirmation of the correct adjustment of equipment and detectability of welding imperfections, being the object of interest in such tests, and provides higher assurance of discontinuity detection. The standard also specifies requirements related to the quality of obtained test results (TOFD images), provides guidance on the interpretation and classification of detected imperfections as well as on the reporting of results. The standards also provide guidance on identifications at the test specification stage, personnel qualification, information to be provided to the operator prior to the performance of a test and requirements concerning test specification. In addition, the standard constitutes the source of guidelines concerning the design of master samples for the verification of equipment settings and detectability in tests utilising the TOFD technique.

Guidance on the evaluation of welded joints based on the TOFD test results is described in PN-EN ISO 15626 *Non-destructive testing of welds. Time-of-flight-diffraction technique (TOFD). Acceptance levels.* The standard specifies three acceptance levels, i.e. 1, 2 and 3, corresponding to quality levels B, C and D set out in PN-EN ISO 5817 accordingly. In addition, the standard specifies the primary symbols and definitions, provides information on principles of determining the length and height of a discontinuity on the basis of TOFD test results. The standard also discusses the principles of dimensioning and summing as well as presents three alternative techniques of measurement cursor positioning. It should be noted that, unlike in conventional ultrasonic tests, where acceptance

is conditioned by the amplitude and length of indications, in TOFD tests, assessments are based on the height, length and location of indications (reaching the surface or internal).

Primary Requirements of TOFD Tests According to PN-EN ISO 10863

The primary requirement as far as TOFD tests are concerned is the assurance of detectability over the entire area of interest. When testing welded joints during their formation it is assumed, accordance with valid standards, that the required area contains the entire volume of a weld along with the adjacent area including 10 mm on each side of the weld or the entire heat affected zone, whichever is greater. This area is tantamount to the area most likely to contain discontinuities formed during the making of welded structures. When testing objects during their operation, the standard allows the reduction of the above-presented test area and requires the identification of the minimum size of a discontinuity to be detected in an area subjected to a test.

The positioning of transducers during tests should ensure the coverage of the entire area of interest and the obtainment of imaging (diffraction) signals from discontinuities, should the latter occur. In cases of joints characterised by simple geometry and the narrow excess weld metal (of the face or root) on the side opposite to the surface subjected to scanning, guidelines concerning the positioning of transducers, presented in Table 2 of standard [5], guarantee the coverage of the entire area of interest. In cases of joints characterised by wide excess weld metal on the opposite side, e.g. when testing thick X-bevelled joints, it may be necessary to perform additional scans further from the weld axis. In such cases, it is necessary to verify detectability using appropriate master samples. It is necessary to use a constant reference system, i.e. master sample, and the same coupling system as the one used during the calibration of a defectoscope. Tests utilising the

TOFD technique do not require previous search for laminar imperfections in sheets, if any, as such imperfections are easily detectible using TOFD tests.

It is worth paying attention to specific terminology used in the ultrasonic echo technique, also appearing in standards concerning the TOFD technique. The notion of time window represents a time interval, during which a signal received by a receiving transducer (receiver), is detalised and recorded. In the TOFD technique, the zero point of the time base corresponds to the moment of transmitting signal initiation. It also means that the time lag, defined as the delay of the time base zero point in relation to the moment of signal initiation, amounts to zero. This notion cannot be identified with the notion of range, as the latter is used to depict a distance and is expressed in millimetres. In PN-EN ISO 10863, the notion of range or depth range is used to depict the range of observation defined as the depth range. Another notion widely used in the TOFD technique is wedge delay representing the time during which an ultrasonic beam passes through the wedges of ultrasonic transducers. The notion of wedge delay should not be identified with the shift of the time base zero point (time lag) used in the echo technique, as it is not connected with the shift of the time base in TOFD imaging, but is only used for the conversion of time at which a beam reaches a specific depth, referred to as linearization in English language publications.

Some attention should also be paid to certain inconsistencies in PN-EN ISO 10863. In item 10.1.1, the standard requires that the depth range and sensitivity be adjusted prior to testing (in accordance with the requirements of EN-583-6 [presently PN-EN ISO 16828]), which would imply the adjustment of gain in relation to the level of structural noise and the verification of detectability. At the same time, in item 10.1.4, the standard requires that the amplitude of a lateral wave amount to 40-80% of the screen height, which, in fact, imposes the

test gain. The noise level exceeding 20% of the screen height and the achievement of the entire screen height by the lateral wave require the repetition of the test.

It is required that, in the case of tests involving the single scan of the entire depth range, the time window start at least 1 μs before the signal of a lateral wave and finish after the first signal of a transformed wave. In cases of tests divided into zones, time windows should overlap by a minimum of 10% of the depth range.

In order to determine the distance between the centres of PCS transducers, it is the most favourable if the conversion of the time of linearization (i.e. when a beam reaches the deposition depth) is conducted through calibration using a lateral wave reflected at a known sonic velocity. It is required that the result of depth measurement be verified using an element of a known depth and that a measurement error not exceed 0.2 mm. However, the standard does not specify the manner of calibration. It should be noted that in order to obtain such a precise and verified result of depth measurement, an element subjected to a test, an element on which the system is calibrated and an element on which calibration is verified, should demonstrate the same sonic velocity. It should also be noted that the TOFD technique is significantly more sensitive to errors resulting from the difference in an ultrasonic wave velocity than the echo technique utilising a transmitting-receiving transducer. In addition, the standard requires the verification of test fixtures operational stability, i.e. gain and depth, at least prior to a test, every 4 h during the test and following the completion of the test.

Standard PN-EN ISO 10863 defines four test levels, i.e. A, B, C and D. The lowest level, i.e. level A does not require the use of a master (reference) sample but only the use of an element having a known thickness allowing the determination of linearization parameters (flight time–deposition

depth conversion). Test level A can be used only in cases of 6-50 mm thick joints representing quality level D. Test level B is used when testing joints representing quality level C and having a thickness of 6- 300 mm. In such a case, it is necessary to use a master sample for gain verification. In both cases it is not necessary to use test procedures and specimens for the verification of detectability. In cases of test levels C and D, e.g. used for joints representing quality level B, it is necessary to use a master sample for the verification of detectability and performing the above named tests on the basis of a written test procedure. Test level D is connected with the use of the highest requirements in terms of master samples and the validation of test procedures. Test level D is recommended when testing elements having complicated shapes and during operational tests [5].

Adjustment of Parameters for the TOFD Technique

Table 2 of standard [5] presents guidelines concerning the adjustment of the TOFD technique test parameters in relation to the thickness of a joint being tested. The table contains information related to the necessary number of scans and parameters of heads used for searching a given joint zone (depth range). In addition, the table provides information about frequency, transducer size, nominal beam insertion angle and the beam intersection point. Joints having thicknesses of up to 50 mm require a single TOFD scan including the entire joint thickness range (from 0 to t). In such a case, the beam intersection point is located at 2/3 of the depth.

Table 2. Parameters recommended during the TOFD technique tests of butt joints having a thickness of 6 to 50 mm [5]

Joint thickness t, mm	Frequency f, MHz	Wedge refraction angle α, °	Transducer size d, mm
6 to 10	15	70	2 to 3
>10 to 15	15 to 10	70	2 to 3
>15 to 35	10 to 5	70 to 60	2 to 6
>35 to 50	5 to 3	70 to 60	3 to 6

For thickness t=50÷100 mm it is necessary to divide a joint into two zones (Fig. 5). The first zone includes the range of 0 to $t/2$, whereas the second zone includes the range of $t/2$ to t. The beam intersection point for the first zone is located at a depth amounting to $1/3\ t$. For the second zone, the beam intersection point is located at a depth amounting to $5/6\ t$. As a rule, each of the zones requires the use of different test parameters. An increase in the depth of a given zone is accompanied by a decrease in required frequency and angle and by an increase in the transducer size. Similarly, for thickness t =100÷200 mm, a joint must be divided into three zones, whereas for thickness t=200÷300 mm it is necessary to divide a joint into four zones. Exemplary parameters for joints having a thickness of up to 50 mm are presented in Table 2.
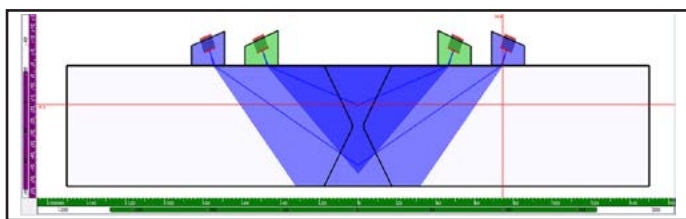

Fig. 5. Exemplary design of TOFD technique tests with division into zones using the NDT Setup Builder software developed by Olympus; joint thickness: 52 mm; beam intersection point for the first pair of heads is located at a depth of 17 mm, for the second pair of heads it is located at a depth of 43 mm

Most of the parameters are presented in the form of a range. This is because of the fact that a change in the joint thickness of several millimetres entails a significant change in the length of the wave in the material, particularly in cases of large beam insertion angles. Using high frequency waves significantly reduces the amplitude of diffracted waves due to damping and, as a result, leads to the lack of distinct indications in the TOFD imaging, hence the gradual reduction of frequency and wedge refraction angle accompanying the increase in joint thickness. The precise adjustment of test parameters must be determined experimentally so that the obtained TOFD imaging could satisfy the

requirements of related standards in terms of the amplitude of lateral wave as well as of structural and electronic noise. Test levels C and D require additional verification of the correctness of settings using the specimen for the verification of detectability.

Standard PN-EN ISO 16828 also provided information on the recommended test parameter ranges in the TOFD method, yet they are significantly wider than those described above according to PN-EN ISO 10863. It should be noted that the requirements of both standards are not always coherent. For instance, according to standard [5] concerning tests of welded joints, the testing of a 10 mm thick joint requires using the frequency of 15 MHz (Table 2 in [5]). In turn, according to PN-EN ISO 16828, a thickness of 10 mm is located on the border of thickness ranges and, because of that, requires the frequency range of 5 to 10 MHz (Table 1 in [7]). In such a case it seems more favourable to satisfy the requirements of the standard concerning the testing of welded joints [5] and to use a frequency of 15 MHz.

Summary

Because of high detectability and the entire archiving of results, tests of welded joints using the TOFD technique constitute an advantageous alternative to relatively expensive and problematic X-ray radiographic or conventional ultrasonic tests, where the correctness of results is highly dependent on operator knowledge and experience. An additional advantage connected with the use of modern TOFD test systems is the possibility of evaluating results on an "off-line" basis, using compatible computer software, while the testing equipment can be used to perform further series of tests, significantly increasing its efficiency. Another important aspect is the possibility of performing tests using the TOFD technique combined with the Phased Array technique, which, presently, is the most effective system of detecting, characterising and dimensioning imperfections in welded

joints. For this reason, the article is concerned with discussing the most important requirements contained in standards related to the NDT of welded joints using the TOFD technique. In addition, the article analyses the essence of the formation of discontinuity indications using imaging (diffraction) signals and discusses standard documents concerning tests utilising the TOFD technique as well as the primary requirements related to the performance of tests and the selection of parameters.

References

[1] Charlesworth J. P., Temple J. A. G.: *Engineering applications of ultrasonic time-of-flight diffraction*. Second edition. Research Studies Press Ltd, Baldock, 2001.

[2] Mackiewicz S., Kopiński J.: *Doświadczenia z zastosowań ultradźwiękowej techniki TOFD*. Materials of the Seminar "Non-Destructive Testing of Materials", Zakopane, 2001.

[3] Olympus NDT: *Introduction to Phased Array Ultrasonic Technology Applications R/D Tech Guideline*. Published by Olympus NDT, Canada, 2004.

[4] Ginzel E., Honarvar F., Yaghootian A.: *A Study of Time-of-Flight Diffraction Technique Using Photoelastic Visualisation*. The 2nd International Conference on Technical Inspection and NDT (TINDT2008), Teheran, Iran, October, 2008.

[5] PN-EN ISO 10863:2011: *Non-destructive testing of welds – Ultrasonic testing – Use of time-of-flight diffraction technique (TOFD)*

[6] PN-EN ISO 15626:2014: *Non-destructive testing of welds – Time-of-flight diffraction technique (TOFD) – Acceptance levels*

[7] PN-EN ISO 16828:2014: *Non-destructive testing – Ultrasonic testing – Time-of-flight diffraction technique as a method for detection and sizing of discontinuities*

Paweł Irek, Łukasz Rawicki, Karol Kaczmarek

Dye Penetrant Testing of Welded Joints Made of Nickel and its Alloys

Abstract: The article presents tests involving natural cracks, including measurements of the width of cracks and the profile of their surface roughness. The investigation also involved tests performed in order to observe how a given factor affects development times in penetrant tests as well as to determine what time of development is recommended for nickel and its alloys in order to detect unacceptable welding imperfections (cracks). The article also discusses the effect of penetration times on the duration of development times and sizes of indications in penetrant tests.

Keywords: non-destructive testing, dye penetrant testing, nickel alloys

Introduction

Welding processes can be accompanied by the formation of welding imperfections compromising the strength of welded joints. The most important imperfections in terms of welded structures are cracks. Surface cracks can be detected using various non-destructive testing methods. One of the most popular NDT methods is penetrant testing. During penetrant tests, a penetrant, supported by a developer, "leaves" a discontinuity to reach the surface subjected to the test. As a result, a dye or fluorescent technique-based indication is obtained (Fig. 1). The time after which a penetrant reaches the surface,
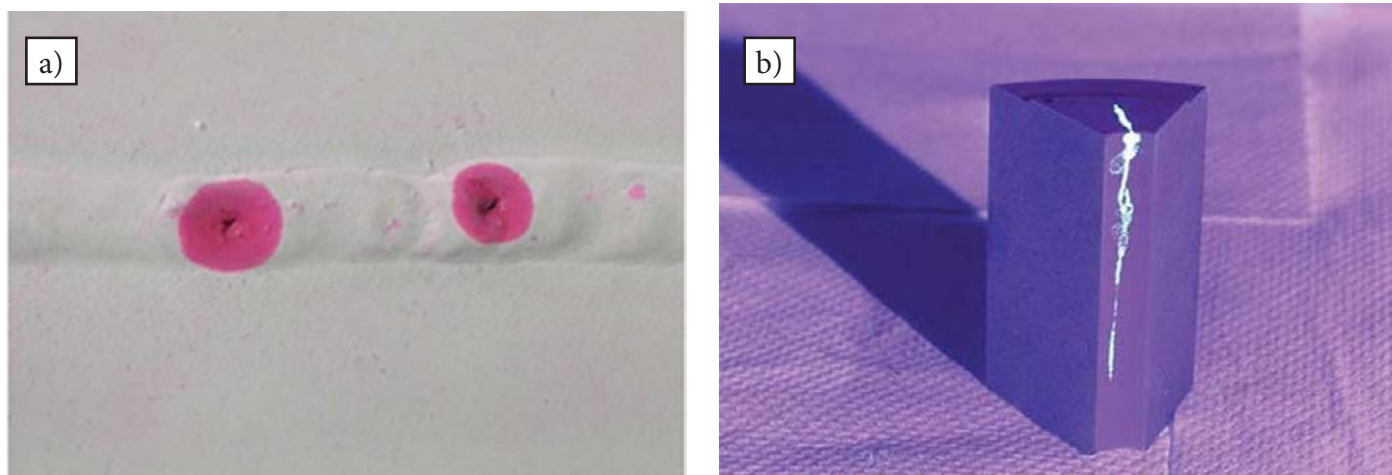

Fig. 1. Indications obtained during penetrant tests: a) using the dye penetrant method (observation of the surface in natural light), b) using the fluorescent method (observation of the surface in UV-A radiation)

dr inż. Paweł Irek (PhD (DSc) Eng.), mgr inż. Łukasz Rawicki (MSc Eng.), dr inż. Karol Kaczmarek (PhD (DSc) Eng.), – Instytut Spawalnictwa, Welding Education and Supervision Centre
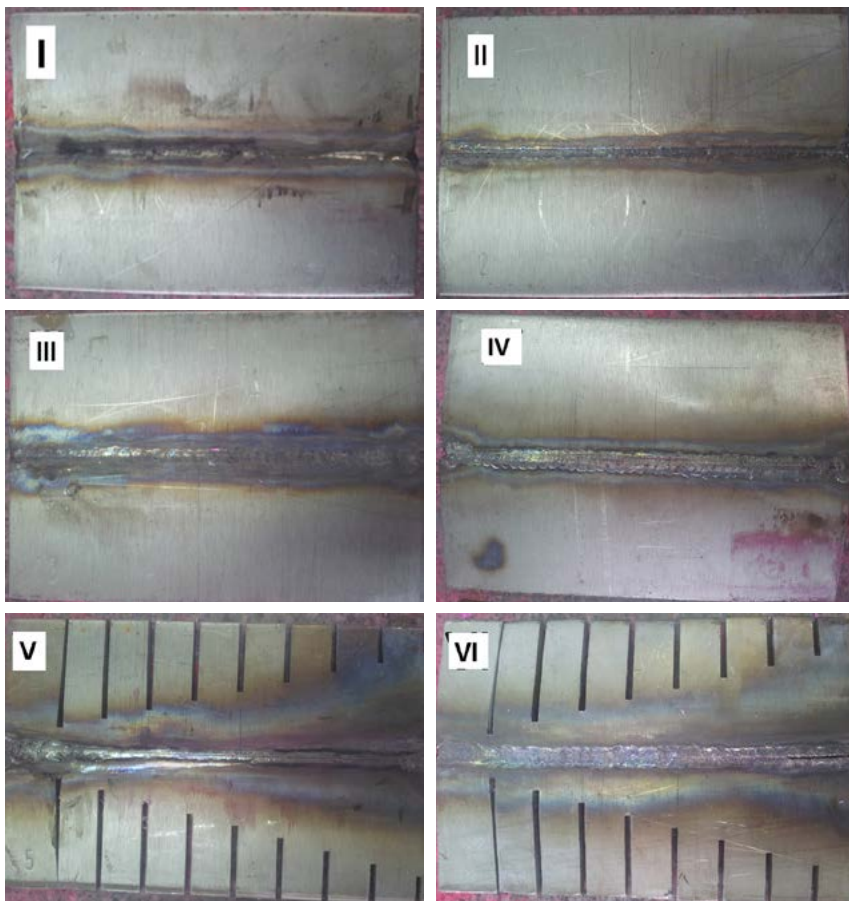
Fig. 2. Butt joints made of Nickel 200. Roman numerals represent numbers of successive joints
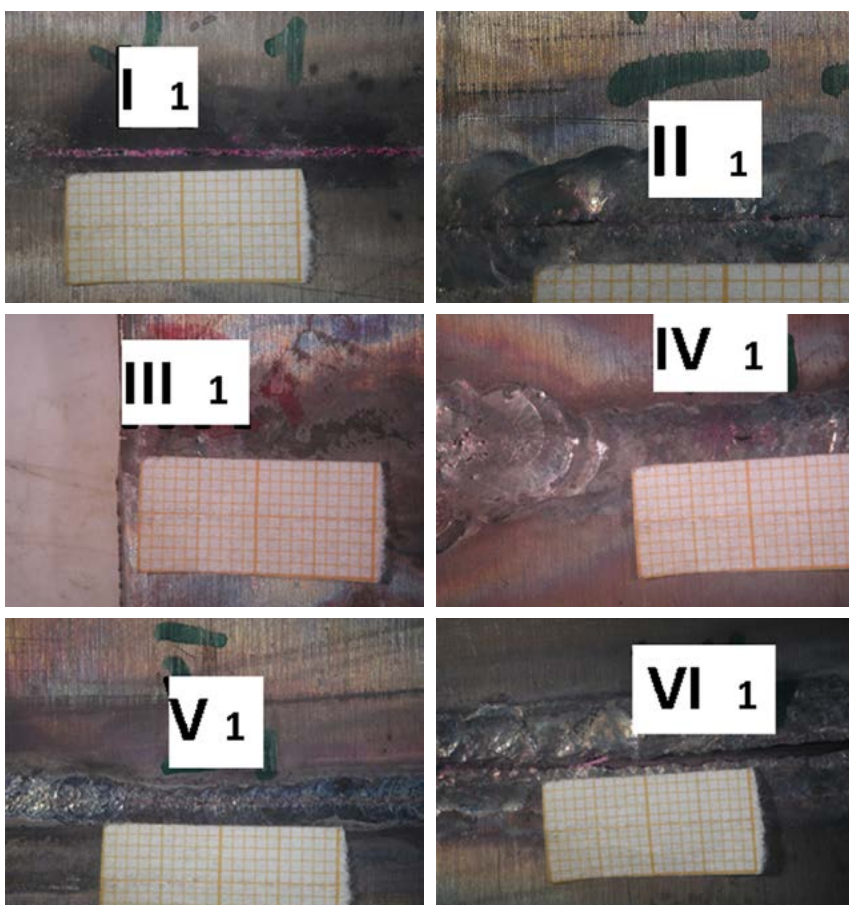
Fig. 3. Exemplary cracks in the butt joints made of nickel (magnified 4x). Roman numerals represent numbers of successive joints; Arabic numerals represent number of successive cracks in a given joint

referred to as the time of development, may vary from several minutes to even 24 hours. The objective of the investigation was to determine how the width of a crack and the roughness of its surface affect the time of development in welded joints made of nickel and its alloys and what time of development should be used in relation to these materials. In order to obtain more accurate results, the tests described in the article were performed using natural cracks [1-3].

Test Specimens

The tests involved the use of Nickel 200. The determination of crack widths involved making 6 butt joints (140×240×6 mm) (Fig. 2). The melting of plates nos. 5 and 6 was not followed by the formation of cracks. In order to solve this problem and create cracks, plates nos. 5 and 6 were cut at the area of melting and welded. The butt joints were welded using the TIG method without a filler metal. The test joints were provided with numerals.

Tests

Before the tests and measurements, the specimens were thoroughly cleaned, i.e. post-processing remains were removed and the surface to be tested was degreased in an ultrasonic washer using extraction naphtha and cleaning solvent. After washing, the specimens were dried at a temperature of approximately 20°C, using a stream of compressed air. As expected, the butt joints developed cracks (see Fig. 3 and 4).

Macroscopic photographs of the cracks were made using an Olympus szx9 stereoscopic microscope at 4x and 28.5x magnification. The widths of the cracks were measured using the Auto CAD 2012 software programme and digital photographs containing visible cracks. The measurement accuracy amounted to 4 μm. The number of measurements performed for each crack varied as measurements of crack widths were performed at 1 millimetre intervals. Therefore, depending on the length of each crack, the number of measurements varied between a few to more than a hundred. The designations and widths of the cracks in the butt joints are presented in Table 1.

Table 1. Designations and the width of the cracks in the butt joints made of Nickel 200

Number of joint	Crack number	Crack width, μm
I	1	8÷612
	2	28÷368
	3	4÷340
II	1	4÷456
III	1	4÷204
IV	1	4÷272
	2	4÷48
	3	4÷248
	4	4÷104
V	1	4÷684
VI	1	4÷1228

The width of 11 measured cracks was restrained within the range of 4÷1228 μm. Before breaking, the crack areas (in order to measure the roughness profile of crack surfaces) were subjected to dye penetrant tests. The penetrant tests of the cracks involved the use of a set of testing aerosols designated, following the requirements of standard PN-EN ISO 3452-1, as IICe-2, type 'Diffu-Therm", manufactured by H. Klumpf Techn. Chemie KG D-45699 Herten. The aerosols used in the tests were as follows:
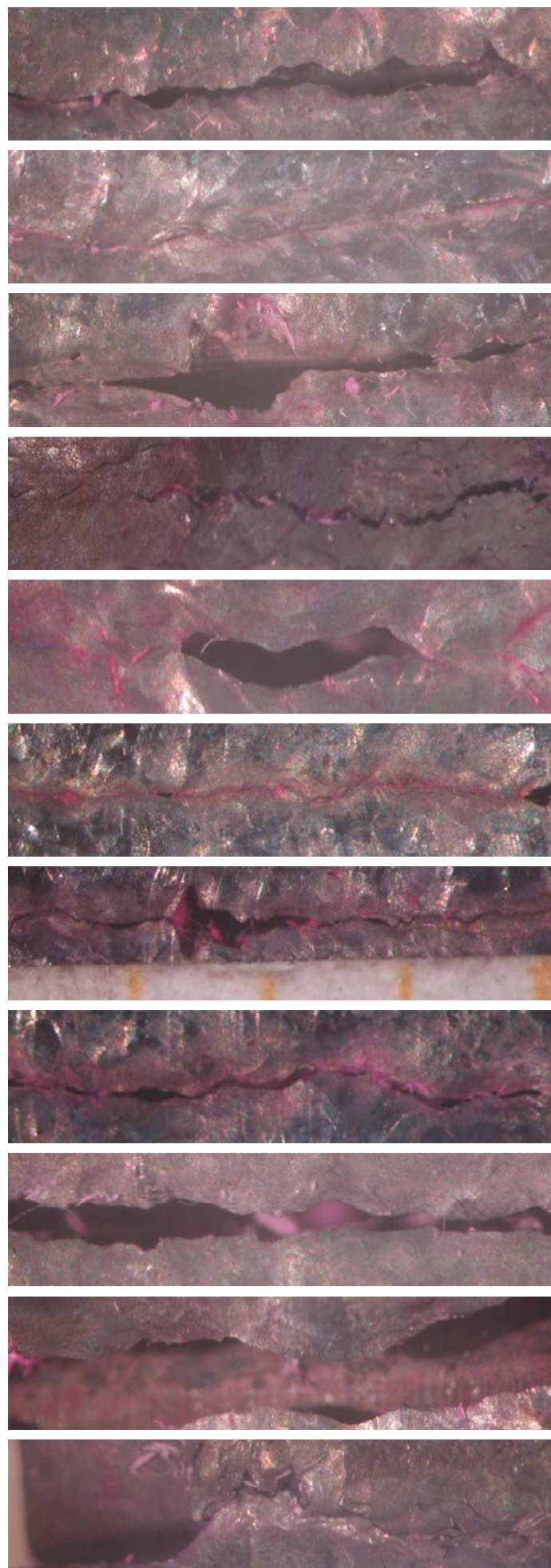– penetrant – red colour, type BDR-L, lot no.: 20 15, filling date: 09/2015;

Fig. 4. Exemplary cracks in the butt joints made of nickel (magnified 28.5x)

– remover – type Bre, lot no.: 22 16, filling date: 02/2015;
– developer – type Bea, lot no.: 23 16, filling date: 06/2015;
– guarantee period – 2 years;
– no chlorine or sulphur compounds in the chemical composition.

The tests involved the use of the following measuring equipment:
– luxmeter – type LX 105 manufactured by the company "LX Lutron";
– thermometer/hygrometer, model 303;
– caliper with measurement accuracy of 0.02 mm;
– workshop magnifying glass (4x);
– non-shredding fabric.

The penetrant tests of the cracks were conducted in the following conditions:
– temperature of tested surface – 22°C;
– ambient humidity – 23%;
– penetration time – 10, 30, 90 and 120 minutes;
– development time – until the end of indication development;
– illuminance of tested surface – 584 lx;
– observation distance – 10-30 cm;
– observation angle – from 60 to 90°.

The tests involved all of the cracks in several tests, where variables were the time of penetration and the time of development. The time of penetration amounted to 10, 30 and 120 minutes; the penetrant was applied several times so that a surface subjected to the tests was permanently covered by the penetrant. The different values of penetration time enabled examining the effect of the time of penetration on the time of development. On the basis of information contained in reference publications, the time of penetration was extended to 120 minutes, in comparison with recommendations of related standards, stating that the time of penetration should be restricted within the range of 5 to 60 minutes. The additional measurement was related to the time of development when the penetrant was applied only one time (90 minutes). The measurements of indications were conducted after 5, 10, 15, 20, 30, 40, 50 and 60 minutes etc., until the end of the development of a given indication (Table 2). Only one indication of the longest crack was recorded for each specimen. Each penetrant test was performed 3 times for specific parameters and the results were averaged.

The measurements performed at the initial stage of indication appearance aimed at the more accurate determination of the dependence being the subject of this work and the dynamics of crack formation. The adopted maximum time of indication development exceeded the recommendations formulated in standard Pn-en iso 3452-1, stating that the time of development should be restricted within the range of 10 to 30 minutes. The time adopted in the tests was extended in order to determine the recommended time of indication development regardless of the recommendation specified in the above named standard. The specimens with developed indications are presented in Figure 5.
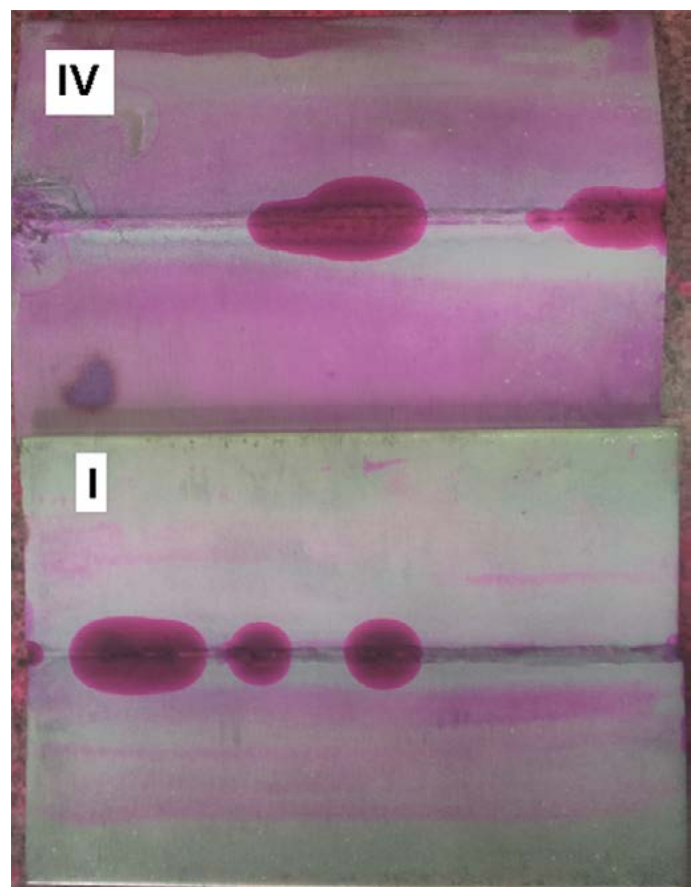

Fig. 5. Selected specimens made of nickel with indications originated in cracks. Roman numerals represent numbers of successive joints

Table 2. Sizes of indications originated in the cracks formed on the joints made of nickel. The penetrant was applied so that the entire tested surface was permanently covered by the penetrant; * - test joint covered by the penetrant once

Specimen no. I

Time of penetration, min	Development time, min																			
	5	10	15	20	25	30	40	50	60	70	80	90	100	110	120	140	170	200	230	260
10	40.5	42.0	43.5	44.5	46.0	47.5	48.5	49.5	51.0	52.0	52.5	53.0	53.5	54.0	54.5	55.0	56.0	-	-	-
30	40.0	42.0	43.5	45.0	46.0	47.5	49.0	50.0	51.5	52.0	52.5	53.0	53.5	54.5	55.0	56.0	57.0	57.5	-	-
120	39.0	41.0	42.5	44.0	45.5	47.0	48.0	49.0	50.0	51.0	52.0	52.5	53.0	53.5	54.0	55.0	56.0	57.0	57.5	-
90*	39.0	41.0	42.0	43.5	45.0	45.5	47.0	48.0	48.5	-	-	-	-	-	-	-	-	-	-	-

Specimen no. II

Time of penetration, min	Development time, min																			
	5	10	15	20	25	30	40	50	60	70	80	90	100	110	120	140	170	200	230	260
10	46.0	48.0	48.5	49.0	49.5	50.0	50.5	51.5	52.0	52.5	53.0	53.5	54.0	54.5	-	-	-	-	-	-
30	47.0	47.5	48.5	49.0	49.5	50.0	50.5	51.0	51.5	52.0	52.5	53.0	53.5	54.0	-	-	-	-	-	-
120	47.0	48.0	48.5	49.0	49.5	50.0	50.5	51.0	51.5	52.0	52.5	53.0	53.5	54.0	54.5	55.0	56.0	57.0	-	-
90*	47.0	48.0	48.5	49.5	-	-	-	-	-	-	-	-	-	-	-	-	-	-	-	-

Specimen no. III

Time of penetration, min	Development time, min																			
	5	10	15	20	25	30	40	50	60	70	80	90	100	110	120	140	170	200	230	260
10	9.0	-	-	-	-	-	-	-	-	-	-	-	-	-	-	-	-	-	-	-
30	8.5	-	-	-	-	-	-	-	-	-	-	-	-	-	-	-	-	-	-	-
120	9.0	-	-	-	-	-	-	-	-	-	-	-	-	-	-	-	-	-	-	-
90*	8.0	-	-	-	-	-	-	-	-	-	-	-	-	-	-	-	-	-	-	-

Specimen no. IV

Time of penetration, min	Development time, min																			
	5	10	15	20	25	30	40	50	60	70	80	90	100	110	120	140	170	200	230	260
10	52.5	56.0	57.0	58.5	59.5	61.0	62.5	64.0	65.0	66.0	67.0	67.5	68.0	68.5	-	-	-	-	-	-
30	53.0	56.5	57.5	59.0	60.0	61.5	63.0	64.5	65.5	66.0	67.0	68.0	68.5	68.5	69.0	-	-	-	-	-
120	53.0	56.0	57.5	59.0	60.5	62.0	63.0	64.0	65.0	66.0	67.0	68.0	68.5	69.0	69.5	70.0	71.0	-	-	-
90*	59.0	59.5	60.0	60.5	-	-	-	-	-	-	-	-	-	-	-	-	-	-	-	-

Specimen no. V

Time of penetration, min	Development time, min																			
	5	10	15	20	25	30	40	50	60	70	80	90	100	110	120	140	170	200	230	260
10	143.0	146.0	148.0	149.0	150.0	151.0	153.0	155.0	156.0	157.0	158.0	159.0	159.5	160.0	-	-	-	-	-	-
30	144.0	146.0	148.0	149.5	151.0	152.0	154.0	155.5	156.0	157.0	158.0	159.0	159.5	-	-	-	-	-	-	-
120	144.0	146.0	148.5	150.0	151.0	152.0	154.0	156.0	157.0	158.0	158.5	159.0	159.0	159.5	160.0	160.5	161.5	162.0	-	-
90*	143.0	146.0	148.0	149.0	150.0	151,0	152,0	-	-	-	-	-	-	-	-	-	-	-	-	-

Specimen no. VI

Time of penetration, min	Development time, min																			
	5	10	15	20	25	30	40	50	60	70	80	90	100	110	120	140	170	200	230	260
10	74.5	76.0	78.0	79.5	80.5	81.0	82.0	83.0	84.0	85.0	85.5	86.0	86.5	-	-	-	-	-	-	-
30	75.0	77.0	78.0	79.0	80.0	81.0	82.5	83.5	84.0	84.5	85.0	86.0	-	-	-	-	-	-	-	-
120	75.0	76.5	78.0	79.0	80.0	81.0	82.5	83.5	85.0	85.5	86.0	86.5	87.0	87.5	88.0	89.0	89.5	-	-	-
90*	77.0	78.0	79.0	80.5	81.0	81.0	81.5	82.5	84.0	-	-	-	-	-	-	-	-	-	-	-

Note: Indication sizes provide information about the greatest values of indication in millimetres

The penetrant tests of the nickel specimens containing the cracks revealed that one of the objectives of the work had been satisfied. The tested differences in penetration time related to the joints made of nickel revealed that at longer penetration times (120 minutes) indications were greater, which could imply the necessity of extending both the time of penetration and the time of development in relation to these materials. Sometimes, at a shorter penetration time (10 minutes), the indications were slightly greater than those obtained at a penetration time of 30 minutes. Such differences rather demonstrated the specific nature of the test process itself as the process of penetrant testing consists of a number of phases, each of which must be performed paying significant attention to detail. Each negligence, usually unintended, in the testing process decreases its sensitivity, leading to the obtainment of a different final result. Knowing this, it is easy to explain detected inaccuracies, i.e. greater indications obtained at shorter penetration times. When the penetrant was applied once, the indications were significantly smaller and the time of development was shorter. It was also noticeable that in most of the cases, the size of indications grew dynamically up to approximately 15-20 minutes of development time. After this time, the increase in indications was very slow and in most of the cases finished after approximately 200 minutes (Fig. 6).
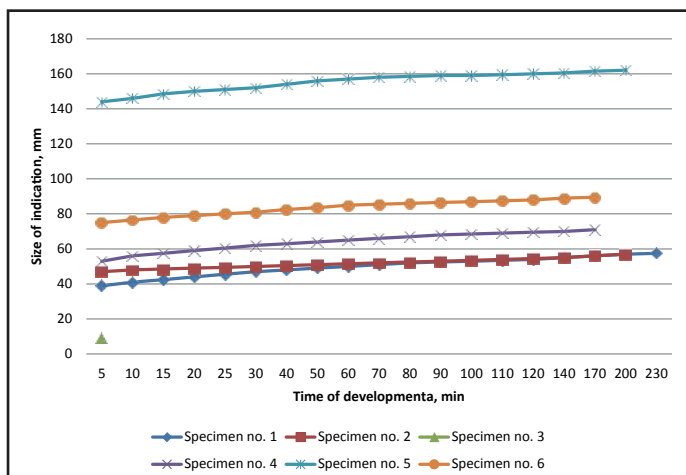
This implies that when performing penetrant tests of joints made of nickel and its alloys, the time mentioned above can be recognised as adequate for detecting unallowed external imperfections (such as cracks). The tests also revealed a tendency that an increase in the width of a crack was accompanied by an increase in the time of development.

Another stage of the tests involved measurements of crack surface roughness. In order to determine profiles of roughness in the cracks, the butt joints were broken in the areas where the cracks were formed. The rig used for testing the profile of roughness was provided with the Turbo Datawin-NT software programme integrated with a Hommel tester T1000 (contact profile measurement gauge) (Fig. 7). The measurement equipment enabled complex dimensional and statistical analyses of microgeometrical parameters as well as the visualisation of the stereometric structure of a surface subjected to measurement. The equipment made it possible to measure the following profiles:

– roughness (R),
– waviness (W),
– primary profile (P) and roughness core parameters (Rk) as well as parameters of the motif-detection method (WD1 and WD2).

Fig. 6. Dependences between indication sizes and development times for the cracks formed in the joint made of nickel

Fig. 7. Hommel tester T1000 contact profile measurement gauge

Such a wide range of measurements was necessary in order to determine correct values of the surface roughness profile. An issue posing difficulty was the waviness of the surface, the roughness of which was to be measured. As a result, the equipment made two measurements, i.e. the surface profile and the roughness profile (Fig. 8).
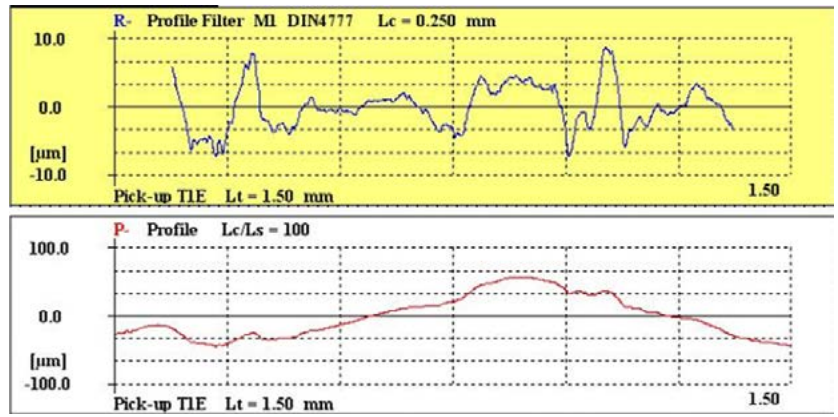
After approximating the value obtained after measuring the surface profile, the software programme converts this value into the profile of roughness. In addition, during measurements, the screen displays the visualisation of the stereometric structure of the surface being measured (Fig. 9).
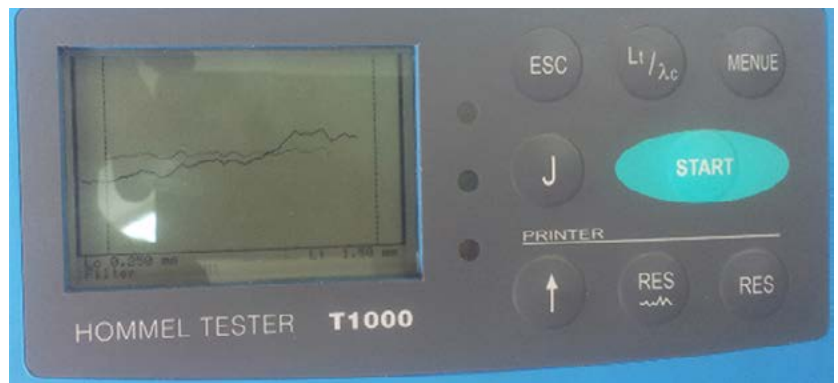
The software programme integrated with the profile measurement gauge provides a lot of data concerning the surface being measured (Fig. 10). This work discusses one of these parameters, namely Ra, i.e. the average arithmetic deviation of the profile from the average line. The profile of roughness was measured for each crack in 3 areas; afterwards, measurement results were averaged (Table 3). Due to the shape of the joint surface after breaking, not all cracks could be measured.
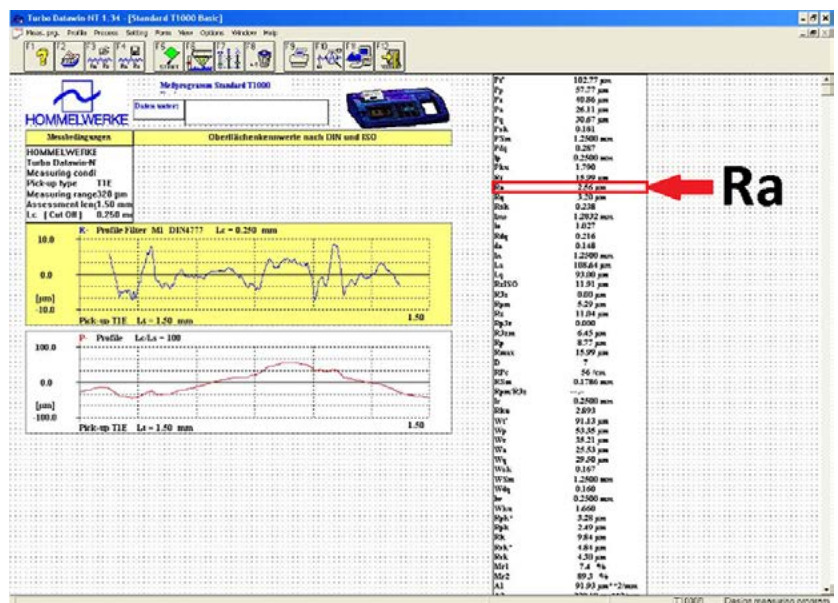
The roughness of surface was measured in accordance with recommendations specified in standard Pn-en iso 4288:2011e. The length of elementary segment l_r amounted to 0.8 mm or 2.5 mm, whereas the length of measurement segment l_t amounted to 4.8 mm and 15 mm respectively.

Fig. 8. Measurement of surface roughness (top) and of the profile (bottom)

Fig. 9. Visualisation of the stereometric structure of the surface being measured

Fig. 10. Window of the Turbo Datawin-NT software programme. The red colour indicates parameter Ra (analysed in the work)

Table 3. Roughness of surfaces of the cracks detected in nickel Nickel 200

Plate/joint	I	I	I	II	III	IV	IV	IV	IV	V	VI
Crack	1	2	3	1	1	1	2	3	4	1	1
Roughness *Ra*, μm	3.98	4.57	5.15	2.41	2.61	7.40	1.39	2.56	3.40	1.66	4.00

Note: Roman numerals represent numbers of successive joints; Arabic numerals represent number of successive cracks in a given joint

The value of the elementary segment and the value of the measurement segment depend on the range of roughness expected on the surface being measured.

The roughness of crack surfaces was restricted within the range of 2.01 to 13.24. When comparing the results concerning the roughness of crack surfaces it was noticed that in relation to previously performed penetrant tests. the time of development was longer in cases of cracks characterised by a greater roughness of surface.

Conclusions

The analysis of the test results led to the formulation of the following conclusions:

1. As regards penetrant tests of nickel and its alloys, the time of penetration significantly affected times of development and sizes of indications and, therefore should be extended to 120 minutes.

2. In most cases, the single-time application of a penetrant resulted in a shorter development time and smaller-sized indications in comparison with situations when a penetrant was applied several times.

3. Each of the tested factors significantly affected development times in the penetrant tests, which was demonstrated by various development times in cases of various cracks.

4. An increase in the roughness of crack surface was accompanied by an increase in the time of development, which could probably be attributed to the greater spread of the surface and, as a result, the greater volume of penetrant located in a given discontinuity.

5. An increase in the width of a crack was accompanied by an increase in the time of development; this was because of the greater volume of penetrant in a given crack.

6. It is recommended that in penetrant tests of nickel and its alloys the time of development be extended to approximately 200 minutes. In most cases, such a time is sufficient for detecting unacceptable welding imperfections.

References:

[1] Czuchryj J., Hyc K.: Dye-penetrant method assessment of the size of surface discontinuities in products made of carbon structural steel. Biuletyn Instytutu Spawalnictwa, 2012, no. 02, pp. 37-45
http://bulletin.is.gliwice.pl/index.php?go=current&ebis=2012_02_04

[2] Czuchryj J., Irek P.: Dye penetrant method of the assessment of the pores size in welded joints made of aluminium and its alloys. Biuletyn Instytutu Spawalnictwa, 2014, no. 4, pp.
http://bulletin.is.gliwice.pl/index.php?go=current&ebis=2014_04_02

[3] Czuchryj J., Irek P.: Dye-Penetrant Method Assessment of the Size of Pores in Welded Joints Made of High-Alloy Steel. Biuletyn Instytutu Spawalnictwa, 2015, no. 1, pp. 21-28
http://bulletin.is.gliwice.pl/index.php?go=current&ebis=2015_01_03

References standards:

- PN-EN ISO 3452-1: *Non-destructive testing — Penetrant testing — Part 1: General principles*
- PN-EN ISO 3452-2: *Non-destructive testing — Penetrant testing — Part 2: Testing of penetrant materials*
- PN-EN ISO 3452-3: *Non-destructive testing — Penetrant testing — Part 3: Reference test blocks*
- PN-EN ISO 3452-4: *Non-destructive testing — Penetrant testing — Part 4: Equipment*
- PN-ISO 3058: *Non-destructive testing — Aids to visual inspection — Selection of low-power magnifiers*
- PN-EN ISO 3059: *Non-destructive testing — Penetrant testing and magnetic particle testing - Viewing conditions*
- PN-EN ISO 12706: *Non-destructive testing — Penetrant testing — Vocabulary*
- PN-EN ISO 6520-1: *Welding and allied processes — Classification of geometric imperfections in metallic materials — Part 1: Fusion welding*

Ryszard Krawczyk, Jakub Kozłowski

Analysing the Effect of Changes in Overlay Weld Geometry on Test SEP 1390

Abstract: The article presents issues related to the assessment of the weldability of thick-walled materials used when making welded steel structures. The article also discusses the analysis of test results based on the technological test concerning the weldability of thick-walled structural materials according to the guidelines of SEP 1390. The tests took into consideration the effect of the change in overlay weld geometry on the technological test, and, as a result, the final result of weldability assessment.

Keywords: weldability, properties of structural materials, bend test, crack assessment, destructive tests

Introduction

The making of thick-walled welded structures continues to pose numerous difficulties in spite of continuous developmental progress in many areas of manufacturing technologies, including welding and metallurgical processes. Thick-walled welded joints require being particularly carefully made, following the development of appropriate technological conditions. One of the key factors affecting the successful making of good quality joints is the proper determination of base material weldability, usually based on both analytical and simulations methods, often involving technological tests [1, 2]. Technological tests serving the above named purpose are usually used to verify analytical methods and confirm quality assumptions required by related standards and guidelines. Recommended technological tests are related to

crack mechanics, i.e. the initiation and propagation of cracks in structural materials and joints [3]. Technological test SEP 1390 recommended by the German Institute of Steel and Iron (ABV) and used for assessing the weldability of thick-walled structural materials also serves the purpose mentioned above.

The objective of this study includes analysing the results of tests performed on the basis of SEP 1390 guidelines and taking into consideration the effect of a change in overlay weld geometry on the proper course and result of test SEP 1390 when assessing the weldability of thick-walled structural materials. Provided that technological test SEP 1390 is performed properly, the analysis of test results should provide valuable information concerning the proper determination of material weldability.

dr inż. Ryszard Krawczyk (PhD (DSc) Eng.), mgr inż. Jakub Kozłowski (MSc Eng.) – Częstochowa University of Technology; Welding Department
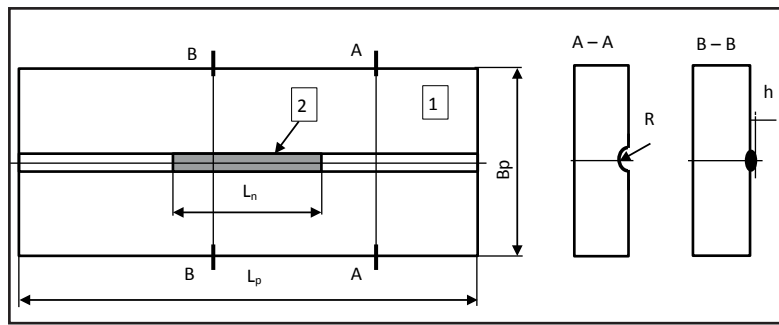
Fig. 1. Scheme of the specimen subjected to test SEP 1390
1: material, 2: overlay weld [4]

Table 1. Dimensions of the specimens in relation to the thickness of tested material [4]

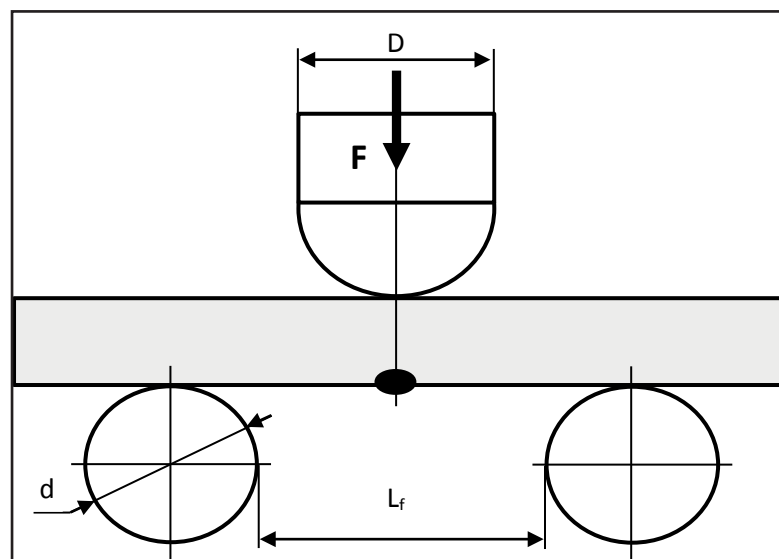| Material thickness g [mm]	Specimen length L_p [mm]	Specimen width B_p [mm]	Overlay weld length L_n min [mm]	Groove radius R [mm]
$30 \leq g \leq 35$	410	200	175	4
$35 < g \leq 40$	440	200	190	4
$40 < g \leq 45$	470	200	220	4
$45 < g \leq 50$	500	200	220	4
$g > 50$	500	200	220	4

Fig. 2. Scheme of the weldability test performed within the bend test [4]

Table 2. Dimensions of the scheme involving the bend tests of the specimens [4]

Material thickness g [mm]	Mandrel diameter D [mm]	Distance between supports L_f [mm]	Support diameter d [mm]
$30 \leq g \leq 35$	105	190	
$35 < g \leq 40$	120	220	
$40 < g \leq 45$	135	250	≥ 50
$45 < g \leq 50$	150	280	
$g > 50$	150	280	

Characteristics of Weldability Test SEP 1390

Test SEP 1390 is focused on the weldability of materials having a minimum yield point restricted within the range of 235 MPa to 355 MPa and a thickness equal to or exceeding 30 mm [4,5]. The weldability tests consist in bending a specimen sampled from a material with an appropriately made overlay weld located in a groove milled along the specimen axis. The bend test assesses the possibility of blocking a crack induced in a special overlay weld subjected to tension during the bending of the specimen. The shape of the specimen sampled for the tests is presented in Figure 1. The dimensions of specimens in relation to the thickness of a material being tested are presented in Table 1 [4].

When testing thicker materials, it is necessary to remove the excess material to a thickness of 50 mm, leaving one post-roll unprocessed surface. The satisfaction of this condition is necessary because of limitations concerning loads of up to 1000 kN on standard testing machines. The scheme of a weldability test performed in a bend test involving a properly prepared specimen is presented in Figure 2. Important dimensions concerning the specimens are presented in Table 2.

The bend tests are performed using a testing machine having a significantly large load range, preferably up to 1000 kN, using appropriate fixtures according to the test scheme presented in Figure 2.

Preparation of Test Specimens

Material

Material for test specimens was sampled from steel 355J2+N (65×1640×3550 mm). Steel 355J2+N is structural unalloyed steel

commonly used in civil engineering structures including halls, containers, bridges, cranes or power engineering structures. According to standard Pn-en 10025-2:2008, the minimum yield point of the above named steel amounts to R_e = 335 MPa, whereas the minimum impact energy at a temperature of -20°c amounts to 27 J. During the production the material was subjected to heat treatment (normalising) [6]. Steel s335j2+n is characterised by good weldability and, according to the manufacturer's certificate of conformity, has a carbon equivalent cev = 0.44 [7].

According to the above named certificate, the mechanical properties of steel s335j2+n are the following [7]:
– yield point R_e = 358 MPa
– tensile strength R_m = 512 MPa
– elongation A_5= 30%
– impact energy KV = 209 J at a temperature of -20°c

Treatment of Specimens

The specimens were thermally cut out of a plate leaving an appropriate allowance. Afterwards, the specimens were subjected to mechanical treatment to reach dimensions of 500×200×50 mm.

In accordance with the requirements of test sep 1390 the specimens were milled to a thickness of 50 mm on only one side of the plate, leaving the other side with a post-roll raw surface. Afterwards, on the untreated (post-roll raw) surface of the specimen, a groove having a radius R=4 mm was milled along the entire length of the plate. The post-treatment view of the specimen is presented in Figure 3.

Overlay Weld

The overlay weld was made in accordance with the guidelines of sep 1390, using mma welding (111) and a rutile electrode. The rutile electrode was thick-covered (Fig. 4) and had a diameter of 5 mm; the electrode was made by Esab under the commercial name of OK Femax 33.80 5.0×450 mm. In accordance with standard En iso 2560-a, the electrode was designated with code e 42 0 rr 73). Before overlay welding, the electrodes were subjected to drying (recommended by the manufacturer) performed at a temperature of 250°c for approximately 2 hours.

According to the certificate of conformity, the mechanical properties of the weld deposit were the following [8]:
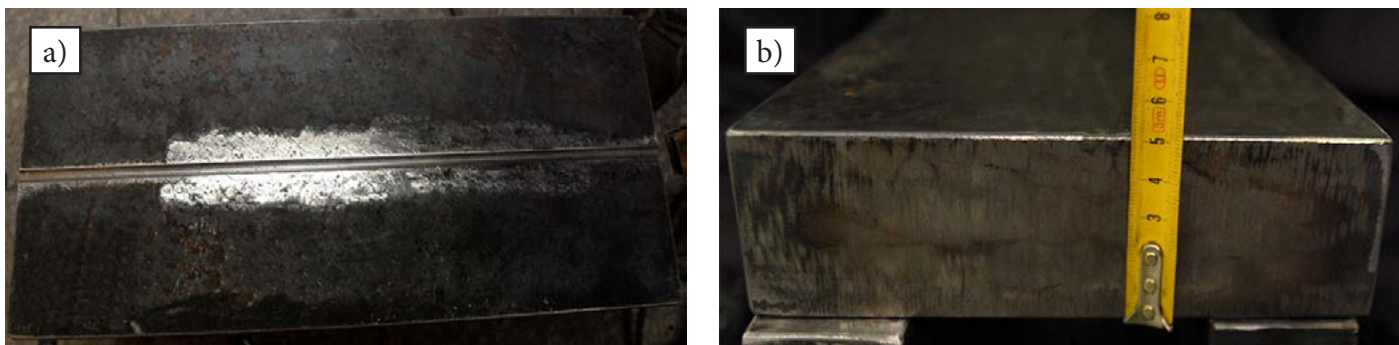

Fig. 3. Post-treatment view of the specimen: a) groove b) front

Fig. 4. Electrodes made by ESAB OK Femax 33.80 5.0x450 mm

– yield point R_{eL} = 480 MPa
– tensile strength R_m = 555 MPa
– elongation A_5 = 26%
– impact energy KV = 60 J at a temperature of 0°C

The preparation of the specimens in accordance with the recommendations contained in SEP 1390 was followed by the adjustment of optimum parameters for surfacing individual specimens. The overlay welds were made in the milled groove using a single run without stopping the process of surfacing. After surfacing, the overlay welds were not subjected to mechanical treatment. All the specimens were subjected to surfacing at a temperature of 19°C and using constant values of welding current and arc voltage (I=246 A, U=29.84 V). In order to test the effect of the change in overlay weld geometry (height of the excess weld metal of the overlay weld) on test SEP 1390, the overlay weld of each specimen was performed using a different welding rate restricted within the range of 2.2 mm/s to 4.9 mm/s. The process of surfacing is presented in Figure 5. The photographs showing the process of surfacing were performed without screening electric arc and using a filter screening arc. The specimens after surfacing and cleaning of the overlay weld are presented in Figure 6.

After cooling, the slag was removed from the specimens using a welding hammer and a wire brush. The removal of the slag was followed by measurements of the widths and heights of the overlay weld faces. Each specimen was subjected to 12 measurements performed every 20 mm. The average heights of overlay weld faces amounted to 0.1; 0.8; 1; 1.2; 2.0 and 2.5 mm respectively, whereas the corresponding heights amounted to 17.9; 18.7; 19.1; 19.4; 24.3 and 24.8 mm.

Tests

After thorough preparation, the test specimens were individually placed in a testing machine manufactured by Heckert EU 100T and provided
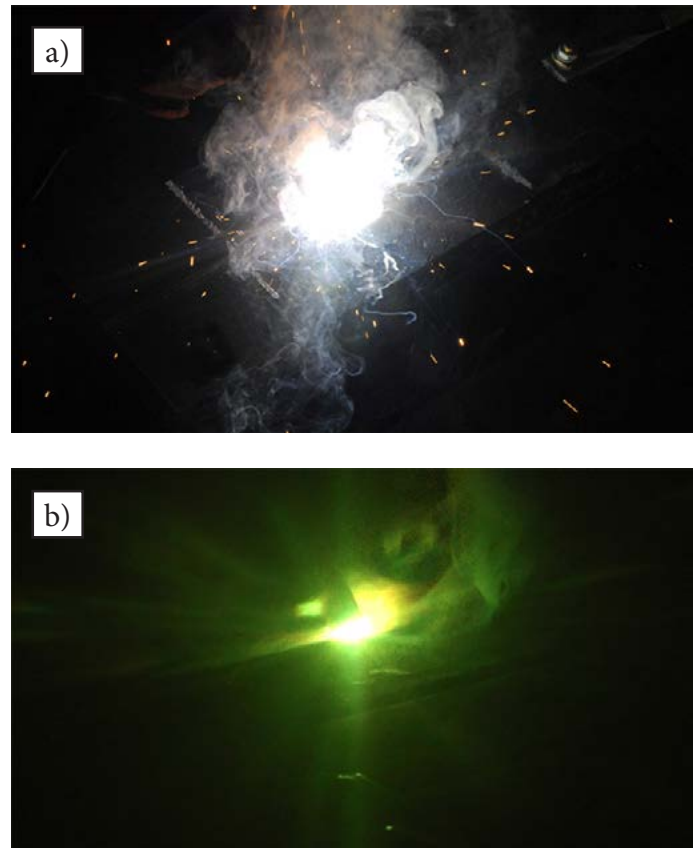
Fig. 5. Surfacing of the specimens: a) without screening arc b) using a filter screening arc

Fig. 6. Test specimen with the overlay weld

with specialist fixtures featuring appropriate mandrel and supports used for the bending of specimens. A given specimen was placed in such a manner that the overlay weld was located in the tension zone during the process of bending. In accordance with the guidelines of SEP 1390, the mandrel diameter related to the test plate having a thickness of 50 mm amounted to 150 mm, the diameters of the supports amounted to 80 mm, whereas the distance between the supports amounted to 280 mm. In order to assess the bend angle of the specimen, the bend tests were continuously monitored by

cameras filming the area of the overlay weld subjected to tension; the testing machine dynamometer (clock) indicating the value of the bend force and the specimen subjected to bending. An exemplary image recorded (and edited) using three cameras during the technological bend test is presented in Figure 7 [9].
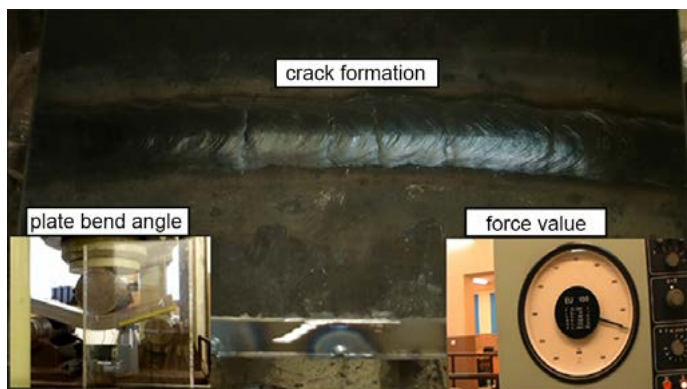

Fig. 7. Image recorded by the cameras during the bend test [9]

The system enabling the continuous monitoring of primary process variables was the basis of the thorough analysis of individual tests.

Test Results

The general characteristics of test results are presented in relation to the individual tests [9].

Test no. 1

In test no. 1 (excess weld metal height of 2.5 mm, bend angle of 65°) 6 cracks were recorded; 4 cracks passed through the heat affected zone and were stopped in the base material. None of the cracks exceeded the boundary value of 80 mm (from the overlay weld centre to the edge of the crack). The test result was positive.

Test no. 2

In test no. 2 (excess weld metal height of 2.0 mm, bend angle of 66°) 6 cracks were recorded; 2 cracks passed through the heat affected zone and were stopped in the base material. None of the cracks exceeded the boundary value of 80 mm (from the overlay weld centre to the edge of the crack). The test result was positive.

Test no. 3

In test no. 3 (excess weld metal height of 0.8 mm, bend angle of 65°) 6 cracks were recorded, all of which cracks passed through the heat affected zone and were stopped in the base material. None of the cracks exceeded the boundary value of 80 mm (from the overlay weld centre to the edge of the crack). The test result was positive.

Test no. 4

In test no. 4 (excess weld metal height of 0.1 mm, bend angle of 67°) 9 cracks were recorded; 7 cracks passed through the heat affected zone and were stopped in the base material. None of the cracks exceeded the boundary value of 80 mm (from the overlay weld centre to the edge of the crack). The test result was positive.

Test no. 5

In test no. 5 (excess weld metal height of 1.2 mm, bend angle of 66°) 7 cracks were recorded; 3 cracks passed through the heat affected zone and were stopped in the base material. None of the cracks exceeded the boundary value of 80 mm (from the overlay weld centre to the edge of the crack). The test result was positive.

Test no. 6

In test no. 6 (excess weld metal height of 1.0 mm, bend angle of 66° 10 cracks were recorded, 6 cracks passed through the heat affected zone and were stopped in the base material. None of the cracks exceeded the boundary value of 80 mm (from the overlay weld centre to the edge of the crack). The test result was positive.

Analysis of Test Results

All the test specimens produced positive results as regards the final assessment concerning the weldability of the material in accordance with criteria presented in the guidelines of SEP 1390. Conditions related to the formation and propagation of cracks within appropriate limits (during bending performed to reach the

boundary angle) were satisfied. Table 3 presents the detailed characteristics of the parameters recorded during the bend tests (taking into consideration cracks formed in relation to the height of the excess weld metal of the overlay weld).

metal. A similar dependence referred to a greater number of cracks crossing the HAZ boundary and entering the base material of the specimens characterised by lower heights of overlay welds. The latest criterion is particularly important as regards the essence of technological tests, where

Table 3. Bend test results [9]

Height of excess weld metal [mm]	2.5	2.2	1.2	1.0	0.8	0.1
Specimen no.	1	2	5	6	3	4
Maximum bend angle [°]	65	66	66	66	65	67
Value of force [kN]	945	930	895	900	910	940
Number of cracks formed in the overlay weld	6	6	7	10	7	9
Number of cracks passing outside the HAZ	4	2	3	6	6	7
Total length of the longest crack [mm]	39.6	36.6	25.3	25.0	70.5	30.0
Longest crack from overlay weld axis [mm]	20.9	16.2	17.7	12.5	37.1	18.0
Bend angle related to the formation of crack no. 1 [°]	20	40	20	8	8	12
Bend angle related to the passage of crack no. 1 through the HAZ [°]	56	48	46	28	24	32
Bend angle related to the formation of the longest crack [°]	36	40	28	8	8	12
Test assessment [ok – positive; neg. – negative]	ok	ok	ok	ok	ok	ok

The test results presented in Table 3 were determined for all of the specimens subjected to bending to a boundary angle restricted within the range of 65÷67° using force restricted within the range of 895 to 945 kN. In the specimens having heights of 0.1, 0.8 and 1.0 mm, the first cracks were initiated at small bend angles restricted within the range of 8° to 12° and were characterised by significant dynamics when crossing the HAZ boundary at bend angles restricted within the range of 24° to 32°. In turn, in the specimens containing overlay welds having higher excess weld metal, i.e. 2.5, 2.0 and 1.2 mm, the first cracks were initiated at greater bend angles restricted within the range of 20° do 40° and were characterised by significantly smaller dynamics making it possible to cross the HAZ boundary at bend angles restricted within the range of 46° to 56°.

It was also possible to observe greater amounts of cracks formed in the specimens characterised by lower heights of the excess weld metal of the overlay weld faces in relation to the specimens characterised by higher excess weld

it is absolutely necessary that a crack be generated in the overlay weld, cross the HAZ boundary to finally enter and be stopped in the base material.

Conclusions

The tests and the analysis of the effect of the change in overlay weld geometry on the course of technological testing used when assessing the weldability of thick-walled materials made of steel S355J2+N according to the guidelines of SEP 1390 enabled the performance of the related assessment and the formulation of the following conclusions:

– first cracks were initiated significantly early and related to the lower excess weld metal of overlay weld faces,

– rate of crack propagation was significantly higher in cases of the lower excess weld metal of overlay weld faces,

– number of cracks passing through the HAZ and reaching the base material was greater in cases of lower excess weld metal,

– number of cracks was also greater in cases of

the lower excess weld metal of overlay weld faces,

– recommendation contained in the technological test according to the guidelines of SEP 1390 concerning the excess weld metal height of approximately 1 mm is fully justified in light of the performed tests as the cracks were initiated early (as early as at an angle of 8°) and satisfied the condition of passing from the overlay weld to the base material at an angle of mere 24°,

– all of the tests performed using the specimens having various heights of excess weld metal produced positive results concerning the weldability of 65 mm thick plates made of steel S355J2+N.

Confirming the rightness of the recommendation concerning the height of the excess weld metal of the overlay weld (approximately 1 mm) is justified, as the range of up to 1 mm undoubtedly offers the most favourable conditions as regards the appropriate dynamics of the test and its high sensitivity without affecting the final result concerning the assessment of weldability. Properly conducted tests make it possible to verify the analytically determined assessment of weldability related to thick-walled structural materials used in welded structures. Particularly important is the test when assessing the weldability of thick-walled structural materials used in structures exposed to significant static loads or to loads of lower intensity but being dynamic in nature. For this reason the test is often recommended by various guidelines or standards, e.g. DIN 18800-7 [10].

References

[1] Pilarczyk J. (ed.): *Poradnik inżyniera – Spawalnictwo*. Vol. II, Wydawnictwo Naukowo-Techniczne, Warszawa 2005

[2] Butnicki S.: *Spawalność i kruchość stali*. Wydawnictwo Naukowo-Techniczne, Warszawa 1979

[3] Brózda J.: S*tale konstrukcyjne i ich spawalność*. Instytut Spawalnictwa, Gliwice 2009

[4] ABV SEP 1390:1996 Requirements

[5] Pakos R.: *Technologiczna próba spawalności według ABV-SEP 1390*. Przegląd Spawalnictwa, 2013, no. 4, pp. 14-17

[6] PN-EN 10025-2:2008: *Hot rolled products of structural steels. Part 2: Technical delivery conditions for non-alloy structural steels*

[7] Świadectwo odbioru wytwórcy 3,1; blacha t65 S355J2+N

[8] Certificate of conformity provided by the manufacturer of welding materials in relation to electrode OK FEMAX 33.80

[9] Kozłowski J.: *Ocena spawalności materiałów wg próby Kommerella i SEP 1390*, Diploma thesis reviewed by dr. inż. R. Krawczyk, Częstochowa University of Technology

[10] DIN 18800-7. *Steel structures - Part 7: Execution and constructor's qualification*